UC Berkeley
SEMM Reports Series

Title
Model studies of curved box-girder bridges

Permalink
https://escholarship.org/uc/item/68c8x31s

Authors
Aslam, Mohammad
Godden, William

Publication Date
1973-03-01

eScholarship.org Powered by the California Digital Library
University of California

REPORT NO.
UC SESM 73-5

STRUCTURES AND MATERIALS RESEARCH
DEPARTMENT OF CIVIL ENGINEERING

MODEL STUDIES OF CURVED BOX-GIRDER BRIDGES

by
M. ASLAM
and
W.G. GODDEN

Report to the Sponsors:
State of California
Business and Transportation Agency
Department of Public Works
Division of Highways; and
U.S. Department of Transportation
Federal Highway Administration

MARCH 1973

STRUCTURAL ENGINEERING LABORATORY
UNIVERSITY OF CALIFORNIA
BERKELEY CALIFORNIA

Structures and Materials Research
Department of Civil Engineering
Division of Structural Engineering
and Structural Mechanics

MODEL STUDIES OF CURVED BOX-GIRDER BRIDGES

A Report of an Experimental Study into the
Behavior of Curved Box-Girder Bridges

by

M. Aslam
Assistant Research Specialist

and

W. G. Godden
Professor of Civil Engineering

to

State of California
Business and Transportation Agency
Department of Public Works
Division of Highways

and

U.S. Department of Transportation
Federal Highway Administration

College of Engineering
Office of Research Services
University of California
Berkeley, California

March 1973

TABLE OF CONTENTS

Page

LIST OF TABLES

LIST OF FIGURES

Page

Page

LIST OF PLATES

SYMBOLS

C	Total compressive force
E	Young's Modulus of Elasticity
I	Moment of Inertia
L	Center line span
L_e	Effective Span
N_{xx}	Longitudinal Force per unit width
M_{yy}	Transverse bending moment per unit length
T	Total tensile force
W	Applied load
ν	Poisson's Ratio
θ	Skew angle

ABSTRACT

This report presents the results of laboratory tests on a series of 1/29 scale aluminum models of curved box-girder bridges. The tests were conducted primarily to provide experimental response data to check the accuracy of proposed analytical solutions for the elastic behavior of bridges of this type. The prototype design was a four cell box section with a total width of 33 ft. 10 in., the radius of curvature was 282 ft. in all cases, and the span varied from 145.0 ft. to 72.5 ft.

All tests were conducted on a single machined aluminum model. Starting with the longest span of 60 in., the model was cut back to 45 in. and 30 in. spans respectively. All models were tested both with and without a midspan radial diaphragm for 10 different locations of a single vertical point load. Reactions were measured by four load cells, deflections at 9 locations by low voltage differential transformers, and strains by 68 rosette gages and four single element gages located on a radial section close to midspan.

All load and strain readings were recorded and reduced by computer, and this data were checked for self-consistency by three independent static checks.

The data presented in this report include external reactions, deflections at selected points along the webs, tangential plate forces and radial plate bending moments on a radial section close to midspan. Also deduced in each test is the distribution of total moment at midspan between the individual I-beams that comprise the box section.

The report concludes with some observations on the general behavior of the curved box-girder bridges tested, and a brief comparison of test and theoretical results.

KEY WORDS

Bridges, curved box-girder bridges, multicell bridges, aluminum models, glued models, diaphragms, curved folded plate structures, Calcomp plotting, strain measurement.

1. INTRODUCTION

1.1 Objective

This investigation is an extension of a previous study on the static response of skew box-girder bridges which was made by the authors and much of the experimental procedure is discussed in greater detail in a previous report (1). The primary objective of this investigation was to develop experimental data on the response of horizontally curved box-girder bridges subjected to static vertical loading. This data was to be sufficiently accurate for checking the validity of proposed analytical solutions.

Bridges curved in plan are an increasingly common feature of highway construction, partly due to the geometrical configurations of highway intersections, and partly due to the restrictions on the location of bridges that occur particularly in built-up areas. Box girder bridges, being torsionally much stiffer than open sections are ideally suited for bridges curved in plan, thus it has become increasingly important to understand the behavior of such bridges and to develop suitable analytical techniques.

Recently, small model studies have been conducted on single cell box-girder bridges either made in plastic [2] or in concrete and steel composite construction [3]. In neither of these studies, was there good agreement between test and analytical results.

Since the accuracy of the test data in this investigation was of primary importance, considerable time and effort was devoted to developing construction and test procedures for the model that would accurately represent the physical system used in the analytical solution. Of particular importance was the continuity between the webs and plates in the construction procedure and checking the test data for self-consistency

in the experimental procedures.

A glued aluminum model of a representative four cell box-girder bridge section was tested. The model was successively cut back to shorter spans so as to study the effect of span length on the response of a curved box-girder bridge of constant curvature. The effect of a midspan radial diaphragm was also studied for each span.

The quantitites to be measured included boundary reactions, deflections at selected points along the webs, and strains at a selected radial section close to midspan. The strains were measured at close intervals so that a complete stress distribution could be determined experimentally at the selected section. This was necessary for internal static checks, as well as for studying the general behavior of the box-section as the span was varied. The quantities to be compared with the analytical results included deflections at selected points, radial distribution of tangential forces, radial distribution of radial plate bending moments, and the distribution of the total bending moment between the I-beams of the box section at the instrumented section.

1.2 Scope of the Investigation

The prototype box-girder bridge design selected for this study is shown in Fig. 1.1a. It is a four-cell bridge, each cell being 7 ft. 3 in. wide by 4 ft. 4 in. deep. The top deck is 6-1/2 in. thick and is continuous with tapered cantilever overhangs at each side. The five webs are all 8 in. thick, and the bottom plate (deck) is 5-1/2 in. thick. The radius of curvature was 282 ft., which represented the steepest curvature on any such existing bridge in the State of California.

A linear scale of 1/29 was chosen for the model study, and the

dimensions of the simplified model corss-section are shown in Fig. 1.1b. The fillets between the webs and plates (decks) were omitted, and the cantilevered part of the top plate was made of constant thickness; this thickness being the same as that of the top plate. A cross-section of the bridge model is shown in Plate 1.1.

The span was considered as a variable, but the radius of curvature and sectional geometry were not changed. Starting with a maximum span of 60 in. for the original Model 1, the span was successively reduced to 45 in. for Model 2 and 30 in. for Model 3. The span in all cases was taken as the horizontal projection of the central web and all dimensions were taken to the center of end diaphragms. Table 1.1 gives plan dimensions of the three models and the corresponding protype dimensions. Plan dimensions of Models 1 through 3 are also shown in Fig. 1.2. All the bridge models were tested with and without a radial diaphragm at midspan. In Table 1.1 and Fig. 1.2, A represents the bridges without midspan diaphragm while B represents the bridges having a midspan radial diaphragm.

A typical curved box-girder aluminum bridge model under test is shown in Plate 1.2. The model was glued together by means of a tape epoxy as it was established in the preliminary coupon studies (see Chapter 2) that this type of model construction would provide the required continuity between webs and plates. The bridge model has two permanent end diaphragms bolted in position and also a collapsible midspan radial diaphragm. The midspan diaphragm could be tightened or loosened externally without removing the top plate. Each bridge model was tested for ten load positions. In each case the load was applied as a point load and the following measurements and self-consistency checks were made.

(1) Boundary Reactions:

The bridge was supported on four point supports R1 through R4 located at the intersection of the outside webs and the end diaphragms - the intersection of mid-thickness planes (Fig. 1.3). All four reactions were measured by load cells (see Plate 1.2). A static check was applied to ensure that the sum of the four reactions equalled the applied vertical load.

(2) Internal Strains:

A radial section designated 0-0 in Fig. 1.3 which is located at an angle of 0.49° from the centerline was closely instrumented with strain gages on top and bottom plates and on all five webs. This enabled a complete stress distribution to be derived at this section. The strains were integrated to get the total compressive and tensile forces as well as internal moment at the section. Comparison of compressive force with tensile force and the comparison of internal moment with the external moment at this section provided two further static checks.

(3) Deflections:

These were measured at nine locations along the webs. Self-consistency checks based upon symmetry and reciprocity were made whenever possible. Reciprocity checks also acted as a check on the linearity of the system.

Load positions and locations of deflection measurements are shown in Chapter 5. Strain gage locations are given in Fig. 3.1.

The following tabulated data is presented in Chapter 5 for all load positions.

(1) Reactions R1 through R4.

(2) Tangential forces N_{xx} in top and bottom plates along Section 0-0 computed from strains at strain gage locations.

(3) Radial bending moments M_{yy} computed from measured strains along

Section 0-0 in plates and webs.

(4) Deflections at selected points.

(5) The total tangential bending moment at midspan computed from external forces.

(6) The distribution of total moment between the I-beams that comprise the box-girder section at Section 0-0, computed from the measured stress distribution.

In addition to the tabulated data, the following data is also presented graphically in Chapter 5 and was plotted automatically by the computer.

(1) Radial distribution of N_{xx} forces in top and bottom plates at Section 0-0 for all the load positions for all bridges tested.

(2) Radial distribution of radial bending moments in plates and webs at Section 0-0 for five midspan load positions for model A series tests i.e. for models without midspan diaphragm.

In Chapter 6 there is a discussion of the self-consistency of the experimental data with regard to static checks, symmetry and reciprocity of deflections. In Chapter 7 there is a general discussion of the behavior of curved box-girder bridges, based on the data presented in Chapter 5.

The report concludes with a brief discussion in Chapter 8 on the comparison between the test and analytical results. The agreement between the two in all cases was considered sufficiently close to validate both studies.

Model Reference No	Model		Prototype	
	Span (in.)	Radius of curvature (in.)	Span (ft.)	Radius of curvature (ft.)
1A, 1B	60	117.6	145.0	282
2A, 2B	45	117.6	108.9	282
3A, 3B	30	117.6	72.5	282

A - Refers to models without midspan radial diaphragm.

B - Refers to models with midspan radial diaphragm.

TABLE 1.1 PLAN DIMENSIONS OF MODEL AND PROTOTYPE

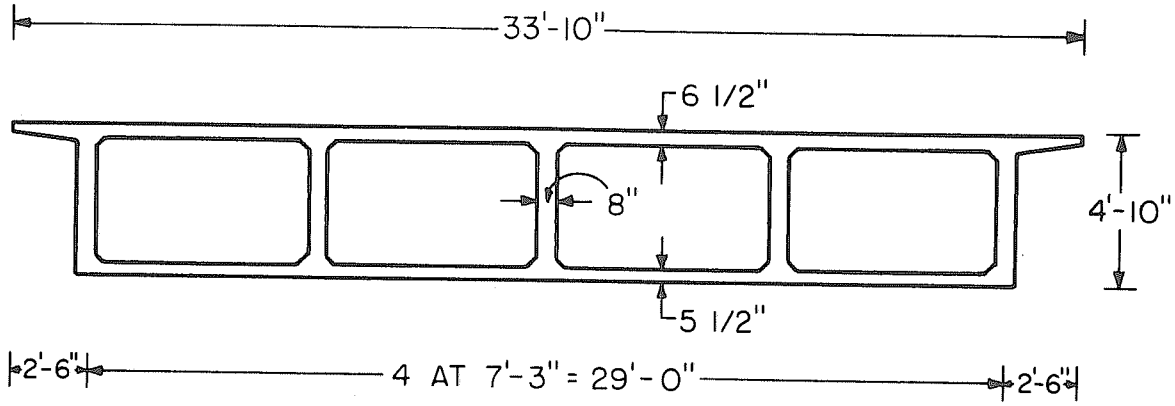

(a) PROTOTYPE

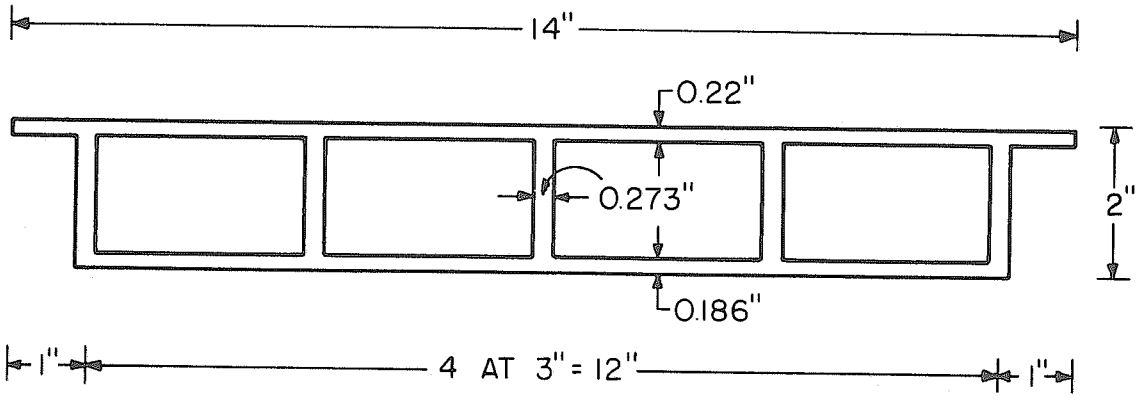

(b) MODEL

FIG. 1.1 DIMENSIONS OF PROTOTYPE AND 1/29th SCALE MODEL CROSS SECTION

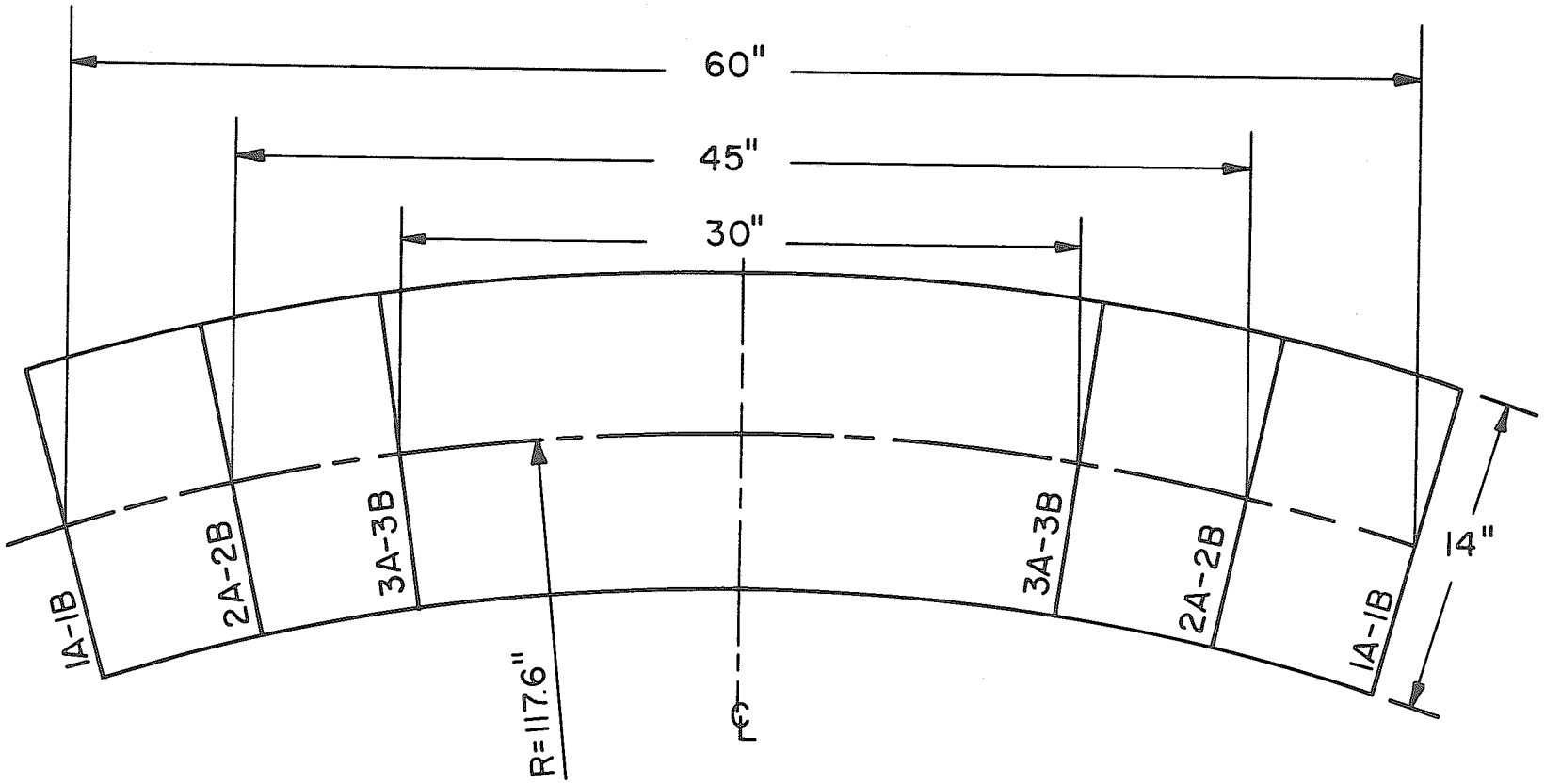

NOTE: ALL DIMENSIONS ARE TO THE CENTER OF END DIAPHRAGM

FIG. I.2 PLAN DIMENSIONS OF MODELS I THROUGH 3

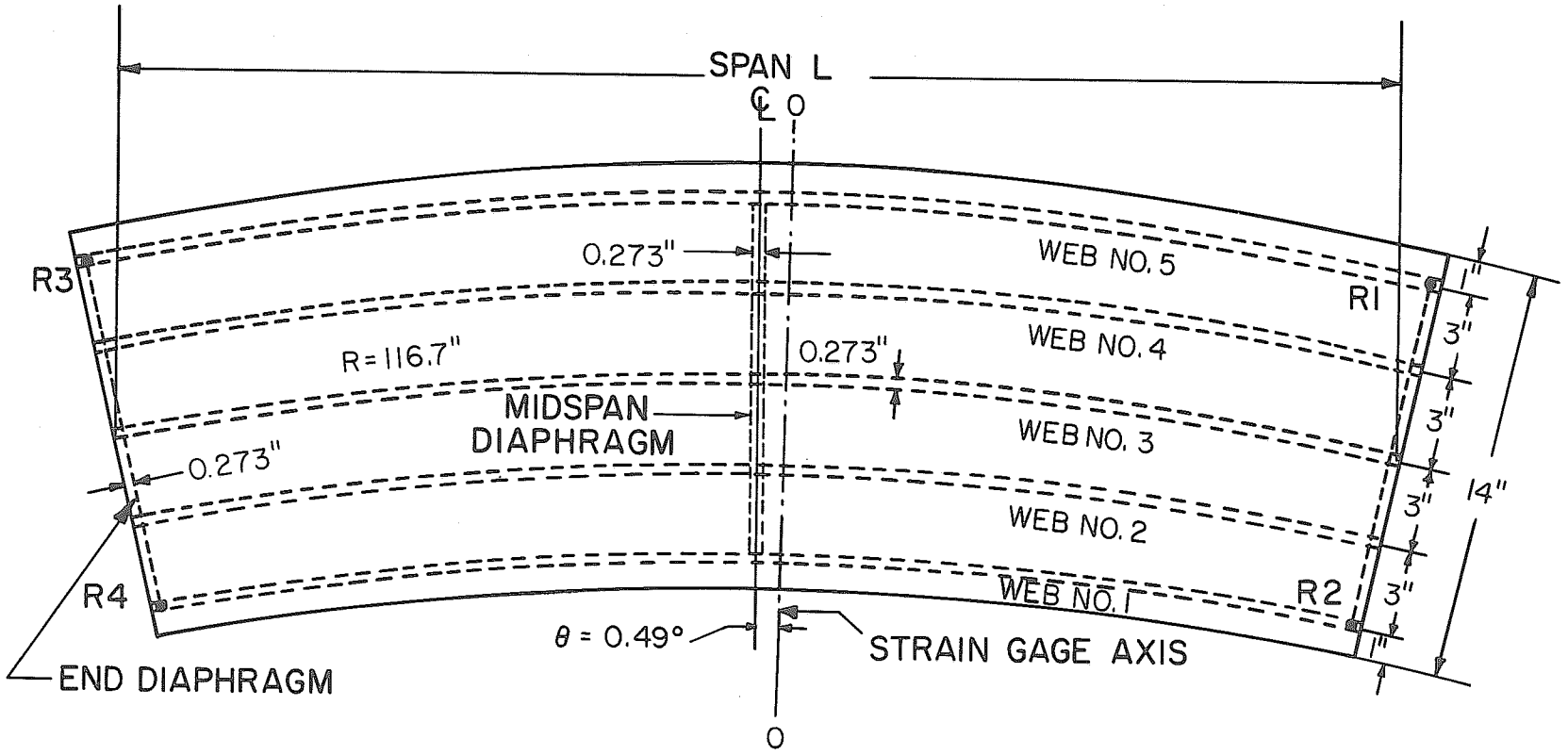

NOTE: THE SPAN L IS TAKEN AS THE HORIZONTAL PROJECTION OF CENTRAL WEB

FIG. 1.3 PLAN VIEW OF A TYPICAL CURVED BOX-GIRDER BRIDGE MODEL

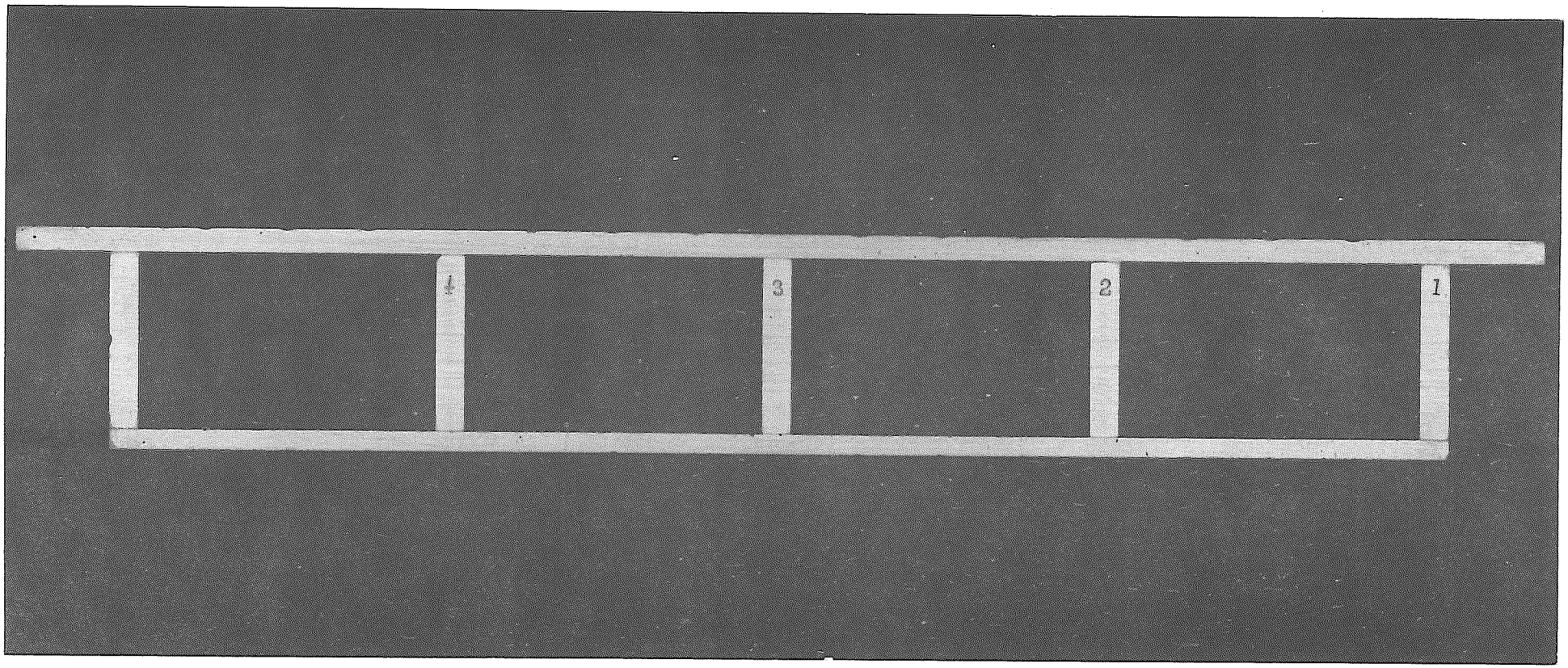

PLATE I.I CROSS SECTION OF THE ALUMINUM BOX GIRDER BRIDGE MODEL

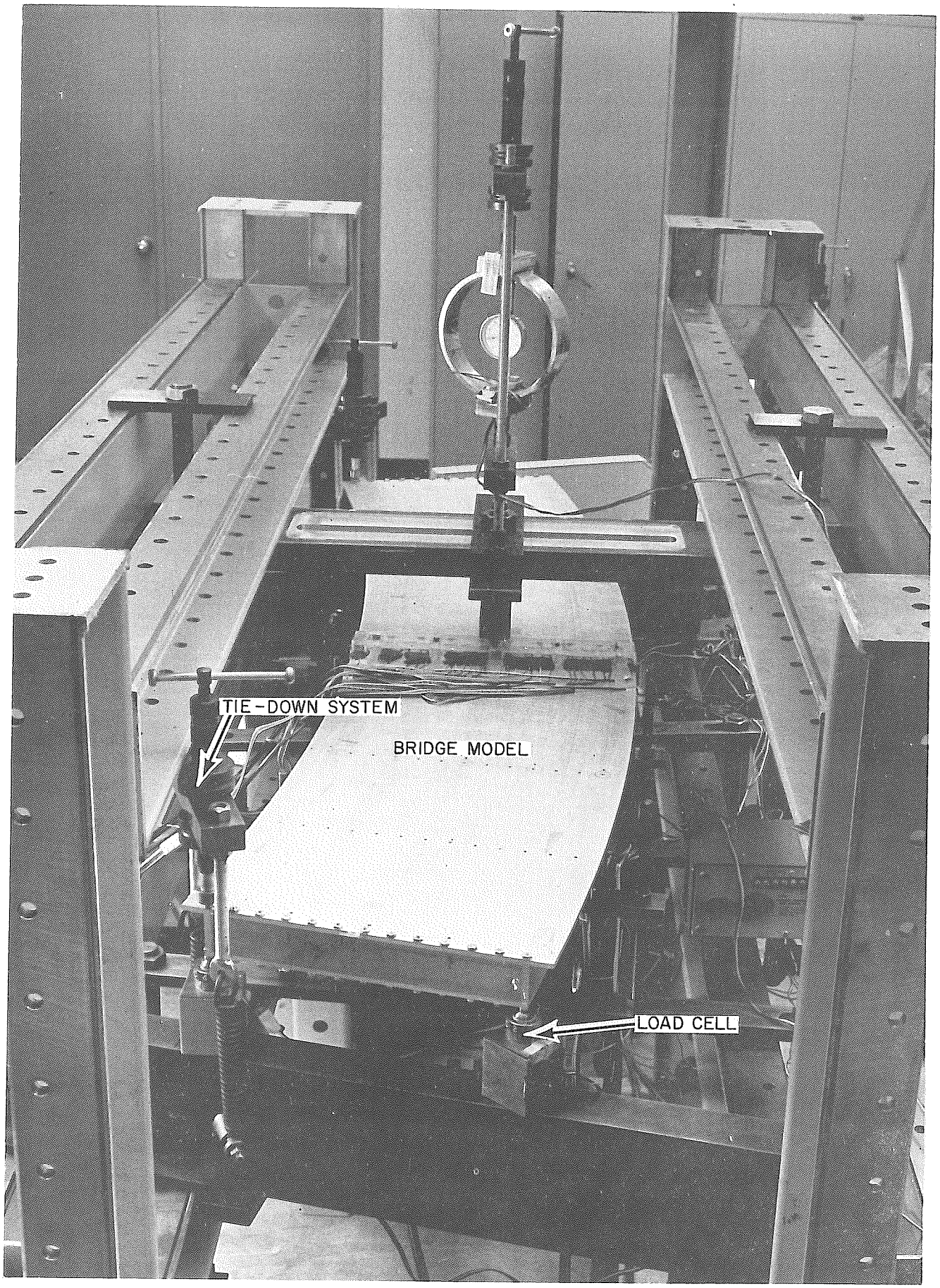

PLATE I.2 A TYPICAL CURVED BOX-GIRDER BRIDGE MODEL UNDER TEST

2. PRELIMINARY STUDIES AND EQUIPMENT DESIGN

2.1 Considerations in the Design of Model

There were three main considerations in the design of the model.

(1) The test data had to be of high accuracy.

(2) The effect of the presence or absence of a midspan radial diaphragm was to be studied on the same model.

(3) The study was to cover a wide range of spans, in order to study general trends in the behavior of curved box-girder bridges.

An aluminum alloy was selected for the model, in preference to the plastics. The properties of the aluminum are neither time nor temperature dependent within known ranges, aluminum can dissipate heat rapidly reducing the strain gage heating problems. Being linear and free from creep problems, an aluminum model is capable of producing test data of higher accuracy than equivalent data from a plastic model.

The model was glued together by means of a tape epoxy, because it was established in the preliminary studies (Secs. 2.2 and 2.3) that a glued web-plate connection behaves closer to a continuous connection than either a screwed or bolted connection. Welding was not considered a possibility on account of the problem of warping and moreover only one plate could be welded to the webs.

When the model is loaded, the web-plate connection is subjected to longitudinal shear as well as transverse bending. Thus the behavior of three types of connections, namely, glued, screwed and bolted web-plate joints was studied separately under longitudinal shear (Sec. 2.2) and transverse bending (Sec. 2.3). The behavior of web-plate connections under shear was studied on I-beam specimens, with section dimensions identical to the model I-beams. The behavior of the web-plate connections

under transverse bending was studied on four-cell Vierendeel girder specimens with dimensions identical to the section of the bridge model. In both of these coupon studies, it was found that the glued specimen was stiffer and closer to the continuum when compared with the screwed and bolted specimens. The glued specimens behaved linearly without showing any slip and the same was found true with the glued model.

The glued model, however, could not be dimantled like a screwed model. This made access to the inside impossible for placing or removing the midspan diaphragm; though it was desirable for economic reasons as well as for consistency of the data to study the effect of a midspan diaphragm on one model. To overcome this difficulty, a collapsible diaphragm was designed and placed in position before gluing the top plate. This diaphragm could then be tightened or collapsed externally to make it effective or ineffective as desired. The collapsible diaphragm was tested for adequate simulation of a solid diaphragm and was found satisfactory (see Sec. 2.4) within a given range of loading.

The concept of using a glued aluminum model with a collapsible diaphragm proved to be useful in reducing the time of construction of the model. It also reduced the testing time by enabling each bridge to be tested both with and without the diaphragm without removing the model from the test bench.

The original long span Model 1 (60 in.) was subseguently cut back to shorter spans and the whole series of tests were conducted on the same basic model. Thus, once the reliability of the strain gages and the basic model was established at the start of the program, the comparative data had a high degree of reliability and consistency. The end diaphragms were not glued, but were bolted to the top and bottom plates as they were

reused on the smaller span models.

During the test program both the longitudinal shear stress and bending moment at the web-plate connection were kept well within safe limits determined from the coupon tests. It was estimated that the maximum transverse bending moment in the model between webs and plates for an applied load of 500 lbs. would not exceed 30 in-lbs./in. and the maximum shear stress would be less than 500 psi. The shear strength of the tape epoxy 'Aerobond 3041', which was used to glue the model was found to be greater than 4000 psi. and the transverse bending moment capacity as tested on a 'T' joint specimen was found to be 120 in-lbs./in.

2.2 Test for Shear Continuity

The test for shear continuity for glued, screwed and bolted specimens was conducted on the I-beam specimens shown in Fig. 2.1. The three specimens were identical except that in one beam, the web and flanges were glued together with the tape epoxy 'Aerobond 3041', in the other the connection between web and flanges was made using 5-40 bolts placed at 1/2 in. centers and torqued to 24 in.-lb., and in the third, the web-flange connection was accomplished using 6-32 steel Allen screws, torqued to 24 in.-lb. and placed at 1/2 in. centers. The beams were 30 in. long and 2 in. deep. The thicknesses of web, top flange and bottom flange were 0.273 in., 0.22 in., and 0.186 in. respectively. The beams were simply supported and the load was applied at midspan in each case. The deflection Δ was measured at the midspan and the load-deflection curves for the three specimens are plotted in Fig. 2.1e. It should be noted that the glued I-beam is stiffer than the other two, its deflection curve

is linear and very close to the theoretical value. The screwed specimen also behaves linearly and does not show shear slip, but the higher deflections are probably due to the reduction of moment of inertia. The deflection curve for the bolted specimen is slightly non-linear and shows some shear slip. The glued I-beam specimen is shown in Plate 2.1.

2.3 Test for Moment Continuity

To study the behavior of the web-plate connection under transverse bending, three vierendeel girder specimens were made as shown in Fig. 2.2. The three specimens were again identical in dimensions and material properties and identical to the section of the model without the cantilevered lengths of the top plate. The top and bottom flange thicknesses were 0.22 in. and 0.186 in. respectively and all five webs were 0.273 in. thick. In the first specimen, webs and flanges were glued together with tape epoxy 'Aerobond 3041'. The glued specimen is also shown in Plate 2.1. In case of second specimen, the webs and flanges were connected by using 5-40 steel bolts torqued to 24 in-lb., and placed at 1/2 in centers (Fig. 2.2c). In the third specimen, 6-32 steel Allen screws were used at 1/2 in. centers torqued to 24 in-lb. to connect the webs and flanges (Fig. 2.2d).

Each specimen was simply supported and a load was applied at midspan. Deflection was recorded under the load. The results of load-deflection relationships are shown in Fig. 2.2e for the three specimens. The glued vierendeel girder behaved linearly and was within 1% of the theoretical curve. Bolted and screwed specimens were considerably more flexible and gave bilinear load-deflection curves, indicating joint opening above a load of 180 lbs.

2.4 Diaphragm Testing

An important question in using a collapsible diaphragm was whether or not it would adequately simulate a solid diaphragm when expanded. This was studied on a single vierendeel girder specimen by first testing it with a solid diaphragm along the center-line of the span and then replacing this with a collapsible diaphragm (Fig. 2.3). The dimensions of the vierendeel girder were the same as for the one used in transverse bending test in Sec. 2.3 and are shown in Fig. 2.3.

The solid diaphragm was simulated by putting four solid rectangular pieces, closely fitting between the webs and flanges of the girder. Each diaphragm piece was securely held to the flanges by three bolts placed at 3/4 in. centers and torqued to 24 in-lb. as shown in Fig. 2.3a. This specimen was then simply supported, load was applied at midspan and the deflection measured at the load.

The solid diaphragm was then replaced with the collapsible diaphragm as shown in Fig. 2.3b and Fig. 2.3c (see also Plate 3.1). To form the collapsible mechanism each of the four solid rectangular diaphragm pieces was taken, a tapered hole was made in the center, then the each piece was slit on both diagonals forming parts designated D in Fig. 2.3b. Pieces D could be driven inwards or outwards by means of a tapered sleeve which was integral with a knurled wheel B with internal threads which could be screwed onto a male threaded unit C as shown in Fig. 2.3c. The knurled wheel unit B could be rotated by means of a bar through a small hole in the top flange. The clockwise rotation of the wheel B pushed the split diaphragm D outwards tightening it between the webs and flanges. Two bolts were used in each cell to keep the different pieces of the split diaphragm in alignment and were tightened when the specimen was being

tested with diaphragm action. Thus the diaphragm could be made effective or ineffective by simply turning the knurled wheel externally through a small hole and tightening or loosening the bolts.

The vierendeel girder specimen was tested with the collapsible diaphragm in the expanded position to simulate diaphragm action.

The results of these tests are shown in Fig. 2.3d. The two curves are almost coincident to a deflection of 0.005 in. It was estimated from a previous study of box-girder bridges that the transverse deflection of the box-section would remain within this limit, and thus the collapsible diaphragm mechanism was considered adequately stiff to simulate solid diaphragm action for this study.

2.5 Straining Frame

The straining frame basically consisted of standard 6 in. x 3 in. double steel channel sections. Two plane frames made up of channel sections and supported on tubular legs were placed parallel to each other to support two cross-beams bolted to the frame as shown in Plate 2.2. The bridge was supported on four load cells which were placed on the cross-beams, and the support points of each cross-beam were also supported directly from the floor so as to eliminate any vertical movement of the reaction points which would otherwise affect the response of the bridge.

Certain load conditions produced negative reactions on the two supports nearest the center of curvature, hence a tie-down procedure was adopted as seen in Plate 1.2 and Plate 2.2. The tie-down system consisted of a hand jack connected to the bridge via a yoke and two helical springs, which provided a constant vertical preload on the support.

2.6 Test Boundary Conditions

The support conditions for the bridge called for no horizontal forces to be applied to the model at the boundries. A series of machined steel blocks and roller assemblies were constructed to provide any required degree of horizontal constraint or freedom at any support. The load cell was cemented to the top plate of the stack. Of the four layers in the stack, all four could be steel plates in which case the support provided two degrees of horizontal constraint. Alternatively, one or two of the plates could be replaced by rollers which provided respectively one or two translational degrees of freedom in the horizontal plane. As the model required three independent horizontal constraints for stability in the horizontal plane, these were applied as shown in Fig. 2.4. R2 and R3 had two and one horizontal constraints respectively. R1 and R4 both had two degrees of freedom. At the point of loading, two degrees of horizontal freedom were achieved by putting a steel ball between the bridge and the loading rod (Plate 2.2).

The final setting up of the model for any test required a precise leveling of the four supports which was accomplished by a pair of machined steel wedges inserted between the test bench and the cross-beam at R4. Using these wedges the four load cells were leveled so that the bridge model rested on all four load points simultaneously, in the unloaded condition. After this a preload of 100 lbs. was always applied to ensure that any clearance between load cells and bridge was eliminated.

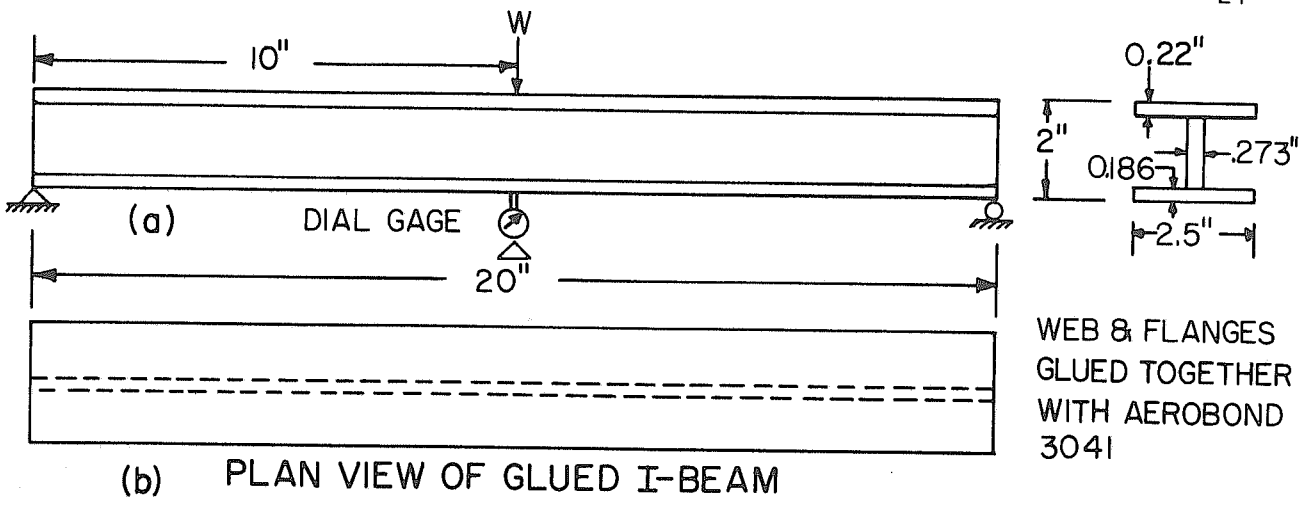

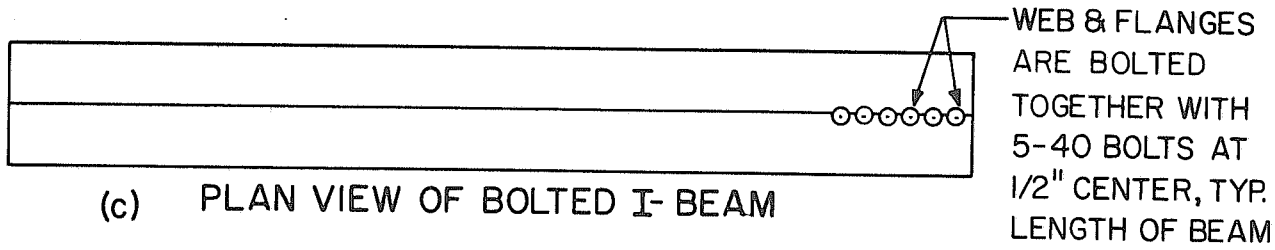

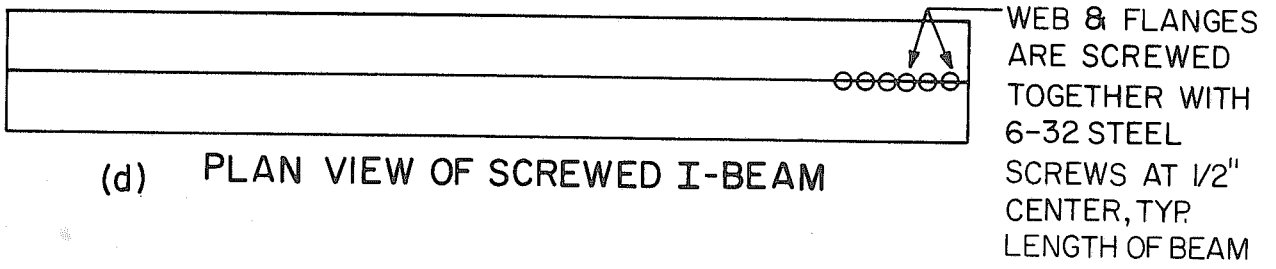

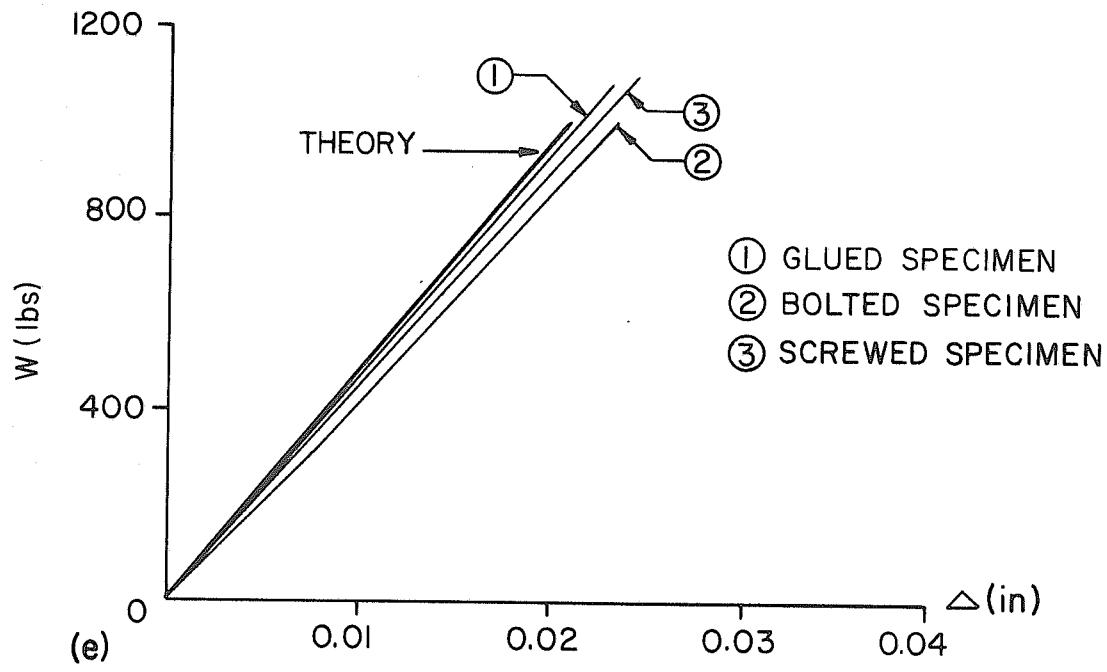

FIG. 2.1 COMPONENT TEST FOR SHEAR CONTINUITY

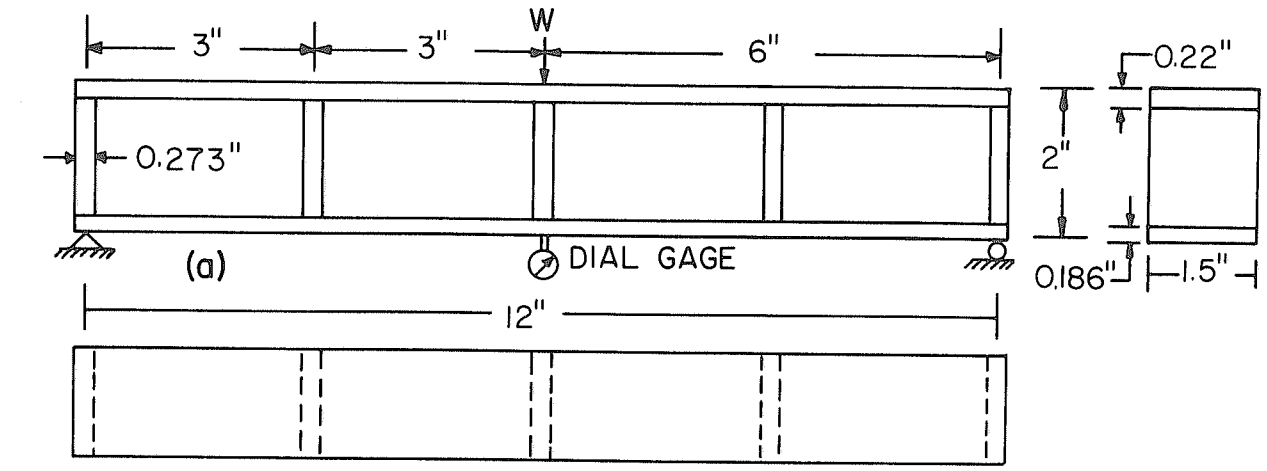

(b) PLAN OF GLUED SPECIMEN

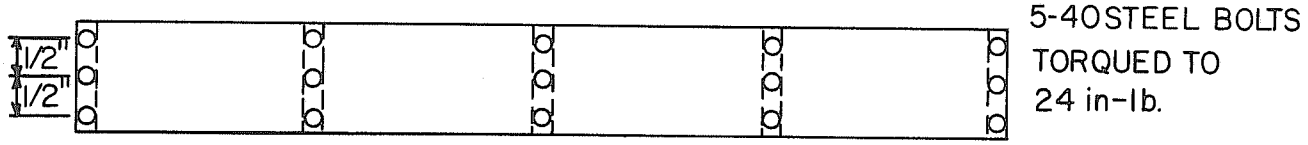

(c) PLAN OF BOLTED SPECIMEN

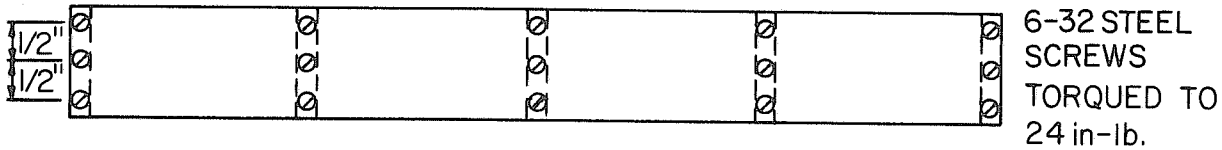

(d) PLAN OF SCREWED SPECIMEN

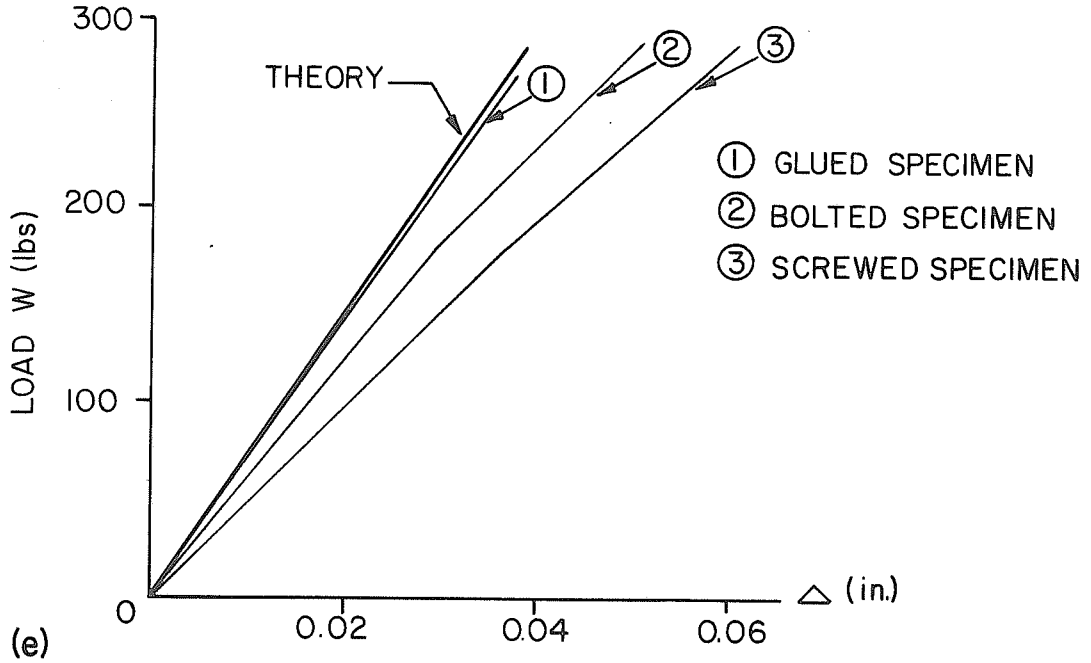

(e)

FIG. 2.2 COMPONENT TEST FOR MOMENT CONTINUITY

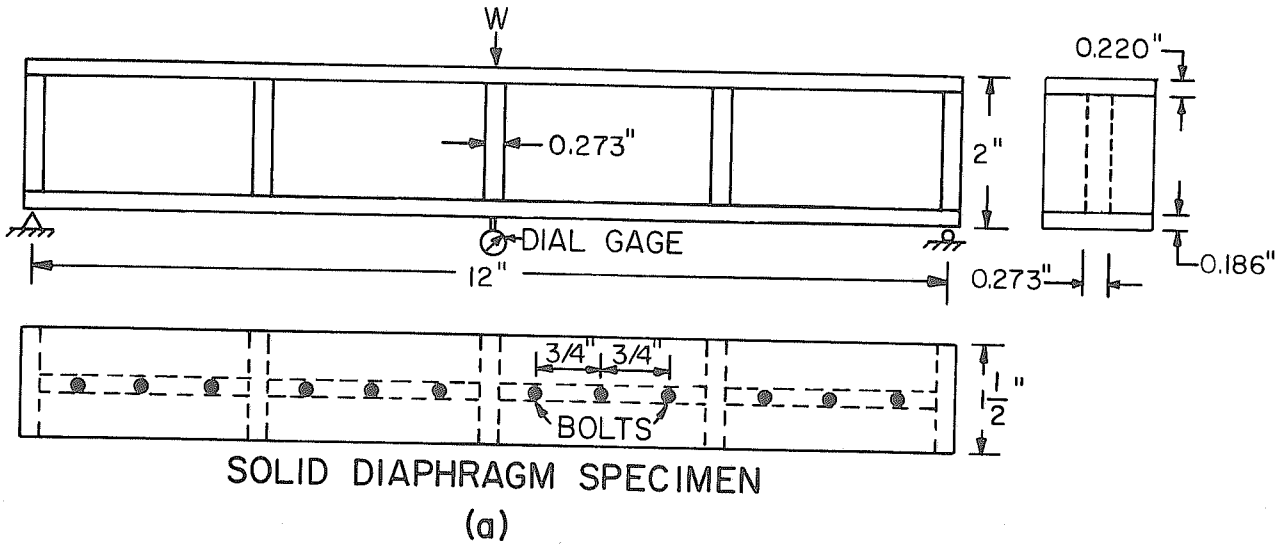

SOLID DIAPHRAGM SPECIMEN

(a)

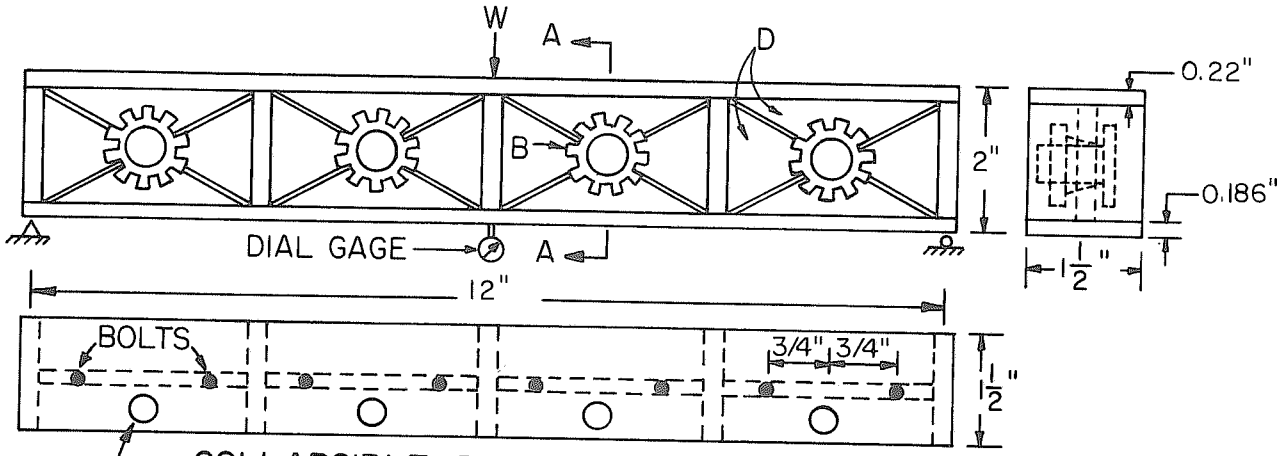

COLLAPSIBLE DIAPHRAGM SPECIMEN

(b)

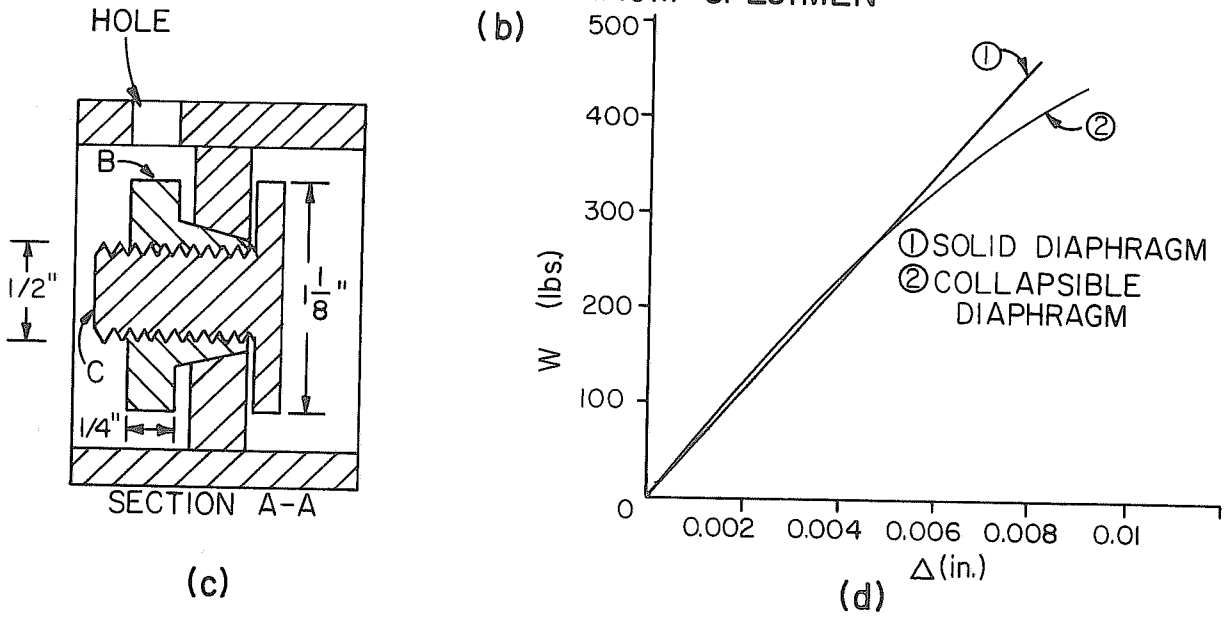

(c)

(d)

FIG.2.3 COMPONENT TESTING OF COLLAPSIBLE DIAPHRAGM

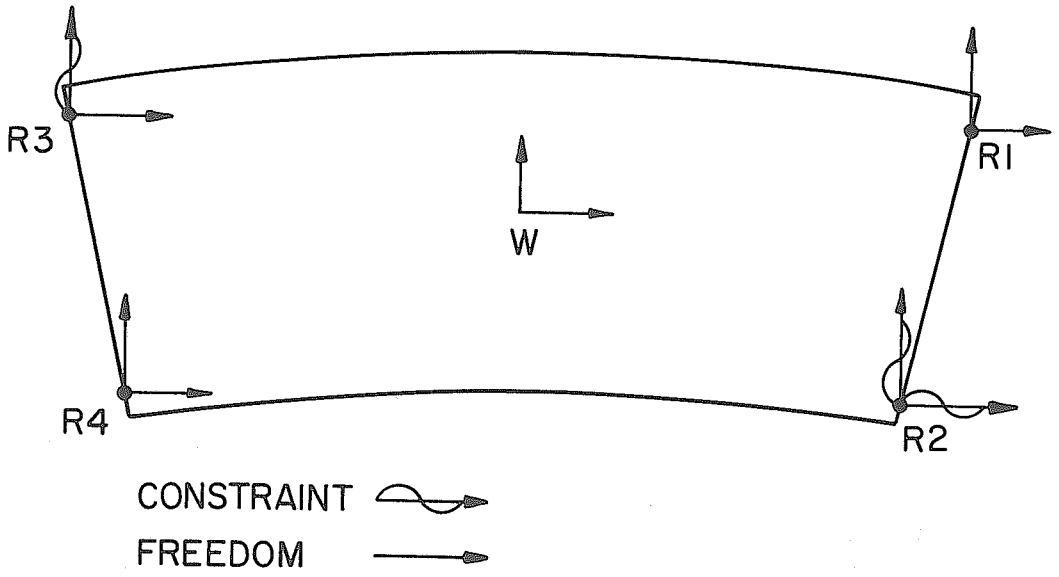

FIG.2.4 TEST BOUNDARY CONDITIONS AND HORIZONTAL CONSTRAINTS AT LOADING POINT

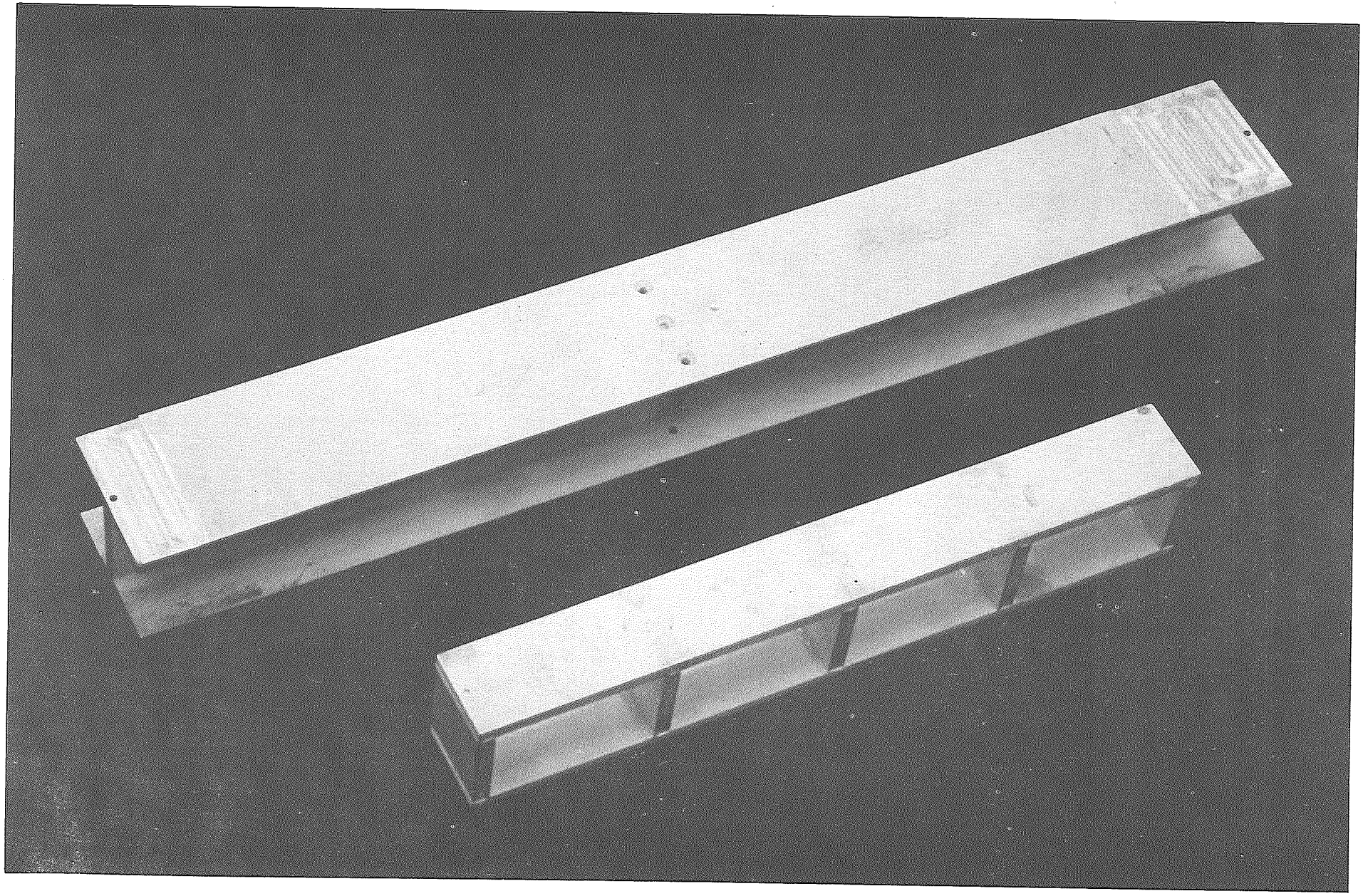

PLATE 2.1 COMPONENT TEST SPECIMENS FOR SHEAR AND MOMENT CONTINUITY

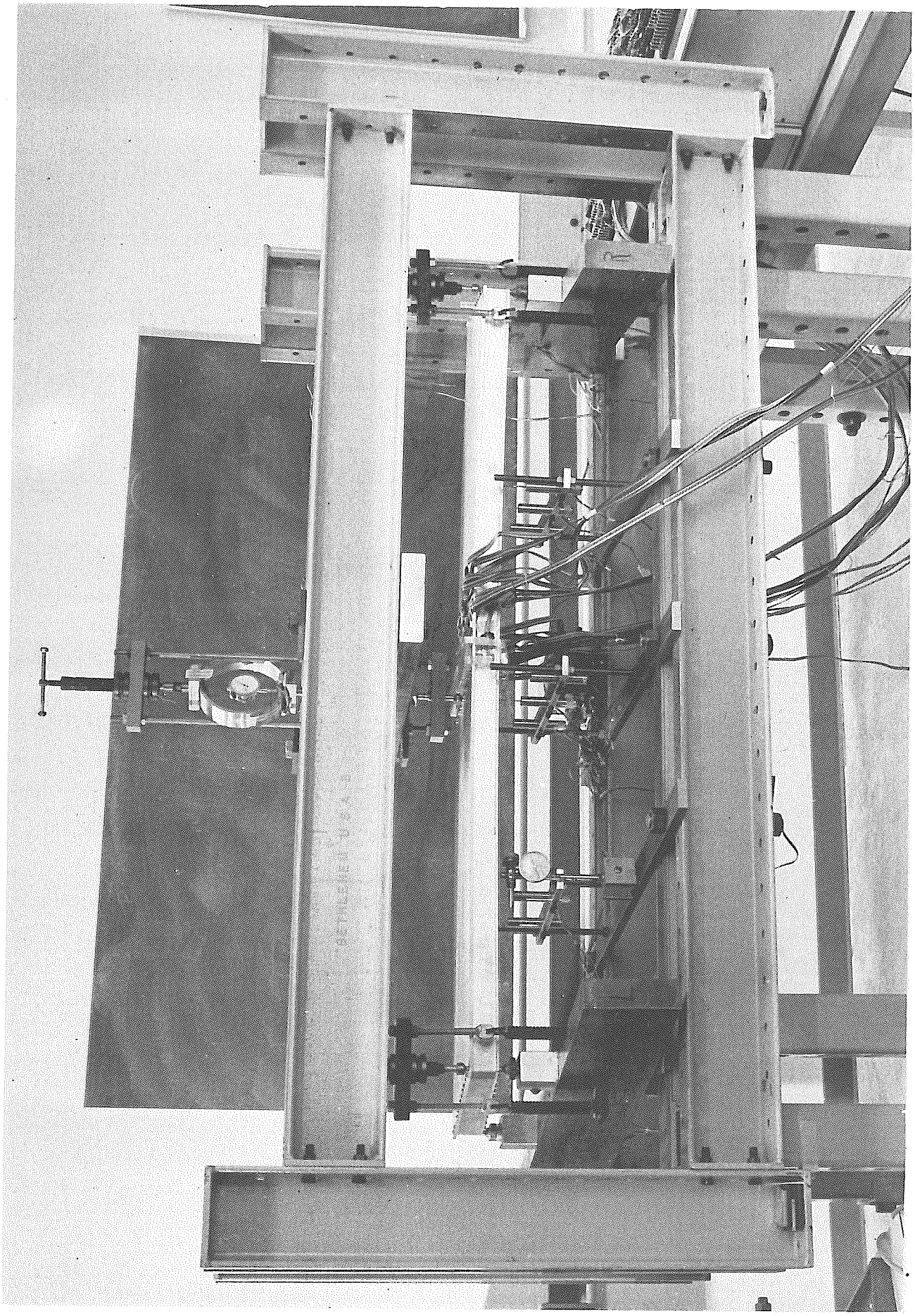

PLATE 2.2 STRAINING FRAME WITH BRIDGE MODEL UNDER TEST

3. MODEL DESIGN AND TEST PROCEDURES

3.1 Fabrication and Description of the Model

The model was constructed out of aluminum alloy reference No. 6061 T-6. The values of Young's Modulus E and Poisson's Ratio ν were determined by individual tests on the five webs before assembling the model. Averaged values were found to be as follows:

$$E = 10.2 \times 10^6 \text{ psi}$$

$$\nu = 0.332$$

The cross-section dimensions of the model are given in Fig. 1.1b. To accomplish the required dimensional accuracy, the aluminum model was constructed with plates and webs machined to the required thickness. As subsequently measured, the plate thicknesses were as follows:

Top plate = 0.220 in.

Webs = 0.273 in.

Bottom plate = 0.186 in.

The webs were machined to the required dimensions, and then rolled to the specified curvature. The plates and webs were then etched to clean the surfaces in a 3:1 solution of sodium dichromate and sulphuric acid for 20 minutes at a temperature of 160°F. The strain gages were fixed on both sides of the webs and on the inside surfaces of top and bottom plates. The performance of all gages was then studied by bending tests conducted on the individual bridge components. These tests were to check for linearity, stability and gage factors and were performed on the low speed scanner. It was essential in this model study to ensure that all the inside gages were working properly prior to assembly, because once the bridge was assembled, there was no possible access to these gages. The bottom plate was then cemented to the webs, and the collapsible diaphragm

was inserted as shown in Plate 3.1. A final check was made on the strain gages and the top plate was then cemented to the webs. The cement used was a tape epoxy, 'Aerobond 3041' manufactured by Adhesive Engineering Company, San Carlos, California. The carrier of the epoxy was a Nylon cloth and the tape had a removeable protective polyethylene cover. The epoxy required a curing time of 2 hours at 160°F under a pressure of 15 psi. For a uniform application of the pressure, the model was placed in a wooden box between two flexible vinyl bags. An air pressure of 2.0 psi applied to the bags exerted a pressure of approximately 15 psi to the glued surfaces. The model under pressure was kept in a heated room for about 10 hours until its temperature reached 160°F and was then cured at this temperature for 2 hours. The temperature of the bridge model was slowly reduced to room temperature before removing the pressure.

The cut-back procedure for making Models 2 and 3 from Model 1 (Fig. 1.2 and Plate 3.2) was accomplished by cutting the assembled bridge on a lathe machine. The solid end diaphragms were inserted between the exterior webs and plates. These diaphragms were not cemented in position, but were fixed to the plates by means of 5-40 steel bolts placed at 1 in. centers and torqued to 20 in.-lb. and passing vertically right through the diaphragm and both plates. Bolts were also used at midspan; one running through each longitudinal web to safeguard against any local failure of the glue line due to any access pressure caused by tightening the collapsible diaphragm.

The original Model 1 which had a span of 60 in., was cut-back successively to spans of 45 in. (Model 2) and 30 in. (Model 3) as shown in Plate 3.2 and Fig. 1.2. This represented the minimum number of spans that could be used for studying general trends of behavior related to span length as a variable.

3.2 Instrumentation

Two types of bridge response measurements were made, namely deflections and strains. Deflections were measured by means of low voltage differential transformers (LVDT's) as shown in Plates 2.2 and 3.3. The LVDT's were linear within 0.18% with a range of ±0.75 in. For an excitation voltage of 6 volts, the output voltage of each LVDT was 6.052 volts/in. The digital voltmeter used could read in micro-volts, thus the deflections could be read accurately to 0.0001 in. The locations of LVDT's are shown in Chapter 5 for each bridge model.

Strains in the bridge were measured at Section 0-0, a radial section making an angle of 0.49° with the midspan axis as shown in Fig. 3.1. Section 0-0 was located far enough from the radial diaphragm to remove the effects of local strain concentrations due to holes at midspan. The strain gages used were 1/8 in. foil resistance gages, reference No. FCA 3-23, made by Tokyo Sokki Kenkyujo Co., Ltd., Japan. The gage locations are shown in Fig. 3.1. All the strain gages were 2-element crosses except for the four linear gages used on the overhangs of top plate. All the gages were oriented along tangential and radial directions as shown in Fig. 3.1.

Strains were directly punched on paper tape as well as being simultaneously typed on a telex typewriter. The equipment used was the slow-speed scanner, designed in the Division of Structural Engineering and Structural Mechanics at the University of California, Berkeley. It consisted of a portable computer, a digital voltmeter and three signal conditioners. Each signal conditioner had 64 channels and each channel could be used as a bridge circuit (see Plate 3.3).

The proving ring, load cells, low voltage differential transformers and strain gages were all connected to the digital voltmeter and portable

computer through the channels of signal conditioners. The channel requirements for the test program were as follows.

		No. of channels
1 No.	Proving ring	1
4 No.	Load cells	4
9 No.	Differential Transformers	9
68 No.	2-Element strain gages	136
4 No.	Linear strain gages	4
	Total	154

3.3 Testing Procedure

The test procedure was arranged to minimize errors due to drift in the instrumentation. The procedure adopted for each test was as follows:

(a) After arranging the bridge on its load cells, and with the loading in position, a careful linearity check was conducted on the model by observing a single deflection, a single reaction and a single strain gage for incremental values of applied load to the full range of loading to be used in the test. Any nonlinearity could have been due to slack in the supporting frame, friction in the loading system, or internal slip in the model. Once linearity was established, the test measurements were taken by the following procedure.

(b) An initial preload of 100 lbs. was applied to the model, and the resulting initial readings of loads, deflections and strains were stored in the scanner. Then as quickly as possible, the full load value was applied and the resulting load, reaction, deflection and strain differences were printed out, as well as punched on a paper tape. The time lag between the initial and final readings was less than one minute, and thus the drift was almost eliminated. Again

the load was taken down to the initial preload and the final values were stored and printed out as a further check against drift and yielding. Each bridge circuit remained closed only for a quarter of a second, virtually eliminating any heating problems in the strain gages. The laboratory itself was under constant temperature conditions.

The gage factors were adjusted such that the applied loading and reactions were printed directly in lbs. and deflections were printed in inches. The print out and punching sequence was as follows:

1. Applied load.
2. Reactions R1 through R4.
3. Deflections.
4. Longitudinal strain readings from left to right along levels A through F in sequence. (see Fig. 3.1)
5. Transverse strain readings from left to right along levels A through F in sequence.

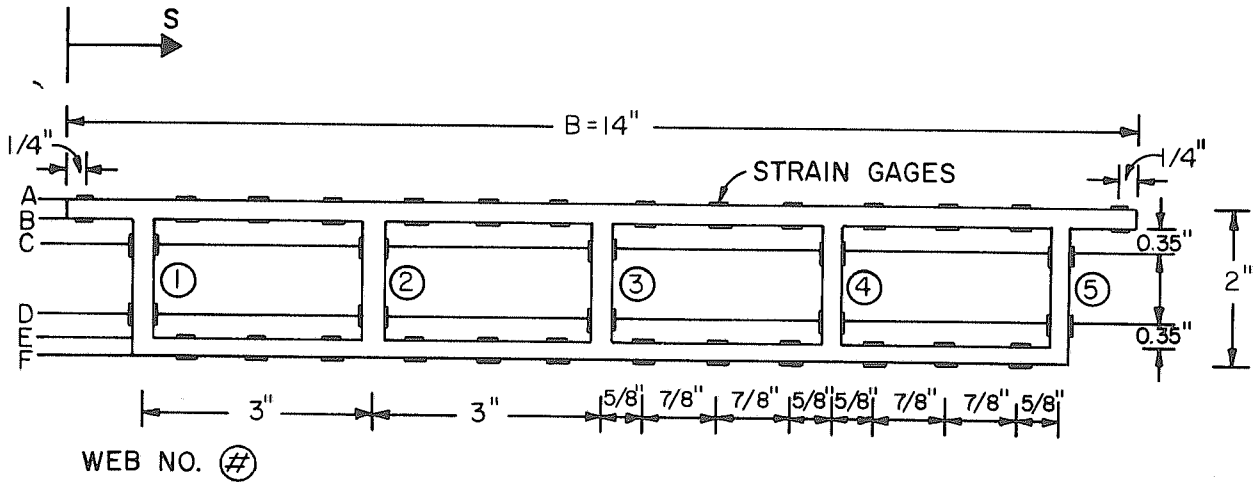

SECTION 0.0

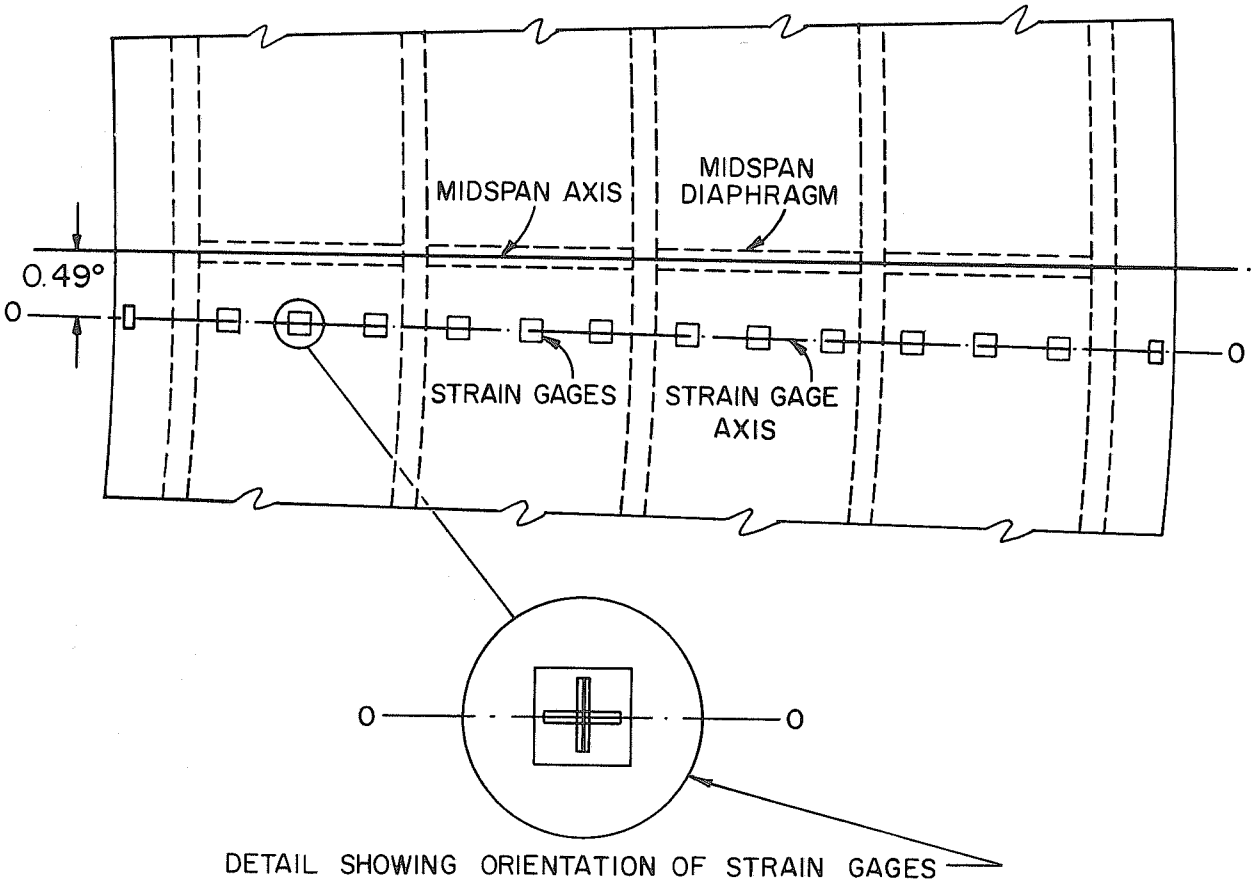

FIG. 3.1 LAYOUT OF STRAIN GAGES AT SECTION 0.0

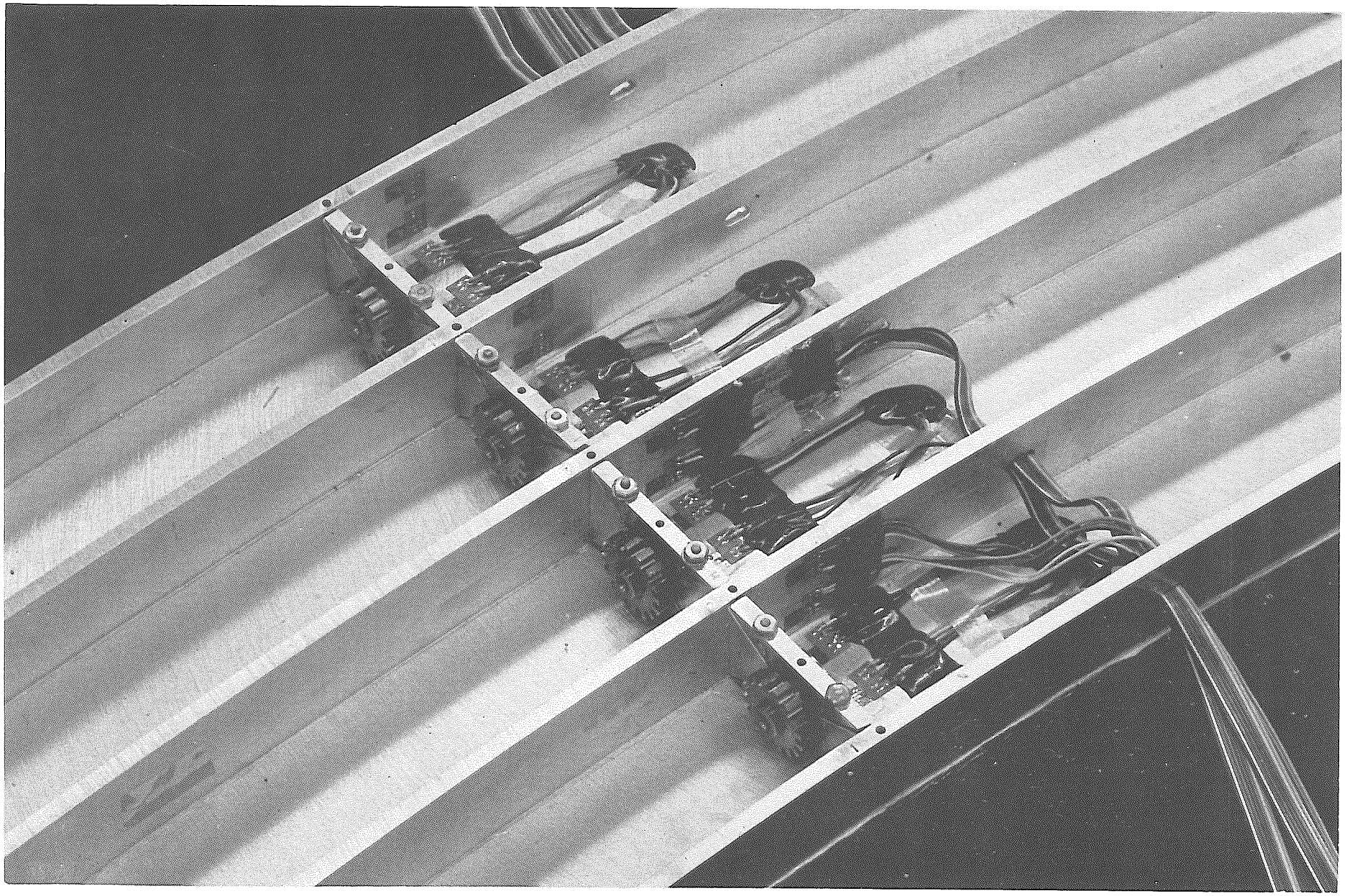

PLATE 3.1 MODEL WITHOUT TOP PLATE SHOWING COLLAPSIBLE DIAPHRAGM AND INSIDE GAGES

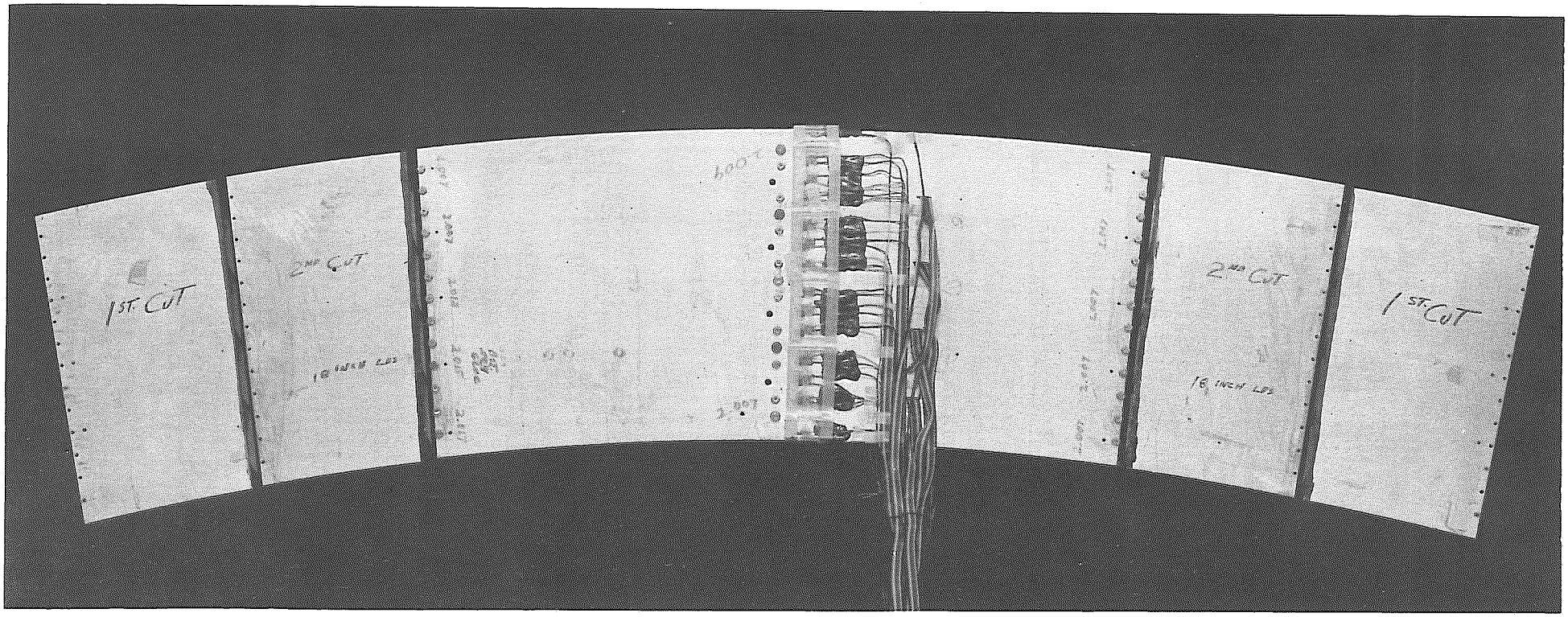

PLATE 3.2 ALUMINUM BOX-GIRDER BRIDGE MODEL SHOWING CUT-BACK PROCEDURE (COMPARE WITH FIG. I.2)

PLATE 3.3 TEST SET UP SHOWING TEST FRAME, MODEL AND SLOW SPEED SCANNER

4. DATA REDUCTION AND PRESENTATION

4.1 General

The reduced response data for each test are presented in Chapter 5 in both tabular and graphical form. The punched strain data on paper tape was reduced and plotted automatically by computer.

All data are given in dimensionless form and hence are applicable directly to any values of loading, elastic modulus and span of bridge provided the bridge is geometrically similar to one of those tested. It will be noted that where the size of the bridge appears in a response quantity, it does so as a single variable L which for convience is taken as the horizontal projection of central web of the model. This value also controls all other dimensions of the bridge which must be kept in proportion to it.

4.2 Static Checks

Three independent static checks were applied to all tests as follows:

(1) Vertical Forces:

The sum of the downward external forces divided by the sum of the upward external forces should equal unity. There were five such forces, the applied loading W and four boundary reactions R1 through R4 measured on load cells. Static check (1) is shown on the first page of computer output and the departure of the values from unity indicates only the experimental error in load and reaction measurements. The sources of error could be (a) friction in the linear motion bearings of loading system, (b) calibration of proving ring and load cells, (c) instrumentation errors.

(2) Horizontal Forces:

Stresses were calculated at strain gage locations, which were then integrated to get the total tensile force T and total compressive force C at Section 0-0. Stress distribution was assumed linear between any two adjacent strain gage locations. Since no horizontal external forces were being applied to the bridge, T and C should be equal. Static check (2) tabulates the value of T/C for each load position, and the departure of the resulting value from unity indicates the experimental error in strain measurements. The sources of error in this case could be (a) the gage factors of individual strain gages (b) instrumentation errors in recording the strains.

(3) Moments:

The internal moment at Section 0-0 was calculated by multiplying the average of T and C forces with the vertical distance between the locations of the resultants of T and C. The external moment at Section 0-0 was taken as the average of the 'left' and 'right' moment at Section 0-0 as computed from the applied load W and boundary reactions. The internal moment divided by the external moment should be unity and the departure of tabulated values from unity indicates the experimental error in relating external forces to internal strains. Accuracy of static check (3) not only depends upon the accurate measurement of applied load, reactions and strains but also on the E value of the material.

4.3 Reactions:

Values of R1 through R4 given as coefficients of the applied load W are tabulated for all load positions. Their accuracy is checked in static

checks (1) and (3). Symmetry checks for reactions are described later.

4.4 N_{xx} Forces in Top and Bottom Plates

The N_{xx} forces in the top and bottom plates are the tangential plate forces per unit width of the plate. In computing these values the calculated stresses from strain readings on the top and bottom surfaces of each plate were averaged and multiplied by thickness of the respective plate. The values of N_{xx} are given at each strain gage point, there being 14 such points in the top plate, and 12 in the bottom plate. The locations of strain gages are defined by the ratio S/B (see Fig. 3.1) which is the distance of the point from the edge of the top plate divided by the total width of the plate. The units of N_{xx} are force per unit width, and the values are tabulated and plotted as coefficients of W/L to make them dimensionless.

4.5 Radial Bending Moments

Radial bending moments at Section 0-0 in top and bottom plates and webs are plotted only for bridges without the midspan diaphragm, but values are tabulated for all bridges. The bending moments given are the moments per unit length of the bridge and are designated as M_{yy}. The units are in.-lb./in., hence tabulated values are given and plotted as coefficients of the applied load W.

The raidal plate bending moments were computed from strain gage readings. At all gaged points in both plates and webs, there were gages on both surfaces which made possible the calculation of curvature both in tangential and radial directions. M_{yy} was then computed by the following relationship.

$$M_{yy} = \frac{Et^3}{12(1-\nu)} \left(\partial^2 w/\partial \gamma^2 + \nu\, \partial^2 w/\partial \theta^2\right)$$

where

E = Young's Modulus

t = thickness of the plate or web

ν = Poisson's Ratio

$\partial^2 w/\partial \gamma^2$ = curvature in the radial direction

$\partial^2 w/\partial \theta^2$ = curvature in the tangential direction

In plotting the distribution of radial bending moments by computer, a linear variation of moment was assumed at Section 0-0 for the bridge models without midspan diaphragm. The extrapolated values at the intersection of center-lines of plates and webs were taken as linear extrapolations of the values at two adjacent gage points.

4.6 Deflections

The deflection values are given as coefficients of W/EL as the quantity $\Delta EL/W$ is dimensionless. The differential transformer positions for each bridge are given with load positions in Chapter 5. Symmetry and reciprocity checks for deflections are given in Chapter 6.

4.7 Total Bending Moment at Midspan, and Distribution between I-beams

The total bending moments on the radial section at midspan are expressed as coefficients of WL and were computed from applied load and external reactions. The moment in each case was taken as the average of the moments computed to the left and right of the section, the average being taken to reduce the effect of experimental error.

In computing the percentage of this total moment being taken by

each of the five I-beams that comprise the box-section (Fig. 7.1), the computation was done at Section 0-0 rather than at midspan, because it is Section 0-0 where the strain and stress distributions were known. Since Section 0-0 is close to midspan, hence errors due to this departure are small. The concept of considering a box-girder as a series of I-beams was suggested in the ASSHO Specifications [4]. In this report, the moment taken by each beam is expressed as a percentage of the total moment at the cross-section. In making this computation, the section was divided into five separate beams as shown in Fig. 7.1; the dividing line between each beam being midway between each web. The moment in each beam was then computed from the tangential force distribution data derived from the strain readings. One difficulty encountered in this calculation is that the value of compressive force C does not necessarily equal that of tensile force T in each individual beam. This is particularly true in case of outside beams where the top plate overhangs the web, and the lower plate does not. The procedure adopted was to find C and T individually for each beam, and the location of each resultant, then the internal moment in that beam was taken as the average of T and C times the distance between the locations of their resultants. In making this computation it was assumed that the stress varied linearly between gage points.

5. TEST RESULTS

5.1 General

The test results for all the curved box-girder models are presented in this chapter. All the results are given in tabular form and some selected and important data are also given in graphical form. The data has been presented in dimensionless form and can be used to determine the elastic response of bridges that are geometrically similar to those tested.

For each bridge, the first figure is a plan view of the model showing the load positions, differential transformer positions where deflections have been measured, and reaction points. Series B and series A models are with and without the midspan radial diaphragm respectively, and all three bridge models were tested in both configurations. The data are presented in the following sequence for each model.

5.2 Graphs

(a) N_{xx} Forces

An automatic Calcomp plot shows the radial distribution of tangential internal forces per unit width (N_{xx}) in the top and bottom plates at Section 0-0 for all the load positions. Load positions 1 through 5 are at midspan while 6 through 10 are at quarter span. These graphs show how the distribution of N_{xx} forces vary at Section 0-0 as the load is moved both across the bridge at midspan and also from midspan to quarter span. The sign convention for N_{xx} is tension positive and and compression negative.

(b) Radial Bending Moments

Following the N_{xx} graphs is a Calcomp plot of the radial distribution

of the radial plate bending moments per unit length (M_{yy}) at Section 0-0 in plates and webs. These bending moment diagrams are plotted for midspan load positions 1 through 5 only. Radial bending moments have not been plotted for series B models, because the presence of the midspan disphragm, reduces the moments to very small values as compared with series A values and hence are not critical in design.

5.3 Tabular Data

At the end of the graphical presentation, the response data and static checks have been given for all load positions. The experimental data for each model is given on four pages in the form of direct computer output. The sequence of the data is as follows:

Page 1:

(a) Three Static Checks

(1) Ratio of downward to upward external forces.

(2) Ratio of horizontal tension to compression forces at Section 0-0.

(3) Ratio of internal to external moments at Section 0-0.

(b) Reactions R1 through R4, expressed as coefficient of the applied load W. Positive reactions are upwards.

Page 2:

N_{xx} forces in top and bottom plates are tabulated as coefficients of W/L at all gage locations along Section 0-0. The locations of strain gages are defined by the ratio S/B (see Fig. 3.1). Tensile forces are positive.

Page 3:

Radial bending moments per unit length (M_{yy}) are tabulated as

coefficients of W in top and bottom plates as well as in webs at the strain gage locations at Section 0-0. The locations of strain gage points for top and bottom plates are specified by the ratio S/B. The locations of points on the webs is specified by web number and section level (see Fig. 3.1). Positive bending moments in plates are taken as those moments which produce compression on the upper surface. The bending moments in the webs are taken as positive if they produce compression on the side which is towards the center of curvature of the curved bridge.

Page 4:

(a) Deflections are tabulated as coefficients of W/EL at all deflection measurement locations. A downward deflection is positive.

(b) Total longitudinal bending moments at midspan are tabulated as coefficients of WL.

(c) The tangential bending moments in the individual I-beams that form the box-section are tabulated as a percentage of the total tangential bending moment in the complete section. This distribution is for Section 0-0 which is adjacent to midspan.

Test Results for Model 1A

Span = 60.0 inches

Radius of Curvature = 116.7 inches

Without midspan radial diaphragm

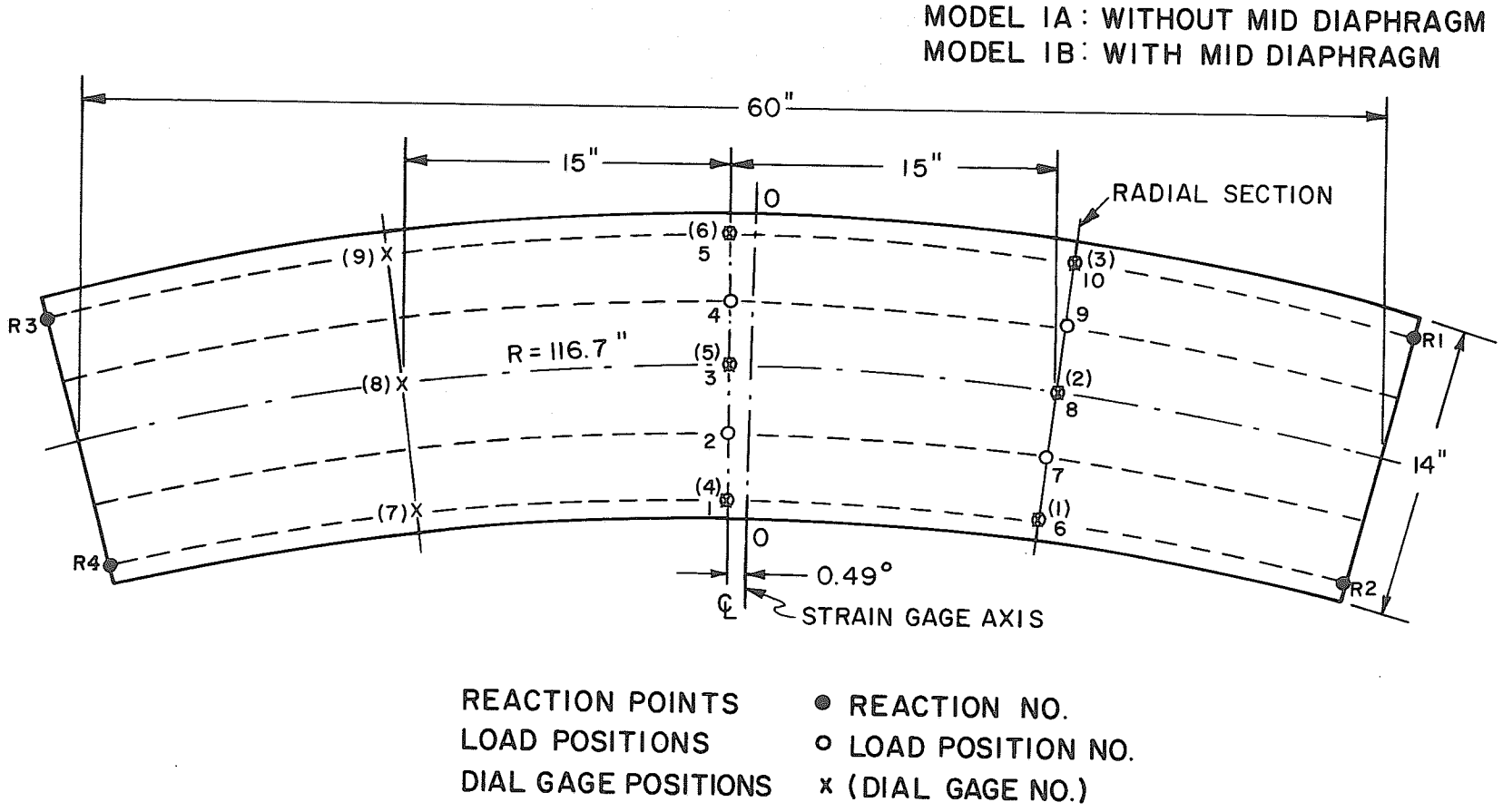

FIG. 5.1 CURVED BOX-GIRDER BRIDGE MODEL NO.1, SPAN = 60 INCHES
RADIUS OF CURVATURE = 116.7 INCHES

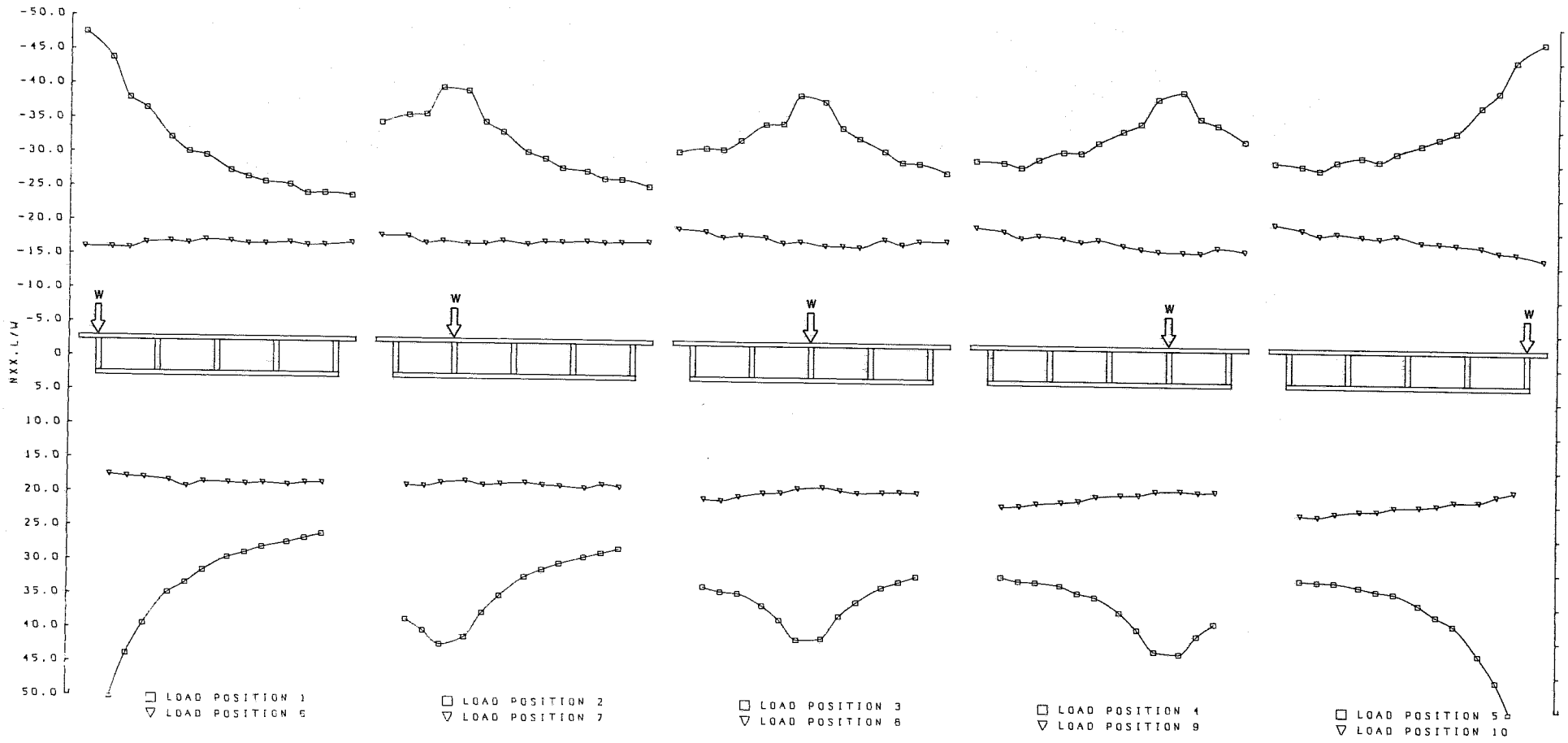

FIG.5.2 RADIAL DISTRIBUTION OF TANGENTIAL FORCES PER UNIT WIDTH IN TOP AND BOTTOM PLATES (NXX) AT SECTION 0-0
MODEL 1A

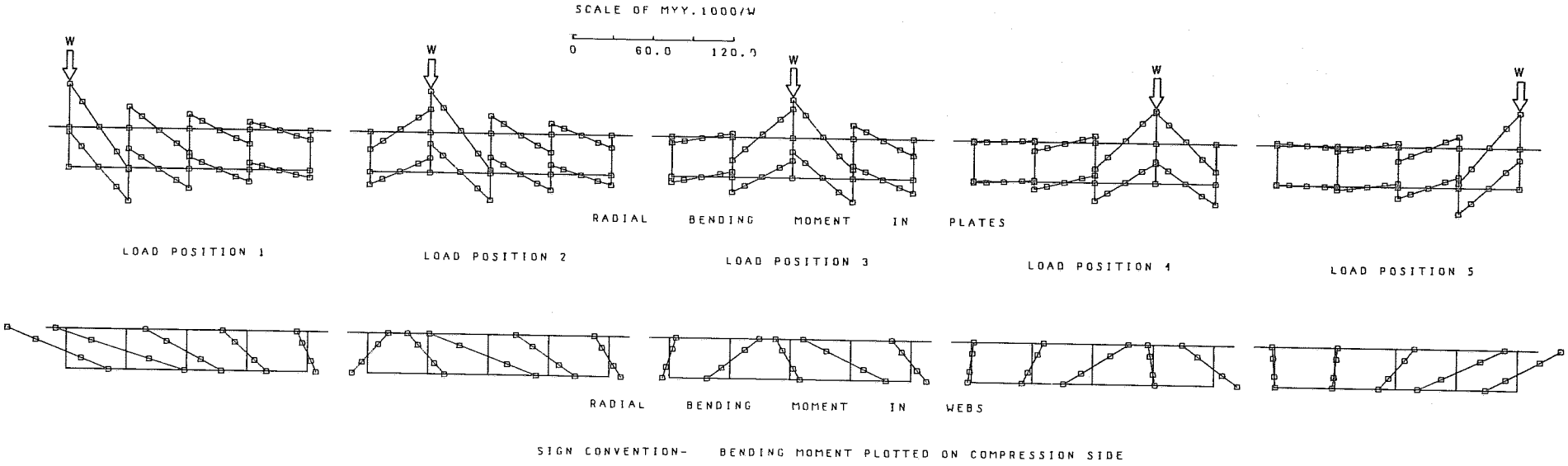

FIG.5.3 RADIAL DISTRIBUTION OF RADIAL BENDING MOMENT PER UNIT LENGTH (MYY) AT SECTION 0-0

MODEL 1A

MODEL NO 1A, SPAN =60.0 INCHES, RADIUS OF CURVATURE =116.7 INCHES, WITHOUT MID DIAPHRAGM

STATIC CHECKS-

(1) RATIO OF DOWNWARD TO UPWARD EXTERNAL FORCES
(2) RATIO OF HORIZONTAL TENSION TO COMPRESSION FORCE AT SECTION O-O
(3) RATIO OF INTERNAL TO EXTERNAL MOMENT AT SECTION O-O

	LOAD POSITION									
	1	2	3	4	5	6	7	8	9	10
(1)	.981	.995	.995	1.007	1.008	.971	.992	1.000	1.011	.999
(2)	1.034	1.022	1.025	1.016	1.011	1.078	1.028	1.034	1.031	1.033
(3)	.980	.994	.993	1.000	1.013	.944	.983	1.006	1.008	1.004

REACTIONS- COEFFICIENTS OF W

	LOAD POSITION									
	1	2	3	4	5	6	7	8	9	10
R1	.160	.292	.418	.547	.679	.151	.336	.522	.707	.893
R2	.350	.204	.080	-.049	-.190	.609	.408	.224	.034	-.152
R3	.165	.291	.419	.536	.672	.096	.163	.232	.296	.373
R4	.348	.216	.088	-.044	-.172	.175	.099	.023	-.047	-.117

MODEL NO 1A, SPAN =60.0 INCHES, RADIUS OF CURVATURE =116.7 INCHES, WITHOUT MID DIAPHRAGM

NXX FORCES- TANGENTIAL PLATE FORCES PER UNIT WIDTH AT SECTION O-O
COEFFICIENTS OF W/L

S/B	LOAD POSITION 1	2	3	4	5	6	7	8	9	10
					TOP PLATE					
.018	-47.51	-34.68	-30.74	-29.98	-30.11	-16.00	-18.04	-19.43	-20.20	-21.09
.116	-43.81	-35.80	-31.33	-29.76	-29.66	-15.95	-18.00	-19.09	-19.66	-20.33
.179	-37.99	-35.95	-31.18	-29.09	-29.09	-15.90	-16.99	-18.28	-18.71	-19.52
.241	-36.47	-39.85	-32.57	-30.28	-30.33	-16.71	-17.33	-18.62	-19.09	-19.85
.330	-32.19	-39.43	-34.94	-31.42	-31.04	-16.90	-16.95	-18.33	-18.71	-19.43
.393	-30.14	-34.85	-35.04	-31.33	-30.47	-16.66	-16.99	-17.52	-18.23	-19.19
.455	-29.61	-33.42	-39.23	-32.80	-31.71	-17.19	-17.42	-17.76	-18.57	-19.62
.545	-26.00	-30.47	-38.33	-34.52	-32.90	-17.00	-16.95	-17.18	-17.76	-18.66
.607	-26.23	-29.53	-34.51	-35.64	-33.85	-16.64	-17.35	-17.17	-17.29	-18.54
.670	-25.33	-28.18	-32.99	-39.28	-34.81	-16.67	-17.28	-17.00	-16.95	-18.33
.759	-26.38	-27.71	-31.14	-40.33	-38.57	-16.86	-17.43	-18.19	-16.85	-18.00
.821	-25.25	-26.61	-29.57	-36.47	-40.71	-16.47	-17.23	-17.47	-16.76	-17.28
.884	-24.24	-26.57	-29.42	-35.52	-45.24	-16.57	-17.33	-18.00	-17.52	-17.04
.982	-23.88	-25.53	-28.07	-33.15	-47.89	-16.89	-17.40	-18.04	-17.02	-16.13
					BOTTOM PLATE					
.116	50.82	38.43	33.16	31.15	31.23	17.55	18.71	20.24	20.85	21.61
.179	43.86	40.04	33.88	31.75	31.35	17.83	18.79	20.44	20.72	21.81
.241	39.39	42.05	34.08	31.87	31.43	17.95	18.27	19.84	20.28	21.29
.330	34.80	40.92	35.81	32.31	32.07	18.31	17.99	19.28	20.08	20.89
.393	33.36	37.30	37.90	33.40	32.64	19.20	18.55	19.20	19.84	20.85
.455	31.51	34.80	40.80	33.96	32.96	18.47	18.35	18.55	19.16	20.24
.545	29.58	32.03	40.60	36.13	34.57	18.59	18.19	18.35	18.91	20.16
.607	28.85	30.95	37.26	38.67	36.22	18.75	18.51	18.75	18.87	19.92
.670	28.01	30.06	35.21	41.85	37.54	18.59	18.63	19.11	18.31	19.36
.759	27.28	29.09	33.00	42.21	41.89	18.83	18.92	18.99	18.23	19.32
.821	26.64	28.45	32.11	39.56	45.75	18.51	18.35	18.91	18.43	18.47
.884	26.00	27.81	31.27	37.70	51.42	18.51	18.71	19.04	18.31	17.87

MODEL NO 1A. SPAN =60.0 INCHES, RADIUS OF CURVATURE =116.7 INCHES, WITHOUT MID DIAPHRAGM

MYY BENDING MOMENTS- RADIAL BENDING MOMENT PER UNIT LENGTH IN PLATES AND WEBS AT SECTION O-O
COEFFICIENTS OF W/1000

S/B	L O A D P O S I T I O N									
	1	2	3	4	5	6	7	8	9	10
					TOP PLATE					
.018	.00	-.00	-.00	.00	.00	-.00	-.00	-.00	-.00	0.
.116	19.13	-6.81	-3.14	-.79	.84	4.04	-.06	.03	.78	2.06
.179	.52	2.23	-.96	-.32	-.03	.06	.43	-.12	-.09	-.12
.241	-17.97	11.08	1.22	.40	-.90	-3.52	1.04	.14	-.67	-1.83
.330	8.78	18.66	-8.90	-4.42	-2.39	3.05	4.24	-.21	-.38	.58
.393	-1.31	1.62	2.73	-1.11	-.53	-.41	.20	.46	-.03	-.26
.455	-11.05	-15.36	13.72	2.47	1.33	-3.81	-3.38	1.07	.29	-1.05
.545	5.76	7.15	17.06	-10.62	-6.66	2.18	3.31	4.21	-.50	-.58
.607	-.90	-1.13	1.11	1.80	-1.24	-.30	-.54	.24	.13	-.42
.670	-6.63	-8.44	-13.00	14.85	4.33	-2.33	-3.17	-2.88	1.34	.26
.759	3.49	4.47	5.40	14.04	-15.24	.64	1.63	2.67	3.14	-.76
.821	-.04	-.50	-1.20	1.57	.61	-.18	-.23	-.21	.17	.08
.884	-4.16	-5.76	-7.62	-11.46	15.35	-1.17	-1.98	-3.03	-2.85	.70
.982	0.	0.	0.	-.00	-.00	-.00	-.00	-.00	.00	-.00
					BOTTOM PLATE					
.116	15.77	-5.35	-2.62	-.83	.41	3.16	-.11	-.11	.46	1.56
.179	.45	.52	-.21	-.27	-.07	.02	.10	-.04	-.06	-.00
.241	-14.20	6.63	2.35	.58	-.52	-2.58	.37	.27	-.67	-1.52
.330	8.29	12.90	-6.32	-3.31	-1.65	2.72	3.14	-.02	-.27	.60
.393	-.40	.68	.62	-.13	-.19	-.11	.19	.10	.06	-.09
.455	-8.67	-11.46	7.81	3.28	1.47	-2.77	-2.74	.52	.25	-.65
.545	5.17	6.77	11.61	-7.69	-5.01	1.74	2.70	2.91	-.33	-.31
.607	-.36	-.23	.54	.47	-.25	-.04	-.00	.04	.06	-.23
.670	-5.36	-7.05	-9.96	8.98	4.63	-1.83	-2.81	-2.56	.64	.10
.759	2.99	3.93	5.36	9.58	-11.33	.66	1.62	2.24	2.18	-.50
.821	-.25	-.36	-.42	.14	.35	-.17	-.08	-.17	-.04	-.06
.884	-3.29	-4.47	-6.09	-8.88	12.51	-.96	-1.69	-2.31	-2.10	.62
WEB NO/LEVEL					WEBS					
1/C	22.85	-8.04	-2.50	-.86	.77	3.77	-.32	-.18	1.04	2.23
1/D	-11.04	4.04	2.04	1.09	-.32	-2.05	.14	.36	-.73	-1.09
2/C	26.08	7.50	-11.22	-4.32	-1.14	6.18	2.82	-.41	.36	2.14
2/D	-17.08	-4.91	6.09	2.86	.63	-4.41	-2.32	-.05	-.59	-1.77
3/C	14.99	21.63	5.86	-13.45	-6.68	5.04	6.22	2.86	-.59	.68
3/D	-10.45	-14.18	-2.41	8.09	5.04	-3.36	-4.09	-1.86	.09	-.59
4/C	9.09	12.04	18.13	2.45	-18.04	2.77	4.68	5.36	1.95	-.77
4/D	-5.64	-7.96	-9.69	0.	10.96	-1.84	-2.84	-3.43	-1.22	1.82
5/C	3.81	5.41	6.95	11.99	-16.77	1.00	1.95	2.82	3.27	.18
5/D	-2.63	-3.50	-4.82	-6.59	8.18	-1.09	-1.14	-1.59	-1.73	.05

MODEL NO 1A, SPAN =60.0 INCHES, RADIUS OF CURVATURE =116.7 INCHES, WITHOUT MID DIAPHRAGM

DEFLECTIONS- LVDTP=LOW VOLTAGE DIFFERENTIAL TRANSFORMER POSITION
COEFFICIENTS OF 1000W/EL

	L O A D P O S I T I O N									
LVDTP	1	2	3	4	5	6	7	8	9	10
1	41.82	41.18	40.55	40.73	41.78	38.51	34.60	33.15	31.95	32.52
2	41.42	43.56	45.40	47.20	49.79	33.21	35.66	39.96	38.83	40.19
3	42.23	45.81	49.41	53.88	59.10	32.82	35.98	40.47	45.16	53.33
4	64.21	60.57	58.61	58.51	59.95	41.93	41.32	41.48	41.08	42.41
5	58.71	62.25	67.13	67.85	70.95	40.81	42.92	45.69	46.80	49.73
6	60.09	65.12	70.77	78.21	89.07	42.21	45.69	50.20	53.90	59.36
7	42.47	41.25	40.88	40.88	42.35	26.68	26.93	27.30	26.56	28.52
8	40.83	43.44	45.12	46.94	49.41	26.35	27.63	29.55	30.01	32.48
9	41.93	45.65	49.08	53.49	58.75	27.38	29.51	32.26	34.14	37.54

TOTAL LONGITUDINAL BENDING MOMENT AT MIDSPAN- COEFFICIENTS OF WL

L O A D P O S I T I O N									
1	2	3	4	5	6	7	8	9	10
.251	.253	.260	.263	.269	.132	.130	.132	.132	.138

DISTRIBUTION OF LONGITUDINAL MOMENT AT SECTION O-O BETWEEN I BEAMS- PERCENTAGE OF TOTAL MOMENT CARRIED BY EACH BEAM

	L O A D P O S I T I O N									
BEAM NO	1	2	3	4	5	6	7	8	9	10
1	23.9	17.8	15.0	14.0	13.5	15.2	16.3	16.9	17.3	17.3
2	24.8	27.4	22.7	20.4	19.5	22.6	22.3	23.0	23.6	23.7
3	20.3	22.2	26.2	22.4	20.7	23.1	22.4	21.9	22.4	22.9
4	18.7	19.6	22.0	26.5	24.2	23.0	22.8	22.3	21.5	21.9
5	12.3	13.0	14.0	16.6	22.1	16.0	16.0	15.8	15.2	14.3

Test Results for Model 1B

Span = 60.7 inches

Radius of Curvature = 116.7 inches

With midspan radial diaphragm

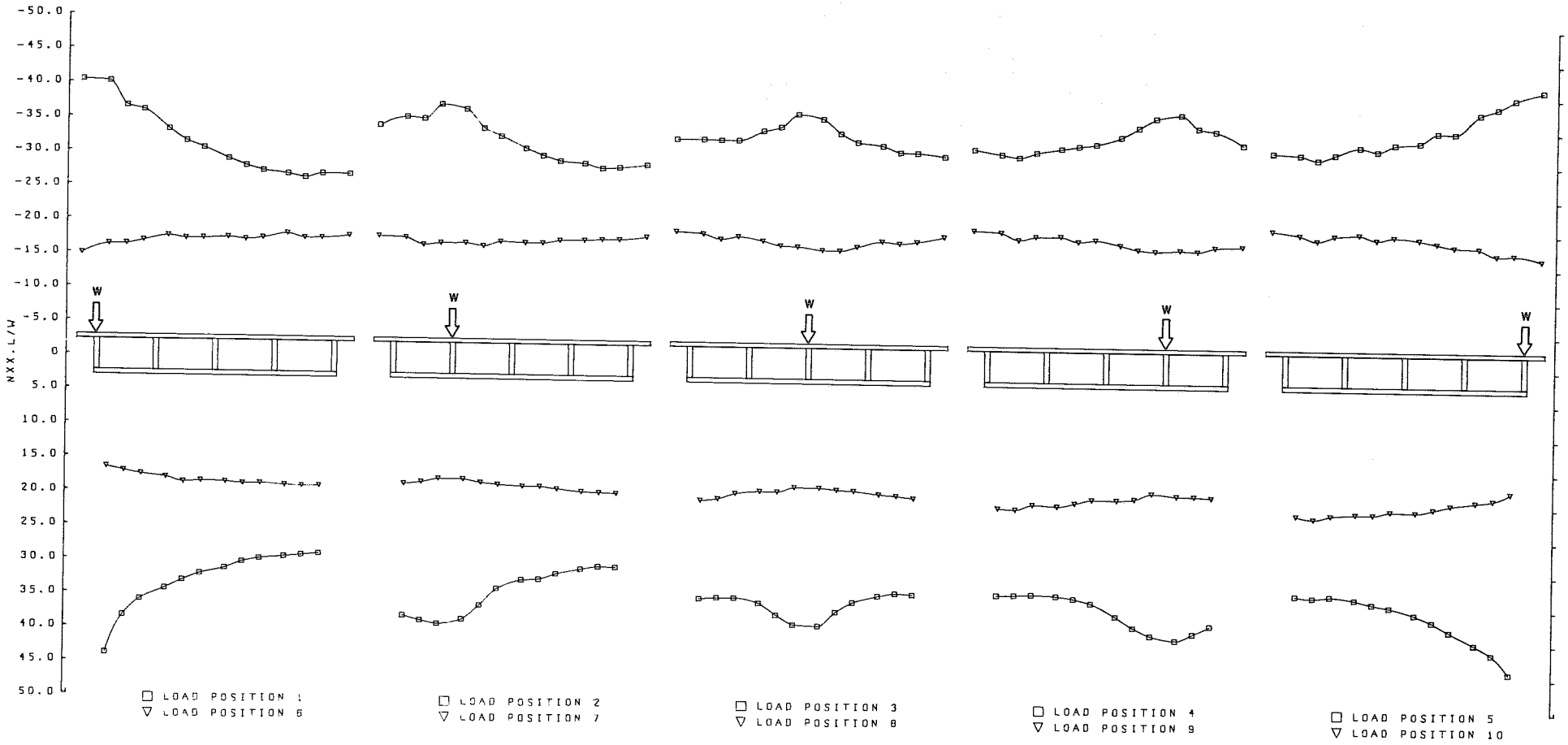

FIG.5.4 RADIAL DISTRIBUTION OF TANGENTIAL FORCES PER UNIT WIDTH IN TOP AND BOTTOM PLATES (NXX) AT SECTION 0-0
MODEL 1B

MODEL NO 18, SPAN =60.0 INCHES, RADIUS OF CURVATURE =116.7 INCHES, WITH MID DIAPHRAGM

STATIC CHECKS-

(1) RATIO OF DOWNWARD TO UPWARD EXTERNAL FORCES
(2) RATIO OF HORIZONTAL TENSION TO COMPRESSION FORCE AT SECTION O-O
(3) RATIO OF INTERNAL TO EXTERNAL MOMENT AT SECTION O-O

	LOAD POSITION									
	1	2	3	4	5	6	7	8	9	10
(1)	.994	.985	.990	1.002	1.016	.982	.992	.999	.998	.998
(2)	1.000	1.011	1.017	1.028	1.001	1.023	1.025	1.026	1.021	1.023
(3)	1.000	.981	.986	.993	1.016	.974	.984	.998	.999	.999

REACTIONS- COEFFICIENTS OF W

	LOAD POSITION									
	1	2	3	4	5	6	7	8	9	10
R1	.160	.292	.424	.550	.679	.151	.340	.519	.704	.896
R2	.342	.213	.080	-.052	-.192	.606	.414	.221	.040	-.149
R3	.160	.291	.421	.544	.672	.091	.160	.232	.299	.371
R4	.342	.222	.091	-.044	-.178	.172	.096	.029	-.044	-.114

MODEL NO 1B, SPAN =60.0 INCHES, RADIUS OF CURVATURE =116.7 INCHES, WITH MID DIAPHRAGM

NXX FORCES- TANGENTIAL PLATE FORCES PER UNIT WIDTH AT SECTION O-O
COEFFICIENTS OF W/L

S/B	LOAD POSITION 1	2	3	4	5	6	7	8	9	10
					TOP PLATE					
.018	-40.42	-34.26	-32.78	-31.82	-31.83	-14.86	-17.91	-19.18	-19.94	-20.45
.116	-40.18	-35.51	-32.81	-31.13	-31.60	-16.28	-17.76	-18.90	-19.71	-19.90
.179	-36.65	-35.28	-32.73	-30.77	-30.93	-16.33	-16.71	-18.14	-18.66	-19.09
.241	-36.05	-37.43	-32.71	-31.48	-31.77	-16.85	-17.04	-18.57	-19.19	-19.85
.330	-33.24	-36.71	-34.14	-32.11	-32.88	-17.57	-17.04	-17.95	-19.23	-20.09
.393	-31.55	-33.95	-34.75	-32.52	-32.32	-17.23	-16.61	-17.28	-18.52	-19.33
.455	-30.57	-32.82	-36.67	-32.85	-33.34	-17.28	-17.33	-17.18	-18.81	-19.81
.545	-29.02	-31.07	-36.00	-33.95	-33.61	-17.47	-17.19	-16.71	-18.09	-19.43
.607	-28.05	-30.05	-33.90	-35.34	-35.13	-17.17	-17.19	-16.68	-17.44	-18.89
.670	-27.36	-29.28	-32.66	-36.75	-35.03	-17.43	-17.62	-17.28	-17.23	-18.38
.759	-26.92	-28.95	-32.18	-37.29	-37.87	-18.09	-17.71	-18.14	-17.42	-18.23
.821	-26.43	-28.29	-31.22	-35.34	-38.74	-17.47	-17.80	-17.85	-17.28	-17.19
.884	-27.01	-28.43	-31.16	-34.92	-40.08	-17.52	-17.85	-18.14	-17.90	-17.28
.982	-26.94	-28.85	-30.69	-32.95	-41.29	-17.91	-18.29	-18.92	-18.04	-16.51
					BOTTOM PLATE					
.116	43.85	37.86	34.78	33.60	33.11	16.50	18.47	20.28	20.77	21.29
.179	38.29	38.55	34.56	33.54	33.36	17.06	18.19	20.00	20.93	21.73
.241	35.91	38.99	34.56	33.43	33.09	17.55	17.67	19.20	20.16	21.17
.330	34.27	38.30	35.29	33.60	33.53	17.95	17.71	18.83	20.36	20.93
.393	33.05	36.22	36.98	33.96	34.15	18.63	18.19	18.87	19.88	20.93
.455	32.07	33.76	38.38	34.61	34.57	18.43	18.43	18.19	19.32	20.44
.545	31.24	32.41	38.54	36.45	35.57	18.55	18.63	18.23	19.36	20.53
.607	30.26	32.26	36.45	38.06	36.62	18.76	18.63	18.47	19.15	20.04
.670	29.74	31.45	34.96	39.25	38.02	18.71	18.95	18.59	18.31	19.44
.759	29.41	30.73	34.00	39.86	39.84	18.92	19.32	19.03	18.67	18.96
.821	29.14	30.33	33.57	38.88	41.30	19.00	19.40	19.24	18.71	18.63
.884	28.90	30.40	33.73	37.68	44.10	18.95	19.48	19.56	18.83	17.59

MODEL NO 1B, SPAN =60.0 INCHES, RADIUS OF CURVATURE =116.7 INCHES, WITH MID DIAPHRAGM

MYY BENDING MOMENTS- RADIAL BENDING MOMENT PER UNIT LENGTH IN PLATES AND WEBS AT SECTION C-C
COEFFICIENTS OF W/1000

S/B	L C A D P O S I T I O N									
	1	2	3	4	5	6	7	8	9	10
						TOP PLATE				
.018	.00	0.	.00	.00	.00	.00	.00	-.00	-.00	.00
.116	4.36	-1.21	-.46	.10	.55	1.11	.09	.05	.14	.49
.179	1.09	.75	-.27	-.27	-.10	-.09	-.02	-.23	-.18	-.16
.241	-3.99	3.92	-.02	-.16	-.31	-.80	.63	.14	-.19	-.33
.330	3.17	8.55	-3.16	-1.29	-.43	1.13	1.64	-.12	-.18	.03
.393	-.32	.71	.69	-.50	-.23	-.07	.16	.05	-.09	-.04
.455	-4.72	-7.13	5.54	.62	.24	-1.48	-1.19	.51	.23	-.32
.545	1.35	2.13	6.85	-3.30	-1.64	.54	.89	1.38	-.14	-.32
.607	-.14	-.50	.39	.56	-.75	-.20	.04	.14	-.05	-.23
.670	-1.43	-2.47	-4.26	5.12	.62	-.45	-.73	-.61	.77	.35
.759	.47	1.03	1.11	5.34	-4.27	-.00	.24	.68	1.22	-.37
.821	.00	.06	-.04	.78	-.25	-.09	-.00	-.16	.12	-.09
.884	-.80	-1.39	-2.13	-3.77	3.59	-.21	-.51	-.75	-.77	.33
.942	.00	.00	.00	-.00	.00	-.00	-.00	-.00	-.00	-.00
						BOTTOM PLATE				
.116	3.84	-1.16	-.46	.05	.45	.95	-.09	-.08	.15	.44
.179	.53	.42	-.28	-.10	.01	-.05	-.00	-.09	-.05	.05
.241	-3.54	2.11	.57	.24	.05	-.65	.39	.19	-.06	-.28
.330	2.69	5.63	-1.98	-.92	-.30	.85	.95	-.05	-.13	.05
.393	-.16	.87	.56	-.30	-.16	.01	.17	.09	.02	-.00
.455	-3.29	-4.85	3.12	1.05	.53	-1.00	-.92	.30	.25	-.15
.545	1.39	1.97	4.15	-2.15	-1.22	.49	.81	.91	-.04	-.20
.607	.13	-.05	.55	.70	-.63	.05	.09	.21	-.05	-.08
.670	-1.24	-2.09	-3.13	3.10	1.13	-.44	-.69	-.70	.31	.19
.759	.68	1.02	1.31	3.19	-3.28	.05	.30	.53	.72	-.26
.821	.16	.06	-.04	.52	-.28	-.13	-.03	-.00	.01	-.06
.884	-.63	-1.12	-1.73	-2.91	3.61	-.19	-.37	-.67	-.65	.34
WEB NO/LEVEL						WEBS				
1/C	5.26	-1.99	-.68	-.14	.38	.90	-.05	-.03	.20	.45
1/D	-3.08	1.42	.46	.05	-.11	-.60	.04	.05	-.08	-.38
2/C	6.83	2.56	-2.90	-1.13	-.10	1.66	.75	-.29	.11	.61
2/D	-5.15	-1.70	2.11	.87	-.04	-1.09	-.56	.10	-.08	-.55
3/C	3.65	5.62	.90	-3.26	-1.25	1.19	1.28	.29	-.14	.11
3/D	-2.75	-4.24	-.60	2.51	.91	-.78	-.87	-.27	.15	-.16
4/C	1.89	3.00	4.76	.26	-4.18	.72	1.16	1.36	.42	-.18
4/D	.08	.10	-.00	.01	.07	.03	.07	.05	.05	.05
5/C	.79	1.36	1.88	3.23	-5.00	.31	.52	.74	.79	-.14
5/D	-.79	-1.05	-1.34	-2.18	2.09	-.26	-.42	-.50	-.53	.03

MODEL NO 18, SPAN =60.0 INCHES, RADIUS OF CURVATURE =116.7 INCHES, WITH MID DIAPHRAGM

DEFLECTIONS- LVDTP=LOW VOLTAGE DIFFERENTIAL TRANSFORMER POSITION
COEFFICIENTS OF 1000W/EL

	LOAD POSITION									
LVDTP	1	2	3	4	5	6	7	8	9	10
1	41.25	41.00	40.88	41.25	41.98	37.94	34.64	32.93	32.93	32.68
2	41.00	43.33	45.78	47.61	50.18	33.29	35.62	39.66	39.41	40.27
3	42.35	45.66	49.94	54.22	59.49	33.05	35.99	40.15	45.53	52.39
4	62.42	60.83	59.36	59.24	60.96	41.98	41.13	41.25	41.49	42.35
5	59.12	61.93	66.34	68.42	71.73	41.00	42.96	45.29	47.37	49.69
6	60.59	65.36	71.85	79.07	87.39	42.60	45.90	50.06	54.47	59.36
7	40.88	41.00	41.13	40.88	41.62	26.93	27.05	26.93	26.68	25.70
8	40.64	43.08	45.53	47.37	49.94	26.68	27.66	29.25	30.72	24.97
9	41.62	45.53	49.69	53.98	59.12	27.54	29.62	32.07	34.64	37.33

TOTAL LONGITUDINAL BENDING MOMENT AT MIDSPAN- COEFFICIENTS OF WL

LOAD POSITION									
1	2	3	4	5	6	7	8	9	10
.246	.256	.263	.265	.267	.129	.130	.132	.135	.139

DISTRIBUTION OF LONGITUDINAL MOMENT AT SECTION O-O BETWEEN I BEAMS- PERCENTAGE OF TOTAL MOMENT CARRIED BY EACH BEAM

	LOAD POSITION									
BEAM NO	1	2	3	4	5	6	7	8	9	10
1	21.3	17.6	15.6	14.7	14.2	14.6	16.0	16.9	17.1	16.9
2	24.2	25.8	22.5	21.1	20.6	22.4	21.9	22.8	23.5	23.8
3	21.2	22.0	24.7	22.4	21.6	23.0	22.4	21.5	22.5	23.2
4	19.7	20.4	22.0	25.0	23.8	23.4	23.1	22.3	21.4	21.8
5	13.6	14.1	15.0	16.7	19.7	16.6	16.7	16.4	15.5	14.3

Test Results for Model 2A

Span = 45.0 inches

Radius of Curvature = 116.7 inches

Without midspan radial diaphragm

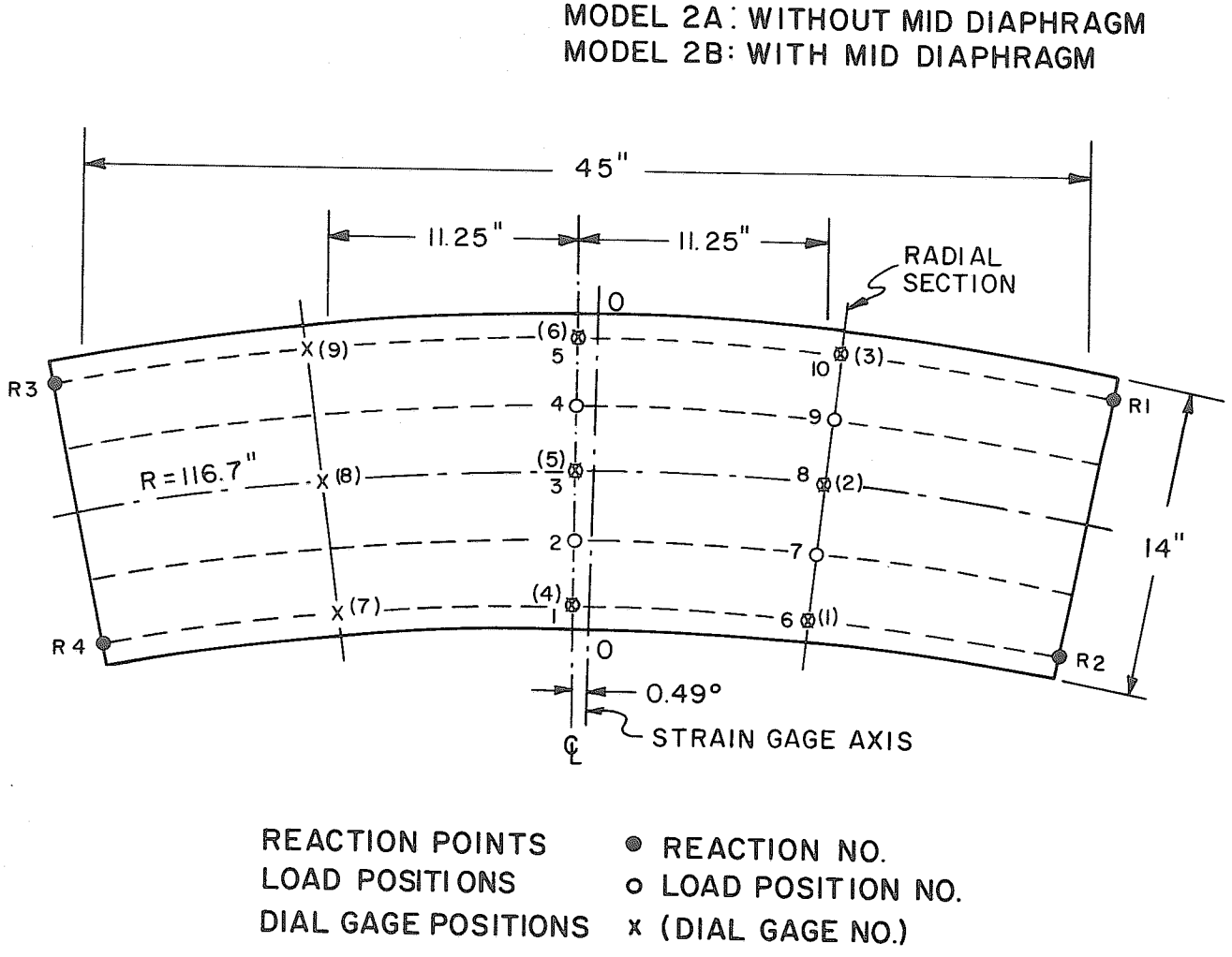

FIG. 5.5 CURVED BOX-GIRDER BRIDGE MODEL NO. 2, SPAN = 45 INCHES
RADIUS OF CURVATURE = 116.7 INCHES

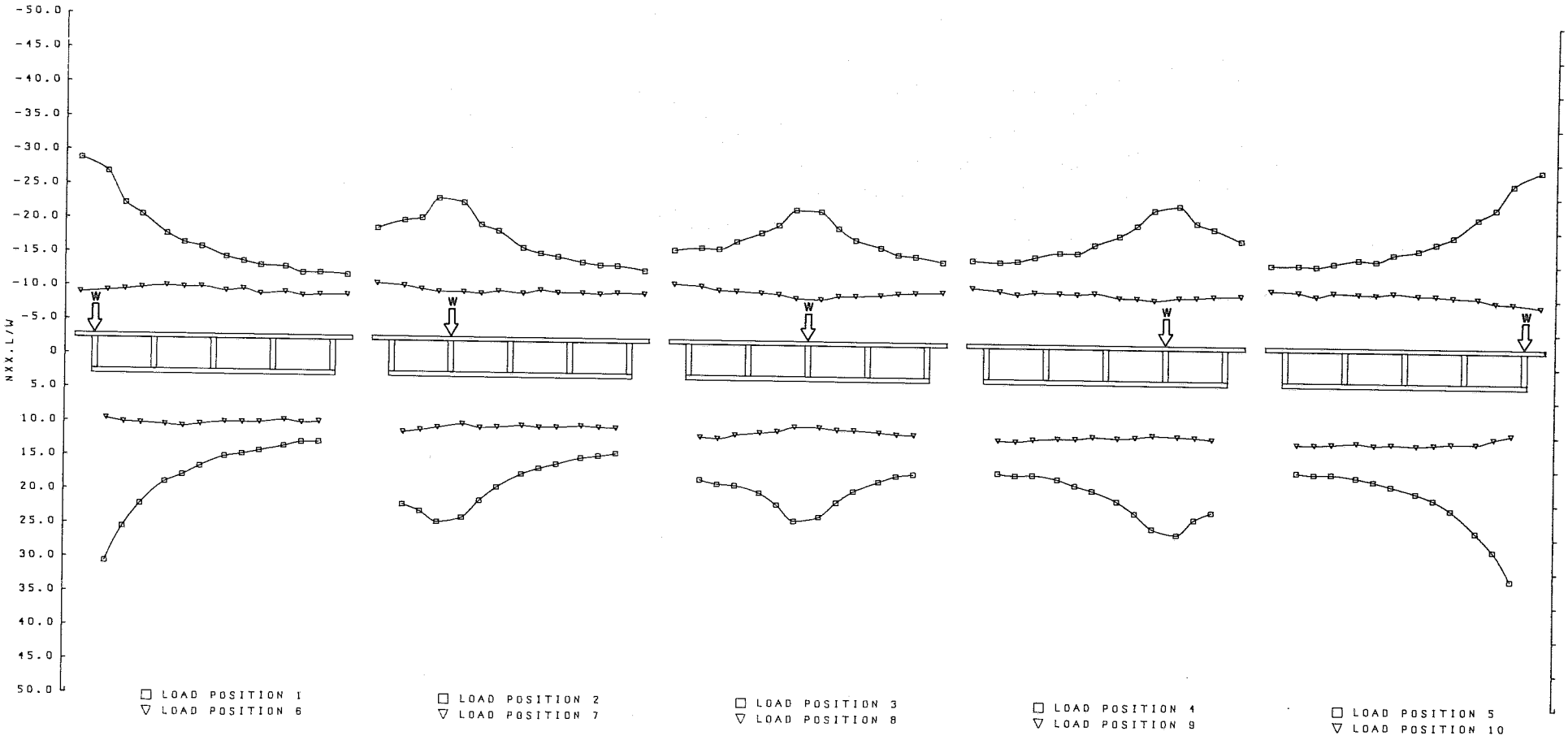

FIG.5.6 RADIAL DISTRIBUTION OF TANGENTIAL FORCES PER UNIT WIDTH IN TOP AND BOTTOM PLATES (NXX) AT SECTION 0-0
MODEL 2A

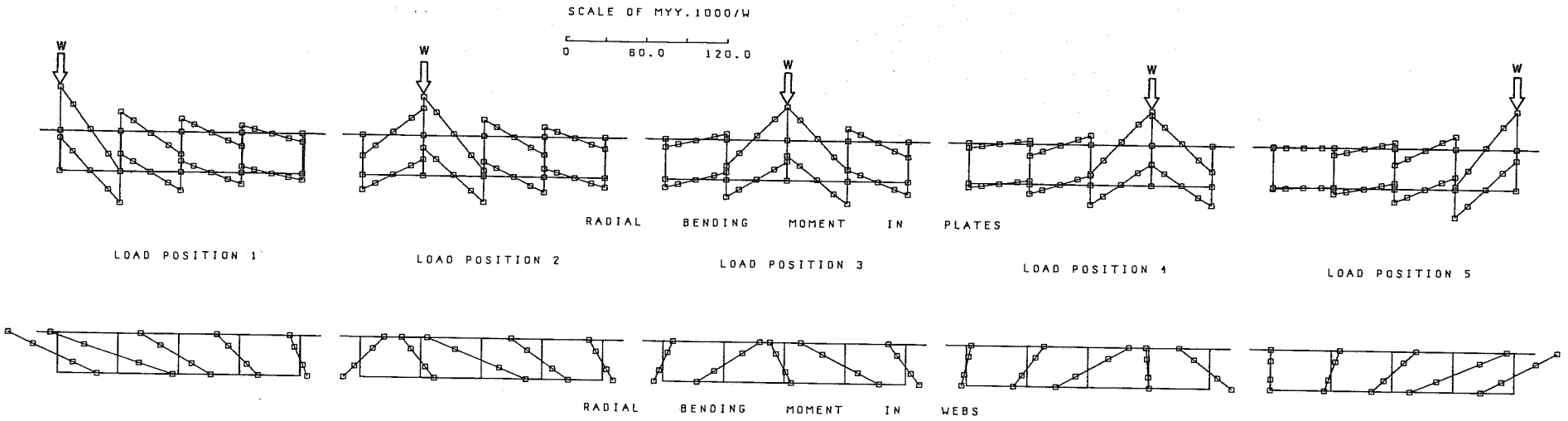

FIG.5.7 RADIAL DISTRIBUTION OF RADIAL BENDING MOMENT PER UNIT LENGTH (MYY) AT SECTION 0-0

MODEL 2A

MODEL NO 2A, SPAN =45.0 INCHES, RADIUS OF CURVATURE =116.7 INCHES, WITHOUT MID DIAPHRAGM

STATIC CHECKS-

(1) RATIO OF DOWNWARD TO UPWARD EXTERNAL FORCES
(2) RATIO OF HORIZONTAL TENSION TO COMPRESSION FORCE AT SECTION O-O
(3) RATIO OF INTERNAL TO EXTERNAL MOMENT AT SECTION O-O

	LOAD POSITION									
	1	2	3	4	5	6	7	8	9	10
(1)	.993	.992	.985	.988	.998	.990	.981	.989	.984	.990
(2)	1.000	1.021	1.027	1.020	1.011	1.039	1.027	1.029	1.023	1.021
(3)	.987	.983	.977	.980	.993	.974	.963	.975	.967	.969

REACTIONS- COEFFICIENTS OF W

	LOAD POSITION									
	1	2	3	4	5	6	7	8	9	10
R1	.099	.223	.350	.484	.611	.108	.283	.462	.650	.828
R2	.400	.278	.153	.020	-.108	.639	.469	.290	.105	-.068
R3	.080	.208	.328	.453	.573	.032	.107	.179	.251	.320
R4	.427	.298	.181	.053	-.076	.228	.158	.079	.006	-.067

MODEL NO 2A, SPAN =45.0 INCHES, RADIUS OF CURVATURE =116.7 INCHES, WITHOUT MID DIAPHRAGM

NXX FORCES- TANGENTIAL PLATE FORCES PER UNIT WIDTH AT SECTION O-O
COEFFICIENTS OF W/L

S/B	LOAD POSITION									
	1	2	3	4	5	6	7	8	9	10
					TOP PLATE					
.018	-28.77	-18.86	-16.10	-15.15	-14.86	-8.95	-10.67	-11.05	-11.05	-11.15
.116	-26.82	-20.10	-16.50	-14.92	-14.89	-9.28	-10.39	-10.78	-10.64	-10.96
.179	-22.21	-20.46	-16.35	-15.10	-14.78	-9.46	-9.92	-10.25	-10.21	-10.39
.241	-20.57	-23.36	-17.46	-15.75	-15.25	-9.75	-9.57	-10.14	-10.53	-10.96
.330	-17.75	-22.75	-18.82	-16.42	-15.85	-10.03	-9.53	-9.92	-10.43	-10.78
.393	-16.46	-19.53	-19.96	-16.39	-15.64	-9.86	-9.35	-9.74	-10.32	-10.71
.455	-15.85	-18.64	-22.25	-17.64	-16.64	-9.93	-9.75	-9.17	-10.53	-11.00
.545	-14.39	-16.14	-22.03	-19.00	-17.25	-9.36	-9.42	-9.07	-9.89	-10.68
.607	-13.75	-15.35	-19.57	-20.53	-18.25	-9.64	-9.93	-9.60	-9.82	-10.61
.670	-13.17	-14.89	-17.89	-22.82	-19.25	-8.96	-9.60	-9.64	-9.57	-10.43
.759	-13.00	-14.10	-16.78	-23.46	-21.96	-9.25	-9.57	-9.78	-9.96	-10.25
.821	-12.14	-13.71	-15.78	-20.96	-23.43	-8.78	-9.43	-10.07	-10.00	-9.64
.884	-12.17	-13.64	-15.53	-20.10	-26.93	-8.93	-9.64	-10.18	-10.21	-9.53
.982	-11.91	-12.96	-14.77	-18.39	-28.96	-8.95	-9.53	-10.29	-10.29	-9.05
					BOTTOM PLATE					
.116	30.60	21.79	17.66	16.15	15.54	9.63	11.17	11.38	11.32	11.44
.179	25.50	22.76	18.26	16.42	15.79	10.14	10.83	11.56	11.44	11.44
.241	22.12	24.36	18.44	16.33	15.72	10.26	10.44	11.02	11.11	11.32
.330	18.86	23.66	19.53	16.93	16.21	10.47	9.93	10.65	10.96	11.08
.393	17.81	21.16	21.22	17.84	16.72	10.69	10.44	10.44	10.96	11.41
.455	16.51	19.16	23.60	18.56	17.41	10.35	10.32	9.75	10.62	11.26
.545	15.06	17.17	22.97	20.04	18.41	10.02	10.08	9.81	10.80	11.41
.607	14.67	16.30	20.79	21.79	19.35	10.05	10.29	10.14	10.62	11.26
.670	14.15	15.66	19.10	24.05	20.83	10.02	10.23	10.17	10.32	11.05
.759	13.43	14.73	17.66	24.90	24.11	9.63	10.05	10.41	10.47	11.08
.821	12.80	14.43	16.78	22.67	26.83	10.02	10.20	10.68	10.59	10.32
.884	12.77	14.00	16.48	21.55	31.09	9.84	10.26	10.74	10.83	9.75

MODEL NO 2A, SPAN =45.0 INCHES, RADIUS OF CURVATURE =116.7 INCHES, WITHOUT MID DIAPHRAGM

MYY BENDING MOMENTS- RADIAL BENDING MOMENT PER UNIT LENGTH IN PLATES AND WEBS AT SECTION O-O
COEFFICIENTS OF W/1000

S/B	L C A C P O S I T I O N									
	1	2	3	4	5	6	7	8	9	10
						TOP PLATE				
.018	-.00	.00	-.00	.00	-.00	.00	-.00	.00	.00	.00
.116	19.33	-8.11	-3.96	-2.21	-.44	5.81	-1.72	-1.92	-.64	.61
.179	.99	2.47	-1.11	-.44	-.35	.09	.52	-.38	-.35	-.15
.241	-17.16	12.73	2.12	1.25	-.15	-4.97	2.91	1.57	.43	-.96
.330	7.88	17.24	-10.03	-5.53	-3.26	4.21	6.02	-2.09	-2.27	-.93
.393	-1.31	1.36	3.17	-.90	-.41	-.47	.46	.78	-.15	-.23
.455	-10.24	-14.43	15.67	3.66	2.32	-5.06	-4.86	3.63	2.06	.41
.545	5.49	6.74	15.09	-11.52	-7.42	2.85	4.19	5.58	-2.53	-2.65
.607	-.56	-.76	1.51	2.58	-1.08	-.41	-.29	.67	.61	-.26
.670	-6.14	-8.11	-11.84	15.61	4.97	-3.23	-4.28	-3.72	3.89	2.27
.759	2.85	3.92	4.88	13.52	-15.79	1.02	2.09	3.08	4.16	-3.35
.821	-.53	-.58	-.99	1.54	1.04	-.35	-.41	-.41	.35	.23
.884	-3.87	-5.18	-7.07	-10.50	16.69	-1.69	-2.79	-3.64	-3.20	3.52
.982	-.00	-.00	-.00	.00	-.00	.00	.00	-.00	-.00	.00
						BOTTOM PLATE				
.116	14.55	-6.15	-3.64	-1.73	-.56	4.63	-1.29	-1.52	-.65	.60
.179	.35	.54	-.27	-.13	-.06	.12	.23	.06	-.06	-.02
.241	-13.41	7.33	3.18	1.43	.31	-3.99	1.62	1.43	.50	-.56
.330	7.50	12.34	-7.17	-4.18	-2.52	3.68	4.34	-1.64	-1.89	-.81
.393	-.17	.72	.48	-.15	-.25	-.13	.33	.25	-.11	-.04
.455	-8.05	-10.87	8.31	4.18	2.35	-3.80	-3.70	2.10	1.91	.60
.545	4.72	6.21	11.08	-8.32	-5.78	2.41	3.32	3.64	-2.04	-2.04
.607	-.17	-.21	.72	.62	-.19	-.15	.02	.17	.17	-.19
.670	-4.97	-6.63	-9.42	9.58	5.24	-2.62	-3.51	-3.18	2.29	1.87
.759	2.68	3.57	4.80	9.20	-11.87	1.18	1.97	2.60	2.76	-2.56
.821	-.29	-.29	-.25	.27	.43	-.13	-.13	-.04	.06	.12
.884	-2.89	-4.24	-5.57	-8.23	12.88	-1.21	-2.04	-2.83	-2.31	2.76
WEB NO/LEVEL						WEBS				
1/C	18.13	-9.45	-3.59	-1.82	-.18	5.68	-1.77	-1.41	-.50	.77
1/D	-11.54	4.18	2.72	1.36	.05	-3.00	.77	1.68	.45	-.73
2/C	24.90	7.32	-13.63	-6.18	-3.18	8.99	2.95	-3.68	-2.77	-.23
2/D	-15.86	-3.50	7.04	3.95	2.00	-5.91	-2.04	1.86	1.45	.18
3/C	13.54	19.72	6.36	-15.17	-8.59	6.68	8.31	1.95	-4.45	-2.77
3/D	-9.77	-13.22	-.86	8.99	5.95	-4.63	-5.45	-1.36	2.23	1.91
4/C	8.18	11.08	16.76	1.36	-19.76	4.09	5.86	6.63	.50	-5.09
4/D	-5.73	-8.00	-9.45	.23	12.36	-1.93	-2.89	-3.62	-1.35	1.87
5/C	3.68	4.95	6.41	11.54	-15.86	1.50	2.82	3.54	3.41	-2.95
5/D	-2.18	-3.18	-4.09	-6.00	9.32	-1.04	-1.68	-2.18	-1.82	1.64

MODEL NO 2A, SPAN =45.0 INCHES, RADIUS OF CURVATURE =116.7 INCHES, WITHOUT MID DIAPHRAGM

DEFLECTIONS- LVDTP=LOW VOLTAGE DIFFERENTIAL TRANSFORMER POSITION
COEFFICIENTS OF 1000W/EL

	LOAD POSITION									
LVDTP	1	2	3	4	5	6	7	8	9	10
1	14.29	13.23	12.16	11.68	11.56	14.38	11.38	9.68	8.95	8.54
2	12.44	13.50	14.53	14.90	15.35	9.84	11.32	13.56	12.39	12.18
3	11.65	13.18	15.15	17.55	20.19	8.52	10.04	11.95	14.82	19.35
4	22.59	19.49	17.73	17.00	16.85	14.38	13.42	12.50	11.98	11.91
5	17.58	19.32	22.05	21.51	21.90	12.29	13.47	14.56	14.91	15.41
6	16.68	18.87	21.77	25.89	31.38	11.71	13.29	15.27	17.66	20.37
7	14.41	13.13	12.21	11.75	11.38	8.72	7.99	7.80	7.44	7.07
8	12.62	13.67	14.65	15.14	15.41	8.12	8.74	9.16	9.53	9.90
9	11.91	13.48	15.35	18.02	20.67	7.84	8.86	9.87	11.18	12.56

TOTAL LONGITUDINAL BENDING MOMENT AT MIDSPAN- COEFFICIENTS OF WL

LOAD POSITION									
1	2	3	4	5	6	7	8	9	10
.243	.250	.258	.263	.268	.124	.129	.131	.135	.138

DISTRIBUTION OF LONGITUDINAL MOMENT AT SECTION O-O BETWEEN I BEAMS- PERCENTAGE OF TOTAL MOMENT CARRIED BY EACH BEAM

	LOAD POSITION									
BEAM NO	1	2	3	4	5	6	7	8	9	10
1	26.7	18.3	14.5	13.0	12.4	15.6	17.1	17.3	16.7	16.6
2	25.3	29.0	22.5	19.3	18.0	23.5	22.4	23.1	23.1	23.2
3	19.7	22.1	27.5	22.3	20.0	23.2	22.3	21.1	22.4	23.3
4	17.1	18.5	21.9	28.1	25.0	22.3	22.4	22.2	21.8	22.5
5	11.2	12.0	13.6	17.2	24.6	15.5	15.8	16.3	15.9	14.3

Test Results for Model 2B

Span = 45.0 inches

Radius of Curvature = 116.7 inches

With midspan radial diaphragm

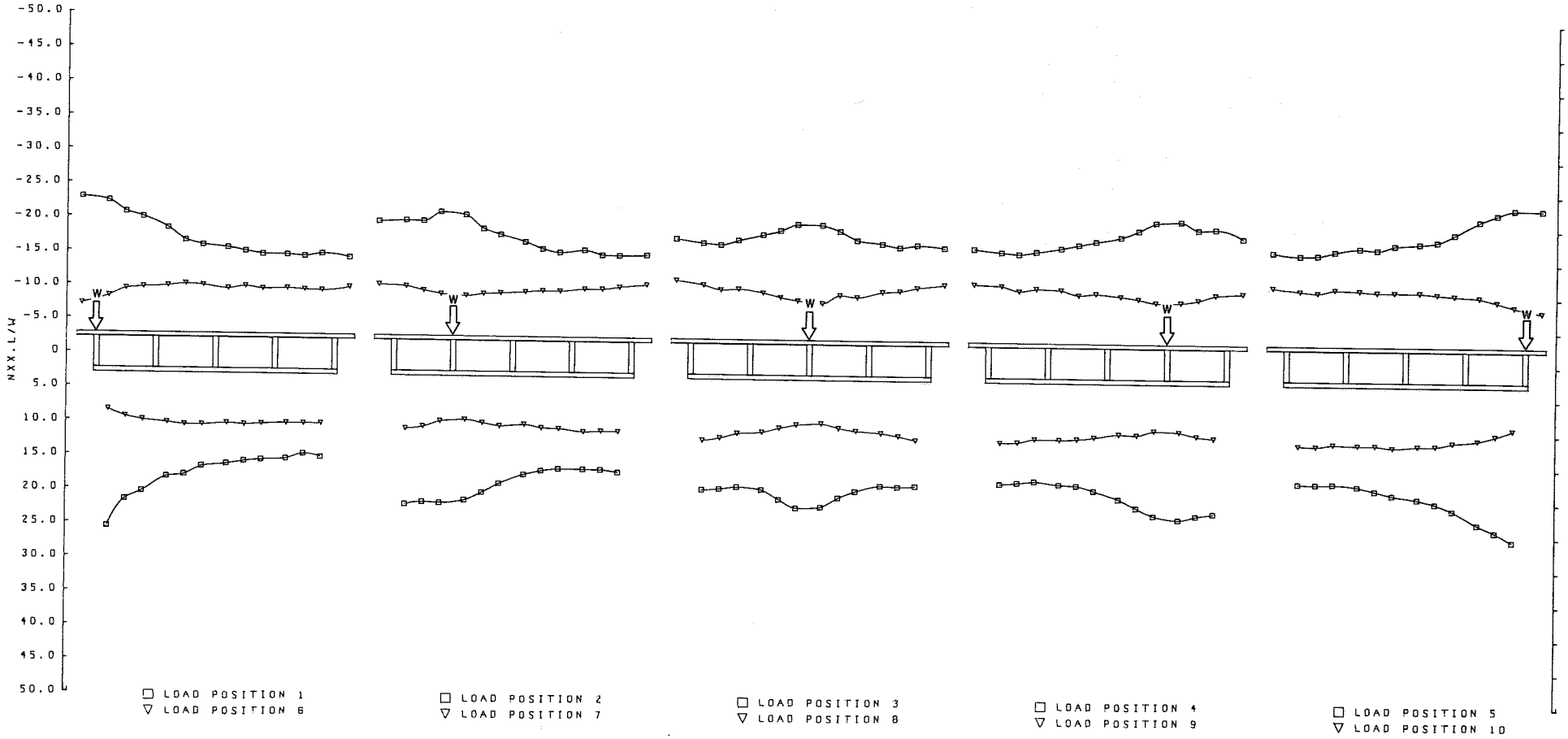

FIG.5.8 RADIAL DISTRIBUTION OF TANGENTIAL FORCES PER UNIT WIDTH IN TOP AND BOTTOM PLATES (NXX) AT SECTION 0-0
MODEL 2B

MODEL NO 2B, SPAN =45.0 INCHES, RADIUS OF CURVATURE =116.7 INCHES, WITH MID DIAPHRAGM

STATIC CHECKS-

(1) RATIO OF DOWNWARD TO UPWARD EXTERNAL FORCES
(2) RATIO OF HORIZONTAL TENSION TO COMPRESSION FORCE AT SECTION 0-0
(3) RATIO OF INTERNAL TO EXTERNAL MOMENT AT SECTION 0-0

	LOAD POSITION									
	1	2	3	4	5	6	7	8	9	10
(1)	.988	1.002	1.000	.998	1.007	.985	.990	.993	.999	.996
(2)	.988	1.013	1.035	1.027	1.001	1.023	1.023	1.018	1.016	1.024
(3)	.978	.999	.994	.990	1.006	.965	.981	.982	.987	.986

REACTIONS- COEFFICIENTS OF W

	LOAD POSITION									
	1	2	3	4	5	6	7	8	9	10
R1	.097	.223	.352	.475	.604	.115	.287	.465	.643	.822
R2	.411	.273	.146	.020	-.109	.631	.463	.287	.108	-.068
R3	.085	.205	.328	.451	.571	.035	.099	.179	.248	.317
R4	.424	.295	.172	.053	-.076	.228	.158	.076	0.	-.070

MODEL NO 2B, SPAN =45.0 INCHES, RADIUS OF CURVATURE =116.7 INCHES, WITH MID DIAPHRAGM

NXX FORCES- TANGENTIAL PLATE FORCES PER UNIT WIDTH AT SECTION O-O
COEFFICIENTS OF W/L

S/B	LOAD POSITION									
	1	2	3	4	5	6	7	8	9	10
					TOP PLATE					
.018	-22.90	-19.70	-17.67	-16.61	-16.57	-7.14	-10.38	-11.53	-11.43	-11.43
.116	-22.32	-19.90	-17.09	-16.17	-16.15	-8.28	-10.18	-10.89	-11.25	-10.96
.179	-20.71	-19.83	-16.86	-15.96	-16.21	-9.39	-9.57	-10.21	-10.53	-10.75
.241	-19.98	-21.19	-17.56	-16.32	-16.80	-9.64	-9.07	-10.35	-10.89	-11.25
.330	-18.37	-20.79	-18.39	-16.90	-17.32	-9.86	-8.85	-9.82	-10.75	-11.11
.393	-16.60	-18.74	-19.03	-17.41	-17.10	-10.14	-9.17	-9.17	-10.03	-10.89
.455	-15.93	-17.93	-19.98	-17.93	-17.79	-9.96	-9.32	-8.71	-10.25	-10.89
.545	-15.56	-16.88	-19.88	-18.60	-18.07	-9.50	-9.50	-8.35	-9.89	-10.89
.607	-15.07	-15.86	-19.00	-19.56	-18.36	-9.89	-9.71	-9.60	-9.53	-10.68
.670	-14.63	-15.35	-17.71	-20.79	-19.50	-9.50	-9.68	-9.32	-9.03	-10.50
.759	-14.62	-15.75	-17.21	-20.97	-21.43	-9.64	-10.03	-10.10	-9.07	-10.25
.821	-14.43	-15.05	-16.70	-19.74	-22.41	-9.46	-10.03	-10.28	-9.46	-9.61
.884	-14.82	-15.01	-17.06	-19.89	-23.19	-9.39	-10.39	-10.78	-10.21	-8.89
.982	-14.28	-15.10	-16.67	-18.53	-23.09	-9.91	-10.76	-11.24	-10.48	-8.10
					BOTTOM PLATE					
.116	25.56	21.86	19.19	17.85	17.33	8.42	10.78	11.92	11.77	11.71
.179	21.57	21.50	19.06	17.64	17.36	9.45	10.44	11.53	11.68	11.77
.241	20.36	21.62	18.73	17.39	17.27	9.93	9.63	10.86	11.14	11.41
.330	18.19	21.19	19.10	17.84	17.59	10.26	9.38	10.62	11.20	11.56
.393	17.86	20.05	20.52	17.95	18.24	10.57	9.84	10.01	11.08	11.53
.455	16.63	18.71	21.74	18.68	18.81	10.57	10.26	9.50	10.80	11.83
.545	16.26	17.32	21.57	19.86	19.34	10.32	10.02	9.32	10.29	11.56
.607	15.85	16.75	20.19	21.12	19.98	10.47	10.47	9.96	10.41	11.53
.670	15.61	16.45	19.19	22.26	20.97	10.35	10.56	10.32	9.75	11.02
.759	15.43	16.48	18.35	22.81	22.99	10.20	10.99	10.59	9.90	10.66
.821	14.67	16.52	18.47	22.24	24.10	10.23	10.84	11.02	10.50	9.96
.884	15.16	16.85	18.35	21.85	25.43	10.17	10.90	11.59	10.78	9.12

MODEL NO 2B, SPAN =45.0 INCHES, RADIUS OF CURVATURE =116.7 INCHES, WITH MID DIAPHRAGM

MYY BENDING MOMENTS- RADIAL BENDING MOMENT PER UNIT LENGTH IN PLATES AND WEBS AT SECTION O-O
COEFFICIENTS OF W/1000

S/R	LOAD POSITION									
	1	2	3	4	5	6	7	8	9	10
					TOP PLATE					
.018	-.00	-.00	0.	.00	0.	-.00	-.00	.00	-.00	.00
.116	4.74	-1.57	-.70	-.12	.29	1.39	-.30	-.37	-.16	.33
.179	.89	.41	-.45	-.31	-.20	.09	-.04	-.25	-.16	-.16
.241	-4.43	3.66	-.04	-.09	-.16	-.84	1.08	.31	.12	-.16
.330	2.66	9.04	-3.65	-1.66	-.79	1.01	1.81	-.40	-.68	-.47
.393	-.29	.99	.78	-.34	-.23	-.28	.23	.12	-.23	-.26
.455	-4.22	-7.15	5.99	1.12	.68	-1.41	-1.45	1.22	.75	.09
.545	1.28	1.99	6.60	-3.47	-2.17	.63	1.22	1.92	-.82	-.89
.607	.07	-.38	.91	.83	-.63	-.05	.31	.44	-.09	-.37
.670	-1.42	-2.42	-4.26	5.51	.94	-.73	-1.06	-.93	1.24	.77
.759	.43	1.01	.87	4.67	-4.85	.21	.33	.68	1.53	-.96
.821	.32	.03	-.15	.78	.24	-.09	.09	.24	.36	-.16
.884	-.46	-1.23	-1.97	-3.11	5.30	-.37	-.65	-.87	-.84	1.03
.982	-.00	-.00	.00	.00	0.	.00	.00	.00	.00	-.00
					BOTTOM PLATE					
.116	4.31	-1.39	-.59	-.22	.25	1.13	-.39	-.34	-.10	.15
.179	.61	.23	-.12	-.08	.01	.11	-.03	-.10	-.01	-.10
.241	-3.67	2.22	.59	.37	.12	-.89	.64	.30	.16	-.00
.330	2.12	5.54	-2.41	-1.14	-.51	.87	1.21	-.30	-.46	-.31
.393	-.08	.96	.52	-.26	-.11	-.15	.07	.02	-.06	-.13
.455	-2.88	-4.86	3.61	1.23	.70	-.92	-.90	.74	.57	.27
.545	1.13	1.89	4.12	-2.39	-1.47	.55	.87	1.13	-.59	-.54
.607	.11	-.15	.56	.62	-.45	-.01	.29	.32	-.11	-.25
.670	-1.17	-1.97	-3.12	3.13	1.31	-.54	-.72	-.80	.81	.63
.759	.50	.88	1.17	2.96	-3.74	.10	.40	.59	.92	-.71
.821	.08	.07	-.02	.56	.15	-.06	.04	.14	.10	-.20
.884	-.40	-.85	-1.54	-2.42	4.19	-.14	-.46	-.67	-.64	.90
WEB NO/LEVEL					WEBS					
1/C	5.19	-2.11	-1.01	-.44	.19	1.06	-.35	-.26	-.04	.19
1/D	-3.01	1.50	.74	.27	-.01	-.53	.26	.20	.08	-.10
2/C	6.53	1.47	-3.46	-1.72	-.67	1.70	.71	-.76	-.49	-.01
2/D	-4.93	-1.17	2.62	1.27	.42	-1.21	-.46	.53	.29	.01
3/C	3.27	5.38	.65	-3.57	-1.80	1.06	1.27	.05	-.72	-.42
3/D	-2.48	-4.24	-.35	2.68	1.35	-.75	-.97	-.22	.48	.42
4/C	1.69	2.79	4.42	.22	-4.80	.79	1.24	1.36	-.10	-.97
4/D	.03	.11	.01	-.01	-.00	0.	.01	-.01	-.05	.05
5/C	.68	1.28	1.68	2.88	-4.08	.31	.68	.93	.86	-.68
5/D	-.63	-.94	-1.28	-2.10	2.28	-.29	-.49	-.61	-.60	.50

MODEL NO 2B, SPAN =45.0 INCHES, RADIUS OF CURVATURE =116.7 INCHES, WITH MID DIAPHRAGM

DEFLECTIONS- LVDTP=LOW VOLTAGE DIFFERENTIAL TRANSFORMER POSITION
COEFFICIENTS OF 1000W/EL

	LOAD POSITION									
LVDTP	1	2	3	4	5	6	7	8	9	10
1	13.95	13.13	12.30	11.84	11.75	13.77	11.29	9.82	9.00	8.63
2	12.58	13.49	14.41	14.96	15.61	10.01	11.29	13.31	12.48	12.21
3	11.84	13.40	15.51	17.44	20.01	8.72	10.10	11.84	14.78	18.73
4	21.48	19.37	18.08	17.35	17.07	13.86	13.04	12.48	12.03	12.03
5	17.72	18.82	21.30	22.31	22.58	12.39	12.94	14.32	14.50	15.61
6	17.17	19.37	22.67	25.61	30.20	11.84	13.40	15.42	17.53	19.83
7	14.05	13.13	12.39	12.03	11.66	8.81	8.26	7.80	7.44	7.34
8	12.67	13.31	14.32	14.78	15.51	8.17	8.45	9.09	9.36	9.91
9	11.93	13.59	15.70	17.72	20.47	7.89	8.72	9.91	11.02	12.30

TOTAL LONGITUDINAL BENDING MOMENT AT MIDSPAN- COEFFICIENTS OF WL

LOAD POSITION									
1	2	3	4	5	6	7	8	9	10
.246	.247	.254	.260	.265	.125	.127	.130	.132	.136

DISTRIBUTION OF LONGITUDINAL MOMENT AT SECTION O-O BETWEEN I BEAMS- PERCENTAGE OF TOTAL MOMENT CARRIED BY EACH BEAM

	LOAD POSITION									
BEAM NO	1	2	3	4	5	6	7	8	9	10
1	22.9	18.2	15.4	14.2	13.5	13.7	16.8	17.7	17.6	16.8
2	24.4	26.5	22.3	20.2	19.7	23.1	21.0	22.7	23.6	23.8
3	20.5	21.8	25.3	22.3	21.2	23.7	22.0	20.0	22.2	23.7
4	19.0	19.7	21.9	25.9	24.3	23.2	23.2	22.1	20.6	22.2
5	13.1	13.7	15.0	17.3	21.3	16.3	16.9	17.4	16.0	13.4

Test Results for Model 3A

Span = 30.0 inches

Radius of Curvature = 116.7 inches

without midspan radial diaphragm

MODEL 3A: WITHOUT MID DIAPHRAGM
MODEL 3B: WITH MID DIAPHRAGM

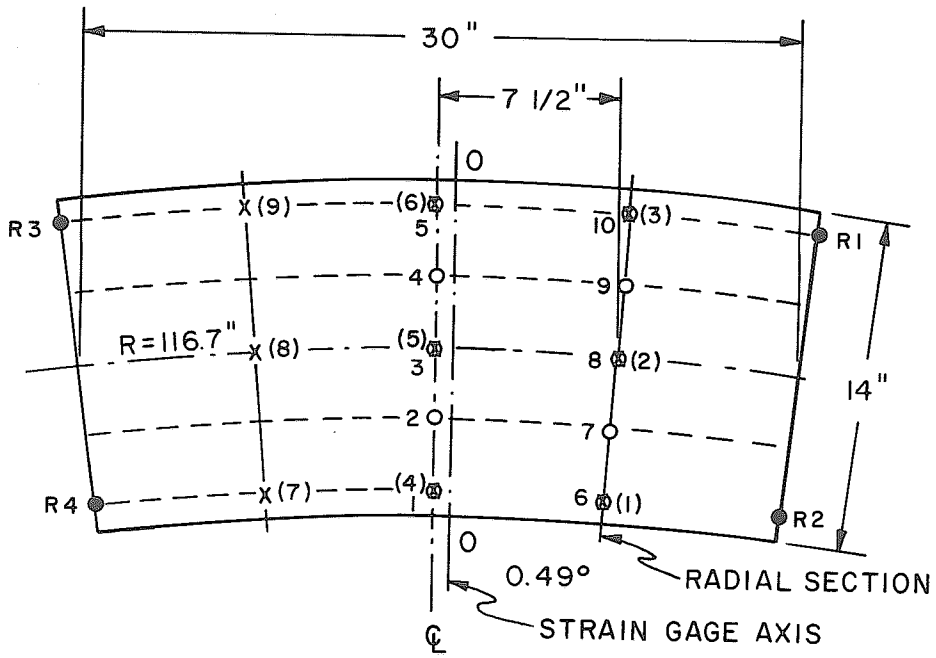

REACTION POINTS ● REACTION NO.
LOAD POSITIONS ○ LOAD POSITION NO.
DIAL GAGE POSITIONS X (DIAL GAGE NO.)

FIG. 5.9 CURVED BOX-GIRDER BRIDGE MODEL NO. 3, SPAN = 30 INCHES
RADIUS OF CURVATURE = 116.7 INCHES

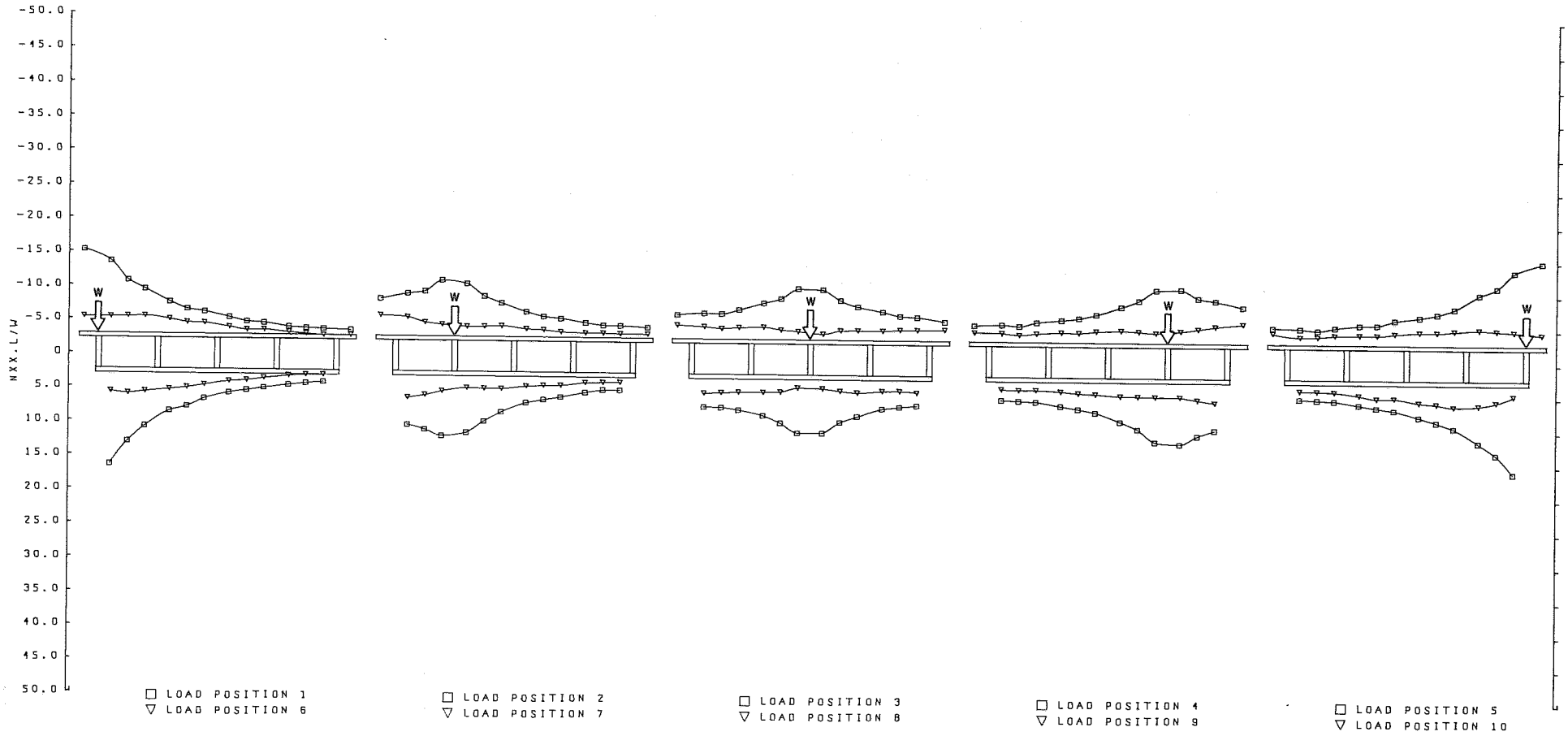

FIG. 5.10 RADIAL DISTRIBUTION OF TANGENTIAL FORCES PER UNIT WIDTH IN TOP AND BOTTOM PLATES (NXX) AT SECTION 0-0 MODEL 3A

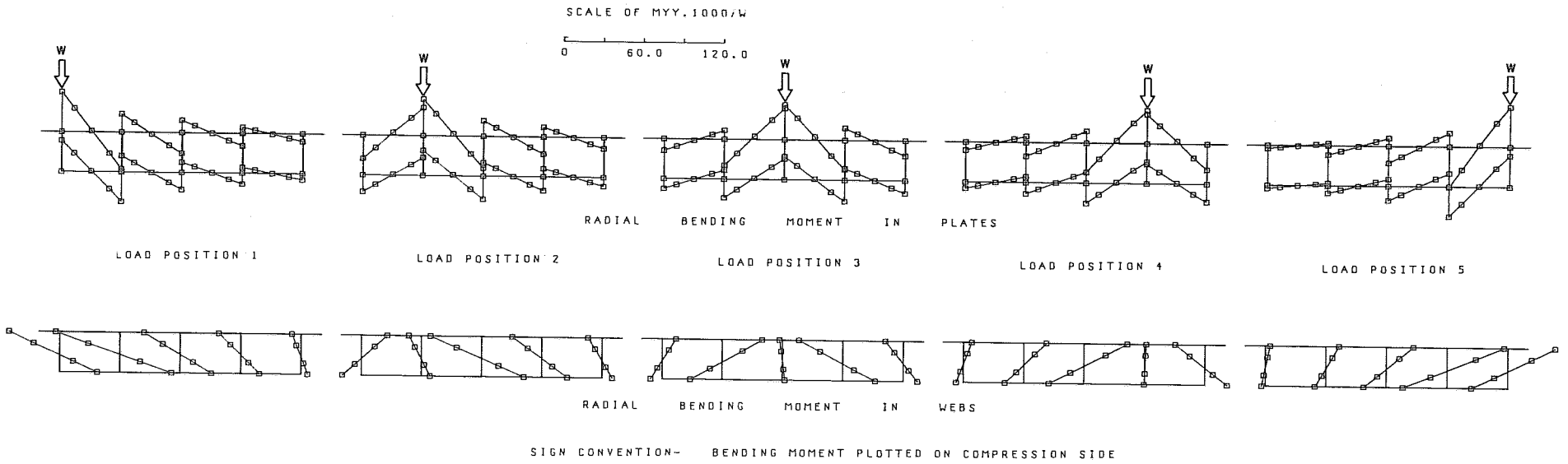

FIG.5.11 RADIAL DISTRIBUTION OF RADIAL BENDING MOMENT PER UNIT LENGTH (MYY) AT SECTION 0-0

MODEL 3A

MODEL NO 3A, SPAN =30.0 INCHES, RADIUS OF CURVATURE =116.7 INCHES, WITHOUT MID DIAPHRAGM

STATIC CHECKS-

(1) RATIO OF DOWNWARD TO UPWARD EXTERNAL FORCES
(2) RATIO OF HORIZONTAL TENSION TO COMPRESSION FORCE AT SECTION 0-0
(3) RATIO OF INTERNAL TO EXTERNAL MOMENT AT SECTION 0-0

	LOAD POSITION									
	1	2	3	4	5	6	7	8	9	10
(1)	.985	.979	.983	.983	.996	.997	.991	.997	.986	.992
(2)	1.046	1.027	1.011	1.034	1.006	1.029	1.045	1.036	1.020	1.042
(3)	.983	.968	.979	.973	.996	.983	.990	.998	.979	.990

REACTIONS- COEFFICIENTS OF W

	LOAD POSITION									
	1	2	3	4	5	6	7	8	9	10
R1	.038	.162	.287	.408	.532	.060	.223	.385	.570	.716
R2	.466	.338	.219	.094	-.031	.687	.525	.364	.187	.040
R3	.051	.176	.304	.427	.552	.019	.091	.171	.253	.344
R4	.453	.339	.208	.079	-.053	.234	.164	.079	0.	-.099

MODEL NO 3A, SPAN =30.0 INCHES, RADIUS OF CURVATURE =116.7 INCHES, WITHOUT MID DIAPHRAGM

NXX FORCES- TANGENTIAL PLATE FORCES PER UNIT WIDTH AT SECTION 0-0
COEFFICIENTS OF W/L

S/B	LOAD POSITION									
	1	2	3	4	5	6	7	8	9	10
					TOP PLATE					
.018	-15.24	-8.38	-6.41	-5.27	-5.27	-5.33	-5.91	-4.89	-4.25	-4.51
.116	-13.59	-9.21	-6.71	-5.43	-5.19	-5.33	-5.69	-4.71	-4.21	-4.00
.179	-10.76	-9.57	-6.64	-5.24	-4.95	-5.40	-4.93	-4.50	-3.95	-4.02
.241	-9.47	-11.19	-7.26	-5.83	-5.40	-5.45	-4.64	-4.66	-4.19	-4.28
.330	-7.62	-10.71	-8.28	-6.19	-5.78	-5.02	-4.36	-4.74	-4.38	-4.33
.393	-6.55	-8.85	-8.95	-6.47	-5.81	-4.55	-4.40	-4.35	-4.33	-4.33
.455	-6.16	-7.88	-10.43	-7.02	-6.52	-4.47	-4.50	-4.14	-4.59	-4.59
.545	-5.36	-6.59	-10.31	-8.19	-7.00	-3.93	-4.07	-3.78	-4.71	-4.83
.607	-4.76	-5.93	-8.73	-9.12	-7.47	-3.52	-3.95	-4.35	-4.57	-4.83
.670	-4.59	-5.66	-7.83	-10.69	-8.28	-3.57	-3.69	-4.36	-4.49	-5.05
.759	-4.07	-5.06	-7.11	-10.82	-10.34	-3.24	-3.58	-4.34	-4.68	-5.24
.821	-3.90	-4.71	-6.50	-9.55	-11.33	-3.05	-3.57	-4.50	-5.02	-5.09
.884	-3.81	-4.69	-6.35	-9.14	-13.67	-2.88	-3.50	-4.50	-5.38	-4.95
.982	-3.68	-4.45	-5.72	-8.26	-15.05	-2.92	-3.49	-4.57	-5.78	-4.57
					BOTTOM PLATE					
.116	16.42	10.24	7.14	5.71	5.23	5.71	6.24	5.15	4.12	4.00
.179	13.06	10.90	7.20	5.82	5.33	5.98	5.83	5.03	4.25	4.04
.241	10.80	11.83	7.57	5.94	5.43	5.69	5.23	4.93	4.21	4.13
.330	8.51	11.33	8.39	6.54	6.00	5.33	4.73	4.93	4.39	4.57
.393	7.83	9.66	9.46	6.94	6.40	5.09	4.83	4.87	4.63	5.01
.455	6.70	8.25	10.89	7.44	6.74	4.67	4.83	4.22	4.73	4.97
.545	5.77	6.86	10.88	8.77	7.71	4.10	4.43	4.32	4.99	5.56
.607	5.41	6.38	9.27	9.86	8.47	3.94	4.31	4.69	5.01	5.76
.670	5.03	5.95	8.39	11.71	9.32	3.60	4.24	4.87	5.05	6.14
.759	4.57	5.25	7.20	11.99	11.43	3.20	3.80	4.63	5.09	5.96
.821	4.27	4.87	6.92	10.76	13.18	3.04	3.74	4.59	5.49	5.47
.884	4.06	4.87	6.68	9.92	15.94	3.00	3.70	4.81	5.88	4.53

MODEL NO 3A. SPAN =30.0 INCHES, RADIUS OF CURVATURE =116.7 INCHES, WITHOUT MID DIAPHRAGM

MYY BENDING MOMENTS- RADIAL BENDING MOMENT PER UNIT LENGTH IN PLATES AND WEBS AT SECTION 0-0
COEFFICIENTS OF W/1000

S/B	LOAD POSITION									
	1	2	3	4	5	6	7	8	9	10
					TOP PLATE					
.018	0.	0.	.00	-.00	0.	-.00	.00	-.00	-.00	-.00
.116	17.70	-9.28	-5.53	-3.66	-1.46	8.31	-4.51	-4.25	-2.82	-.35
.179	.75	2.21	-1.08	-.35	-.35	.55	.78	-.50	-.29	-.20
.241	-15.99	13.26	3.52	2.53	.84	-7.53	6.19	3.26	2.03	-.00
.330	7.38	16.69	-10.47	-6.28	-4.10	5.73	8.69	-4.86	-4.54	-2.33
.393	-1.31	1.68	2.44	-.76	-.41	-.50	.78	1.48	-.29	-.64
.455	-9.68	-13.29	14.77	4.97	3.37	-6.57	-6.60	7.21	3.98	1.42
.545	5.26	6.60	16.31	-11.87	-7.85	3.63	5.26	8.34	-5.47	-4.74
.607	-.29	-.50	2.47	2.24	-1.22	-.35	-.18	1.07	1.22	-.96
.670	-5.73	-7.74	-11.72	15.32	5.41	-4.30	-5.67	-5.79	7.47	3.08
.759	2.41	4.12	4.87	13.49	-17.21	1.82	3.10	4.19	6.40	-10.16
.821	-.47	-.41	-1.02	1.89	1.16	-.18	-.41	-.61	.67	.23
.884	-3.61	-5.09	-7.07	-10.41	17.91	-2.59	-4.04	-5.32	-5.00	10.35
.982	0.	-.00	-.00	-.00	.00	.00	.00	-.00	0.	-.00
					BOTTOM PLATE					
.116	13.88	-7.05	-4.51	-2.83	-1.29	6.57	-3.58	-3.45	-2.14	-.31
.179	.47	.58	-.25	-.10	.02	.23	.29	-.00	-.10	-.06
.241	-12.79	8.10	3.86	2.51	1.08	-5.97	3.82	2.97	1.77	.23
.330	7.09	11.37	-7.84	-4.97	-3.28	4.84	5.88	-3.85	-3.53	-1.60
.393	-.23	.79	.83	-.06	-.17	-.15	.41	.41	.08	-.27
.455	-7.59	-9.85	9.45	4.82	2.97	-5.07	-5.07	4.70	3.47	1.35
.545	4.43	6.01	10.45	-8.61	-6.34	3.07	4.36	5.38	-4.24	-3.58
.607	-.02	-.10	.56	.79	-.02	-.13	-.13	.27	.35	-.25
.670	-4.78	-6.19	-9.04	9.85	5.76	-3.22	-4.47	-4.61	4.84	3.10
.759	2.47	3.59	5.03	8.69	-12.89	1.77	2.81	3.78	4.18	-7.73
.821	-.17	-.08	-.33	.39	.52	-.06	-.12	-.33	.10	.17
.884	-2.74	-3.95	-5.74	-7.71	13.88	-1.97	-3.20	-4.10	-3.87	8.17
WEB NO/LEVEL					WEBS					
1/C	19.22	-10.27	-5.22	-3.09	-1.68	7.72	-4.68	-4.18	-2.45	.09
1/D	-10.14	4.72	3.27	2.04	1.05	-4.27	2.82	3.00	1.95	.09
2/C	23.58	4.86	-14.95	-8.27	-4.81	12.54	2.00	-8.31	-6.45	-1.86
2/D	-15.08	-2.32	9.04	5.59	3.18	-8.31	-1.50	5.13	4.22	1.18
3/C	12.99	18.67	1.09	-15.99	-9.63	9.04	10.81	.73	-8.59	-5.04
3/D	-9.50	-12.68	-.68	10.27	6.81	-6.36	-7.54	-.82	5.81	3.91
4/C	7.81	10.54	16.99	-.77	-21.31	5.72	7.72	9.86	-.45	-12.27
4/D	-5.83	-8.05	-8.62	-.18	12.27	-1.32	-1.67	-1.92	-1.78	2.55
5/C	3.32	5.13	6.63	11.36	-17.67	2.36	3.68	5.04	5.86	-9.18
5/D	-2.04	-2.91	-4.22	-6.00	10.09	-1.63	-2.18	-3.00	-2.86	5.31

MODEL NO 3A, SPAN =30.0 INCHES, RADIUS OF CURVATURE =116.7 INCHES, WITHOUT MID DIAPHRAGM

DEFLECTIONS- LVDTP=LOW VOLTAGE DIFFERENTIAL TRANSFORMER POSITION
COEFFICIENTS OF 1000W/EL

	L O A D P O S I T I O N									
LVDTP	1	2	3	4	5	6	7	8	9	10
1	4.25	2.98	2.21	1.74	1.53	4.29	2.70	1.82	1.35	1.18
2	2.54	3.10	3.65	3.28	3.03	1.95	2.90	4.26	3.40	2.91
3	1.72	2.57	2.99	4.14	5.73	1.24	1.92	2.73	4.15	7.64
4	6.75	4.26	3.15	2.56	2.39	3.98	3.12	2.39	1.91	1.78
5	3.45	4.14	5.44	4.52	4.26	2.36	3.10	3.87	3.62	3.50
6	2.44	3.37	4.20	5.82	8.59	1.70	2.39	3.32	4.73	6.77
7	3.98	2.63	1.96	1.90	1.59	1.96	1.47	1.22	.80	.73
8	2.36	2.69	3.56	3.25	3.23	1.35	1.80	2.18	2.13	2.12
9	1.69	2.25	3.09	4.21	5.88	1.04	1.64	2.14	2.90	3.88

TOTAL LONGITUDINAL BENDING MOMENT AT MIDSPAN- COEFFICIENTS OF WL

L O A D P O S I T I O N									
1	2	3	4	5	6	7	8	9	10
.242	.250	.256	.260	.265	.121	.125	.127	.133	.134

DISTRIBUTION OF LONGITUDINAL MOMENT AT SECTION O-O BETWEEN I BEAMS- PERCENTAGE OF TOTAL MOMENT CARRIED BY EACH BEAM

	L O A D P O S I T I O N									
BEAM NO	1	2	3	4	5	6	7	8	9	10
1	33.2	19.9	13.6	10.9	9.9	20.7	20.9	17.1	14.1	13.7
2	27.3	32.6	22.2	17.0	15.1	28.1	24.5	23.6	20.7	20.4
3	17.8	21.7	29.7	22.9	18.7	22.5	22.3	20.9	22.7	23.5
4	13.6	16.0	21.6	31.4	26.6	17.8	19.5	22.5	23.5	26.4
5	8.1	9.8	12.8	18.6	29.7	10.9	12.8	16.0	19.3	16.1

Test Results for Model 3B

Span = 30.0 inches

Radius of Curvature = 116.7 inches

With midspan radial diaphragm

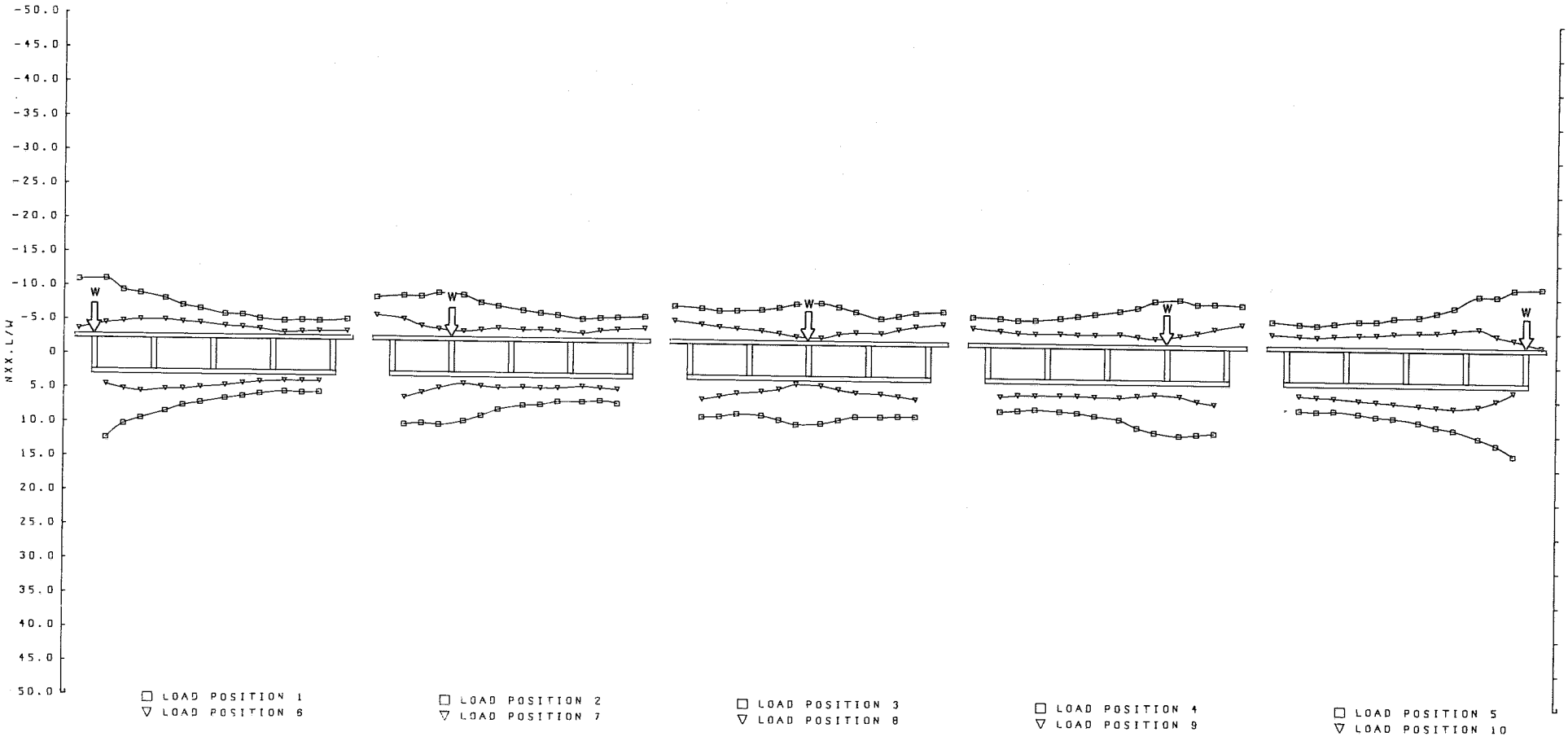

FIG. 5.12 RADIAL DISTRIBUTION OF TANGENTIAL FORCES PER UNIT WIDTH IN TOP AND BOTTOM PLATES (NXX) AT SECTION 0-0
MODEL 3B

MODEL NO 3B, SPAN =30.0 INCHES, RADIUS OF CURVATURE =116.7 INCHES, WITH MID DIAPHRAGM

STATIC CHECKS-

(1) RATIO OF DOWNWARD TO UPWARD EXTERNAL FORCES
(2) RATIO OF HORIZONTAL TENSION TO COMPRESSION FORCE AT SECTION O-O
(3) RATIO OF INTERNAL TO EXTERNAL MOMENT AT SECTION O-O

	LOAD POSITION									
	1	2	3	4	5	6	7	8	9	10
(1)	.998	.993	.979	.983	.985	.990	.989	.998	1.002	1.008
(2)	.990	1.013	1.080	1.024	.992	1.036	1.029	1.024	1.033	1.036
(3)	.982	.979	.967	.969	.988	.983	.983	1.002	1.006	1.027

REACTIONS- COEFFICIENTS OF W

	LOAD POSITION									
	1	2	3	4	5	6	7	8	9	10
R1	.032	.159	.283	.408	.535	.048	.223	.388	.564	.710
R2	.460	.341	.221	.094	-.025	.699	.531	.361	.185	.040
R3	.048	.179	.312	.435	.560	.032	.093	.173	.251	.339
R4	.456	.327	.202	.076	-.055	.225	.161	.076	-.003	-.099

MODEL NO 3B, SPAN =30.0 INCHES, RADIUS OF CURVATURE =116.7 INCHES, WITH MID DIAPHRAGM

NXX FORCES- TANGENTIAL PLATE FORCES PER UNIT WIDTH AT SECTION O-O
COEFFICIENTS OF W/L

S/B	LOAD POSITION									
	1	2	3	4	5	6	7	8	9	10
					TOP PLATE					
.018	-10.91	-8.64	-7.81	-6.66	-6.46	-3.68	-5.97	-5.65	-5.08	-4.64
.116	-11.01	-8.92	-7.52	-6.50	-6.13	-4.52	-5.45	-5.19	-4.69	-4.40
.179	-9.35	-8.85	-7.16	-6.26	-5.99	-4.78	-4.47	-4.83	-4.43	-4.26
.241	-8.92	-9.38	-7.24	-6.33	-6.30	-5.05	-4.04	-4.62	-4.36	-4.48
.330	-8.15	-9.06	-7.38	-6.63	-6.65	-5.02	-3.76	-4.35	-4.43	-4.64
.393	-7.17	-8.00	-7.73	-6.98	-6.63	-4.76	-4.00	-3.95	-4.31	-4.69
.455	-6.70	-7.50	-8.28	-7.29	-7.13	-4.59	-4.28	-3.50	-4.31	-4.93
.545	-5.91	-6.87	-8.43	-7.78	-7.34	-4.19	-4.07	-3.35	-4.43	-5.07
.607	-5.86	-6.50	-7.87	-8.28	-7.96	-4.05	-4.12	-3.93	-4.04	-5.12
.670	-5.30	-6.23	-7.16	-9.29	-8.72	-3.81	-3.97	-4.19	-3.81	-5.43
.759	-5.01	-5.72	-6.23	-9.53	-10.47	-3.31	-3.65	-4.12	-4.27	-5.71
.821	-5.14	-5.87	-6.62	-8.87	-10.40	-3.48	-4.05	-4.67	-4.69	-4.67
.884	-5.08	-5.99	-7.10	-8.96	-11.43	-3.59	-4.26	-5.12	-5.28	-4.09
.982	-5.32	-6.15	-7.33	-8.73	-11.56	-3.62	-4.45	-5.52	-5.97	-3.05
					BOTTOM PLATE					
.116	12.29	9.99	8.45	7.13	6.54	4.53	6.06	5.81	4.95	4.39
.179	10.27	9.78	8.32	6.97	6.67	5.17	5.31	5.33	4.71	4.53
.241	9.41	9.99	7.90	6.76	6.55	5.49	4.61	4.89	4.69	4.63
.330	8.37	9.44	8.13	7.02	6.92	5.17	3.94	4.59	4.67	4.97
.393	7.48	8.61	8.77	7.20	7.33	5.11	4.28	4.22	4.67	5.13
.455	7.03	7.68	9.40	7.62	7.50	4.85	4.51	3.52	4.81	5.33
.545	6.41	7.04	9.22	8.13	8.08	4.55	4.39	3.68	4.85	5.64
.607	6.07	6.88	8.71	9.29	8.73	4.25	4.49	4.24	4.63	5.84
.670	5.68	6.42	8.16	9.95	9.16	3.96	4.45	4.69	4.42	5.98
.759	5.36	6.42	8.17	10.39	10.34	3.80	4.21	4.83	4.65	5.66
.821	5.50	6.24	8.07	10.17	11.36	3.80	4.41	5.13	5.35	4.83
.884	5.41	6.66	8.08	10.00	12.87	3.76	4.57	5.53	5.75	3.60

MODEL NO 3B, SPAN =30.0 INCHES, RADIUS OF CURVATURE =116.7 INCHES, WITH MID DIAPHRAGM

MYY BENDING MOMENTS- RADIAL BENDING MOMENT PER UNIT LENGTH IN PLATES AND WEBS AT SECTION O-O
COEFFICIENTS OF W/1000

S/B	L C A D P O S I T I O N									
	1	2	3	4	5	6	7	8	9	10
					TOP PLATE					
.018	-.00	-.00	.00	0.	0.	.00	.00	0.	-.00	-.00
.116	2.93	-1.41	-.65	-.27	.12	1.85	-1.03	-.73	-.51	-.16
.179	.43	.52	-.35	-.22	-.05	.12	.07	-.33	-.17	-.09
.241	-3.19	3.41	.10	.06	-.07	-1.50	1.92	.66	.23	.03
.330	.73	4.14	-1.99	-1.09	-.68	.92	2.44	-1.10	-1.01	-.61
.393	-.34	.84	.78	-.06	-.21	-.07	.38	.21	-.19	-.33
.455	-2.22	-3.05	3.76	.79	.44	-1.45	-1.78	2.25	.99	.33
.545	.89	1.17	4.93	-3.30	-1.95	.56	1.27	2.88	-1.47	-1.24
.607	.24	.17	.99	.56	-.84	.07	.30	.68	-.10	-.65
.670	-1.09	-1.65	-2.81	4.31	.35	-.73	-1.20	-1.50	2.02	.42
.759	-.03	.19	.23	4.07	-4.01	.02	.31	.64	2.39	-2.51
.821	.15	.42	.45	1.07	.19	.07	.17	.35	.47	-.66
.884	-.21	-.66	-1.12	-2.11	3.87	-.33	-.72	-1.10	-1.36	2.48
.982	0.	.00	0.	-.00	.00	.00	-.00	-.00	.00	.00
					BOTTOM PLATE					
.116	3.04	-1.38	-.77	-.33	.04	1.56	-.96	-.69	-.40	-.05
.179	.18	.44	-.13	-.13	.09	.04	-.03	-.14	-.10	-.09
.241	-2.83	2.15	.57	.39	.16	-1.33	1.16	.69	.46	.10
.330	.97	2.55	-1.17	-.69	-.36	.86	1.60	-.90	-.70	-.41
.393	-.28	.45	.58	.02	-.03	-.00	.06	.07	-.05	-.16
.455	-1.62	-2.12	2.20	.71	.50	-1.03	-1.20	1.18	.78	.26
.545	.76	1.17	2.86	-2.04	-1.26	.57	1.00	1.73	-.98	-.85
.607	.19	.25	.86	.50	-.57	.06	.26	.36	-.25	-.52
.670	-.84	-1.33	-2.09	2.69	.89	-.64	-.98	-1.23	1.27	.73
.759	.20	.50	.85	2.25	-3.08	.29	.46	.82	1.31	-1.96
.821	.08	.24	.33	.72	.17	.04	.11	.14	.25	-.42
.884	-.21	-.58	-.88	-1.73	3.53	-.26	-.59	-.99	-1.05	2.21
WEB NO/LEVEL					WEBS					
1/C	4.50	-2.15	-.83	-.38	-.11	1.44	-.91	-.69	-.33	.01
1/D	-2.59	1.34	.52	.26	.05	-.89	.42	.34	.26	-.04
2/C	5.04	1.09	-2.94	-1.66	-.60	2.28	.35	-1.70	-1.09	-.34
2/D	-3.72	-.95	2.08	1.20	.40	-1.61	-.35	1.10	.72	.14
3/C	2.06	3.50	.14	-2.97	-1.36	1.32	1.68	-.07	-1.27	-.75
3/D	-1.46	-2.58	-.20	2.33	1.16	-1.01	-1.17	.03	.91	.56
4/C	1.28	2.10	3.33	-.99	-4.70	.98	1.49	1.94	-.39	-2.26
4/D	-.37	-.42	-.10	-.11	.08	-.43	-.34	-.31	-.19	.52
5/C	.57	1.06	1.54	2.68	-4.54	.41	.86	1.23	1.47	-2.21
5/D	-.48	-.75	-1.16	-1.79	2.35	-.25	-.65	-.84	-.80	1.50

MODEL NO 3B, SPAN =30.0 INCHES, RADIUS OF CUPVATURE =116.7 INCHES, WITH MID DIAPHRAGM

DEFLECTIONS- LVDTP=LOW VOLTAGE DIFFERENTIAL TRANSFORMER POSITION
COEFFICIENTS OF 1000W/EL

	LOAD POSITION									
LVDTP	1	2	3	4	5	6	7	8	9	10
1	3.61	2.88	2.45	2.02	1.90	3.98	2.69	1.90	1.53	1.35
2	2.57	2.75	3.61	3.55	3.49	2.08	2.88	3.98	3.30	3.12
3	1.77	2.26	3.49	4.65	6.36	1.53	2.08	2.94	4.16	7.22
4	5.63	4.16	3.55	2.94	2.63	3.61	3.12	2.51	2.08	1.84
5	3.43	3.79	5.02	4.71	4.77	2.51	3.06	3.61	3.61	3.73
6	2.57	3.12	4.71	6.43	7.96	2.02	2.69	3.61	4.77	6.55
7	3.55	2.88	2.45	1.96	1.77	2.02	1.41	.98	.80	.73
8	2.45	2.63	3.43	3.30	3.37	1.47	1.71	2.02	2.08	2.08
9	1.84	2.20	3.37	4.59	6.12	1.29	1.65	2.33	2.82	3.67

TOTAL LONGITUDINAL BENDING MOMENT AT MIDSPAN- COEFFICIENTS OF WL

LOAD POSITION									
1	2	3	4	5	6	7	8	9	10
.239	.247	.257	.261	.268	.122	.126	.127	.129	.130

DISTRIBUTION OF LONGITUDINAL MOMENT AT SECTION O-O BETWEEN I BEAMS- PERCENTAGE OF TOTAL MOMENT CARRIED BY EACH BEAM

	LOAD POSITION									
BEAM NO	1	2	3	4	5	6	7	8	9	10
1	26.4	19.6	15.9	13.3	12.0	16.1	20.6	19.2	16.5	14.7
2	26.1	27.8	22.0	18.7	17.6	26.8	21.0	22.5	21.8	21.9
3	19.7	21.3	25.5	21.6	20.1	23.6	21.6	17.7	21.8	24.6
4	16.5	18.2	21.4	27.5	25.7	19.8	21.0	22.0	20.9	26.1
5	11.3	13.0	15.2	18.8	24.5	13.6	15.8	18.6	19.0	12.7

GENERAL COMMENTS ON THE TEST DATA

6.1 Self-Consistency of Test Data

The self-consistency of the test data can be studied in the following three ways:

(a) Static checks

(b) Symmetry checks

(c) Reciprocity checks

The static checks are merely a check on the accuracy of the measurement techniques, as any system must satisfy the conditions of equilibrium. A check on the symmetry of test data checks that the entire system (bridge model, testing frame and bridge supports) are structurally symmetrical. The reciprocity condition depends upon the system behaving linearly, and would break down if there was any significant source of nonlinearity such as initial slack in the testing system or internal slip in the model. The linearity of system was always checked prior to taking response data. All three checks depend on the accuracy of the measurements, but none of the three indicates the accuracy of the modeling technique particularly as it compared with the continuum.

6.2 Static Checks

The results of the three static checks detailed in Sec. 4.2 are tabulated for each test in Chapter 5. Static check (1) on vertical forces was the easiest to obtain as it depended only on the accurate measurement of applied load and reactions. This was generally correct to within 1%.

Static check (2) related to the equilibrium of horizontal force resultants T and C at Section 0-0 depended on the accurate measurement of strains at that section. This check was generally accurate to within 3%.

Static check (3) related to the equilibrium of internal and external moments at Section O-O was not only dependent on static checks (1) and (2) but also on the value of E of the material. The error in this check was generally less than 2%. The accuracy of the three static checks was considered satisfactory.

During the test program the static checks became more of a check on the reliability of the low speed scanner equipment than on the bridge model. It was verified in the first test series that the strain gages and load cells were operating accurately, and hence if the readings were measured accurately the static checks were satisfactory. In subsequent tests the table of static checks was always studied as soon as possible to ensure that the low speed scanner was operating reliably. On several occasions during the testing program poor static checks pointed to a small malfunction in the electronic equipment and without the continuous check of self-consistency the resulting errors would have gone unnoticed.

6.3 Symmetry Checks

Symmetry checks can be applied to reactions and deflections for midspan load positions. For load positions 1-5, reactions R1 and R2 should be equal to R3 and R4 respectively, and the deflections at LVDT locations 1, 2 and 3 should be equal to those at locations 7, 8 and 9 respectively. Taken as a percentage of maximum measured values for the test in each case, the average deviation of reactions and deflections due to lack of symmetry were as follows:

Reaction < 2%

Deflections < 1%

6.4 Reciprocity Checks

Deflection measurements were taken under load positions 1, 3, 5, 6, 8

and 10, and thus it was possible to apply the reciprocity check to these load positions. The average deviation of reciprocal deflections, expressed as a percentage of the maximum measured deflection in each test was within 1%.

It was considered that the symmetry and reciprocity checks were satisfactory within the limits of experimental accuracy.

7. GENERAL BEHAVIOR OF CURVED BOX-GIRDER BRIDGE MODELS

7.1 Total Longitudinal Bending Moment at Midspan

The values of total longitudinal bending moments CWL are tabulated as values of the coefficient C in Chapter 5. Making use of the statics and symmetry conditions, the C values can be calculated for any point load W at midspan, by the following equation.

$$C = \frac{1}{4}\left(1 + \frac{A}{2R} + \frac{X}{R}\cos\phi\right) \quad \ldots\ldots\ldots\ldots\ldots\ldots \quad 7.1$$

where ϕ, R, A, and X are defined in Fig. 7.2. X is measured from the line R1 - R3, and is taken negative when the load lies between the center of curvature and line R1 - R3. The values of C for midspan load positions are summarized in Table 7.1. The following observations can be made regarding the total midspan bending moments.

(a) C varies linearly with X as the load is moved across the bridge. The results are plotted in Fig. 7.3 and compared with skew and straight bridges in terms of the effective span L_e, where L_e is that span which is calculated by equating the total midspan moment to 0.25 WL_e. Substituting the values of X in equation 7.1 for load positions 1 and 5 respectively, gives $C = \frac{1}{4}(1 + \frac{A}{2R})/\cos\phi$ and $C = \frac{1}{4}(1 + \frac{A}{2R})/\cos\phi - A/4R\cos\phi)$ indicating a maximum variation of $C = A/(4R\cos\phi)$.

(b) The bending moment coefficient is dependent on ϕ. This can be seen by comparing the average values of C in Table 7.1. The average value of C for midspan load positions reduces from 0.259 to 0.253 as the span is reduced from 60 in. to 30 in. The average C value will approach 0.250 as the span approaches zero.

(c) As the load is moved from midspan positions (1 through 5) to quarter span positions (1 through 10) the bending moment coefficient values at midspan are reduced to approximately one-half. This can be seen in Chapter 5.

(d) The bending moment coefficients being statically determinate are not affected by the presence or absence of midspan radial diaphragm, for midspan load positions.

(e) The bending moment coefficients can be calculated for uniformly distributed load by using the influence lines as shown in Fig. 7.4. The bending moments expressed as coefficient of WL (where W is the total uniformly distributed load over the entire bridge) are found to be 0.131, 0.129 and 0.127 for 60 in., 45 in. and 30 in. span bridges respectively.

7.2 N_{XX} Forces in Top and Bottom Plates at Section 0-0

From Calcomp plots in Chapter 5 the following trends can be noted in the distribution of N_{XX} forces.

(a) The form of the N_{XX} distribution curve for any given load position on the midspan radial section is sensibly independent of the span of the bridge as may be seen in Fig. 7.5 and Fig. 7.6. It will be seen that the graphs are essentially parallel indicating that the departure from a uniform N_{XX} distribution is a function of local bending in the bridge. If this were so, it would suggest that to increase the span beyond that of Model 1 would merely add a uniform increment to N_{XX} in both top and bottom plates, due to added effect of overall bending.

(b) The local bending effects on the radial distribution of N_{XX} forces at Section 0-0 is damped out as the load is moved from the midspan load positions towards the reaction points. The distribution becomes

uniform at a certain distance from Section 0-0 which is very close to quarter span load positions in Model 2A (see Fig. 5.6). Further, as the load is moved further away from the midspan there is a slight tendency for the form of the distribution curve of N_{xx} to become the reverse of those produced by the midspan load positions at Section 0-0. This can be seen in Fig. 5.2, which shows that where the N_{xx} values are maximum for load positions 1 through 5, they are minimum for the corresponding quarter span load positions 6 through 10. This tendency is more pronounced for bridges with the midspan diaphragm (Figs. 5.4 and 5.8)

(c) It may be noted that the distribution of N_{xx} at Section 0-0 is more nearly uniform for load position 5 than for load position 1 for all models (see Fig. 7.5). A measure of this distribution can be taken as the ratio of maximum and minimum N_{xx} values in each case. These ratios are 1.98 and 1.59 for load positions 1 and 5 respectively for the top plate in Model 1A. Also, higher N_{xx} values are observed in the plates towards the inside edge as compared with the edge farthest from the center of curvature for load position 3.

(d) The effect of midspan radial diaphragm is very noticable on the distribution of N_{xx} as can be seen in Fig. 7.7 for Model 1. The diaphragm flattens the N_{xx} distribution graphs, the maximum flattening effect occuring for load positions 1 and 5. However, the average internal longitudinal forces (average N_{xx}) remain the same with and without the midspan diaphragms for a given bridge. This is due to the fact that for loading at midspan the reactions and the total longitudinal bending moments are statically determinate and independent of the midspan diaphragm.

(e) A comparison of N_{xx} distribution between Model 2A and a 30^{o} skew box-girder bridge model is shown in Fig. 7.8. The skew bridge model has a span of 47.43 in. and its cross-section is the same as that of Model 2A. It can be seen in Fig. 7.8 that the distributions of N_{xx} for the two models are quite similar for load positions 1 and 2 and the difference in distribution trends becomes greater as the load is moved to positions 3, 4 and 5. The reason for greater difference in load positions 3, 4 and 5 is the higher torsional moments in the case of the curved model. Even so, the N_{xx} distribution curves are remarkably similar, even in those cases where extreme differences could be expected.

7.3 Distribution of Total Longitudinal Moment between the I-beams

The concept of dividing a box-girder section into individual I-beams as suggested by AASHO Specifications [4] is shown in Fig. 7.1, along with the percentage of moment of inertia contributed by each beam towards the total moment of inertia of the box-section. The concept is useful for design purposes, the bending moment in each section being considered as a percentage of the total. The division of total moment amongst the five individual beams is tabulated in Chapter 5 for all models and load positions. The following observations can be made from this data:

(a) For a completely uniform distribution of N_{xx}, the moment percentages taken by the individual I-beams should approach their moment of inertia percentages, i.e. 15.8% for the outer beams 1 and 5, and 22.8% for the inner beams 2, 3 and 4. It will be noted in Chapter 5 that the N_{xx} distribution is approximately uniform for Model 2A for load positions 6 through 10, and in these cases,

the computed I-beam moment percentages do approximate to the predicted 15.8% and 22.8% values.

(b) It was shown in Section 7.2 that the N_{xx} distribution graphs are essentially parallel with changing span. This would result in an increasing moment percentage taken by any individual beam as the span gets shorter for a point load directly over that beam. This can be seen in Table 7.2 which gives the maximum I-beam percentages of total moment carried by any beam, and this always occurs when the load is directly over that beam. Table 7.2 shows that the maximum percentage moment increases in every beam as the span is reduced from 60 in. to 30 in. Naturally the increase is much larger for the models without midspan radial diaphragm.

The data of Table 7.2 for beam No. 1 is also plotted in Fig. 7.9 to show the variation with span and the effect of midspan diaphragm. As the span gets very large, the percentage of moment carried by any beam will approach its moment of inertia percentage for the models with and without diaphragm. As the span is reduced the increase in the percentage moment carried by any beam increases at a much higher rate for models without midspan diaphragm as compared with models with midspan diaphragm. This can be seen in Fig. 7.9 where the percentage moment carried by beam No. 1 rises from 23.9% for Model 1A (60 in.) to 33.2% for Model 3A (30 in.) as against an increase from 21.3% for Model 1B to 26.4% for Model 3B. It can be seen in Fig. 7.9 that if the span is reduced beyond 30 in., the percentage moment in beam No. 1 increases very sharply for a bridge without midspan diaphragm but the relative increase

would be much smaller for the same span bridge with midspan diaphragm indicating the usefulness of such a diaphragm at smaller spans.

(c) It will be noted in Table 7.2 that beam No. 1 for load position 1 always takes a greater percentage of total moment than the beam No. 5 for load position 5. However the total moment taken by beam No. 5 may still be greater because the total longitudinal bending moment is 10% higher for load position 5 than for load position 1. The same trend can be seen by comparing beam No. 2 with beam No. 4.

7.4 Radial Bending Moments at Section 0-0

Values of radial plate bending moments per unit length (M_{yy}) in top and bottom plates and in all five webs are tabulated for all strain gage locations in Chapter 5. This data is also plotted for models without midspan diaphragm in Chapter 5 for midspan load positions 1 through 5. A study of this data and plots of Figs. 5.3, 5.7 and 5.11 shows the following trends.

(a) The largest plate bending moments in plates and webs are observed for load position 1 in all models (see Figs. 5.3, 5.7 and 5.11). The largest value of M_{yy} will be seen in web No. 2 of Model 1A and is approximately 0.05W (in-lbs/in). Note that this is an extrapolated value, but it agrees closely with the analytical results. The maximum values of M_{yy} for Models 2A and 3A also occur in web No. 2 and they decrease slightly as span is decreased.

(b) It can be seen by comparing Figs. 5.3, 5.7 and 5.11 that the overall distribution pattern and the order of magnitude of M_{yy} is reasonably independent of the span for all practical purposes. However, as the span is reduced and the curved bridge approaches the case of a straight bridge, the plate bending moments for load position 1 decrease

slightly, while those for load position 5 increase. Clearly as the curved bridge approaches the straight bridge, the M_{yy} values for load positions 1 and 5 become comparable by symmetry. Similar trends can be seen for the central load position 3, where the M_{yy} values become more symmetrical about the center point of the box-section as the span is reduced.

(c) It can be seen from the Calcomp plots of radial bending moments that the variation of bending moments in top and bottom plates at Section 0-0 is approximately linear between the webs for the models without midspan radial diaphragm. There were only two points on each web where plate bending moments were measured, so the linearity of M_{yy} on the web could not be ascertained experimentally. However, the analytical solution showed that the bending moment variation is virtually linear in the webs. This linear variation does not apply to the bridges with midspan diaphragm. Moment diagrams are not shown for bridges with midspan diaphragm, as plate bending moment values were approximately one third of the values encountered in models without diaphragm.

7.5 Deflections

Values of deflections at selected points under the webs are tabulated in Chapter 5. The following observations can be made from this data.

(a) In all cases the twist at midspan taken as the differential displacements between webs 5 and 1 varies linearly as the point load is moved across the midspan radial section as shown in Fig. 7.11 and Table 7.3. The presence of the midspan diaphragm produces only a small reduction in twist values. The variation of midspan twist with span length is shown in Fig. 7.10 for bridges with and without midspan radial

diaphragm for load position 5. The applied load in all cases was 1000 lbs. It can be seen in Fig. 7.10 that the reduction in twist due to the midspan diaphragm was about the same for Models 1, 2 and 3 and was approximately 0.0038".

(c) The radial distributions of vertical deflections at midspan for Models 1A, 2A and 3A are shown in Fig. 7.12 and those for Models 1B, 2B and 3B are plotted in Fig. 7.13. The Calcomp plots of Figs. 7.12 and 7.13 are in dimensionless form and are plotted for the midspan load positions 1 through 5. These plots show how the profile of vertical deflections changes at midspan, with change of span and load position. It will be seen in these figures that the deflection profiles look approximately parallel for load position 1 indicating little change in twist of the bridge section as the span changes. As the load is moved towards load position 5, the twist increases. The effect of span on the deflection profile at midspan can be seen clearly.

(d) The average deflections are not affected by the midspan diaphragm.

7.6 Reactions

The values of reactions are tabulated as coefficients of the applied load W in Chapter 5. The following trends can be observed for the reactions.

(a) The reaction values are not affected by the midspan diaphragm. This is clearly true for the midspan load positions where the reactions are statically determinate and hence are dependent only on the overall geometry of the bridge. However, it will be seen that the reactions are not affected appreciably by the midspan diaphragm even for load positions other than those at the midspan.

(b) The tendency for R2 and R4 to become negative with the load at mid-span, depending only on considerations of geometry and statics, makes it a different problem from the skew bridge where negative reactions are due to continuity effect and torsional stiffness.

7.7 Use of the Data in Design

The data presented in this report is largely in dimensionless form and hence is directly applicable to prototype response data for simply supported curved box-girder bridges within the following limits:

(a) The data is for bridges made of homogeneous, linearly elastic material with a Poisson's Ratio value of $\nu = 0.332$. It is unlikely however that the precise value of ν will have a significant effect on the overall response of a structure of this type.

(b) The cross-sectional geometry must be similar to that used in the model study. There is no way of extrapolating this data to bridges of other cross-sectional geometry, either with a different number of cells or with plate thicknesses which are not to the same scale as those used in the model.

(c) For exact data the prototype bridge should strictly be geometrically similar to a model in all respects including span and radius of curvature. However as the span was varied in this study, it is possible to interpolate the response data for a wide range of spans of the single radius considered.

(d) The loading applied to the models was a point load. But this was applied in a sufficient number of locations directly over the webs to make possible the construction of influence lines or influence surfaces for measured response quantities if these should be required for determining the total effects of multi-point loads or distributed loading.

Model	Span (inches)	Moment Coefficient C for Load Positions										Average Value of C		C for LP 5 / C for LP 1	
		1		2		3		4		5					
		Test	Theory	Test	Theory	Test	Theory	Test	Theory	Test	Theory	Test	Theory	Test	Theory
1A	60.0	.251	.245	.253	.252	.260	.259	.263	.265	.269	.272	.259	.259	1.07	1.11
1B	60.0	.246	.245	.256	.252	.263	.259	.265	.265	.267	.272	.259	.259	1.09	1.11
2A	45.0	.243	.242	.250	.248	.258	.255	.263	.261	.268	.268	.256	.255	1.10	1.11
2B	45.0	.246	.242	.247	.248	.254	.255	.260	.261	.265	.268	.254	.255	1.08	1.11
3A	30.0	.242	.239	.250	.246	.256	.252	.260	.258	.265	.265	.253	.252	1.10	1.11
3B	30.0	.239	.239	.247	.246	.257	.252	.261	.258	.268	.265	.253	.252	1.11	1.11

TABLE 7.1 TEST AND THEORTETICAL BENDING MOMENTS AT MIDSPAN (COEFFICIENTS OF WL) FOR ALL MODELS FOR MIDSPAN LOAD POSITIONS 1 THROUGH 5.

	BEAM NUMBER				
	1	2	3	4	5
Individual I Values (in4)	0.7525	1.0858	1.0858	1.0858	0.7525
Percentage of Total I	15.8	22.8	22.8	22.8	15.8

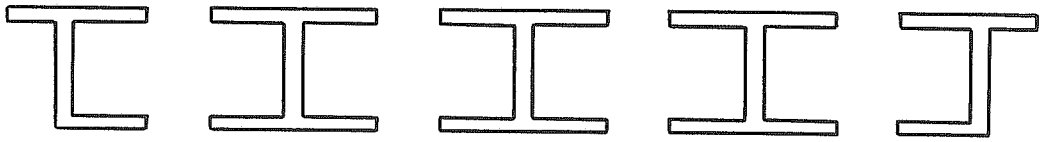

BEAM NO. ① ② ③ ④ ⑤

FIG. 7.1 DIVISION OF BOX GIRDER SECTION INTO I BEAMS

Model	Span (inches)	BEAM NUMBER/LOAD POSITION				
		1/1	2/2	3/3	4/4	5/5
1A	60.0	23.9	27.4	26.2	26.5	22.1
2A	45.0	26.7	29.0	27.5	28.1	24.6
3A	30.0	33.2	32.6	29.7	31.4	29.7
1B	60.0	21.3	25.8	24.7	25.0	19.7
2B	45.0	22.9	26.5	25.3	25.9	21.3
3B	30.0	26.4	27.8	25.5	27.5	24.5

TABLE 7.2 MAXIMUM I-BEAM PERCENTAGES OF TOTAL MIDSPAN MOMENT DUE TO POINT LOADING ON RADIAL SECTION AT MIDSPAN

Model	Span (inches)	Twist (inches) for Load Position W = 1000 lbs.				
		1	2	3	4	5
1A	60.0	-0.0068	0.0074	0.0200	0.0322	0.0476
1B	60.0	-0.0030	0.0074	0.0204	0.0324	0.0432
2A	45.0	-0.0130	-0.0014	0.0088	0.0194	0.0318
2B	45.0	-0.0094	0.0000	0.010	0.0180	0.0286
3A	30.0	-0.0140	-0.0030	0.0032	0.0106	0.0202
3B	30.0	-0.0100	-0.0034	0.0038	0.0114	0.0174

Twist = (Deflection under Web No. 5 - Deflection under Web No. 1) at midspan

TABLE 7.3 VARIATION OF TWIST WITH POSITION OF LOAD AT MIDSPAN RADIAL SECTION

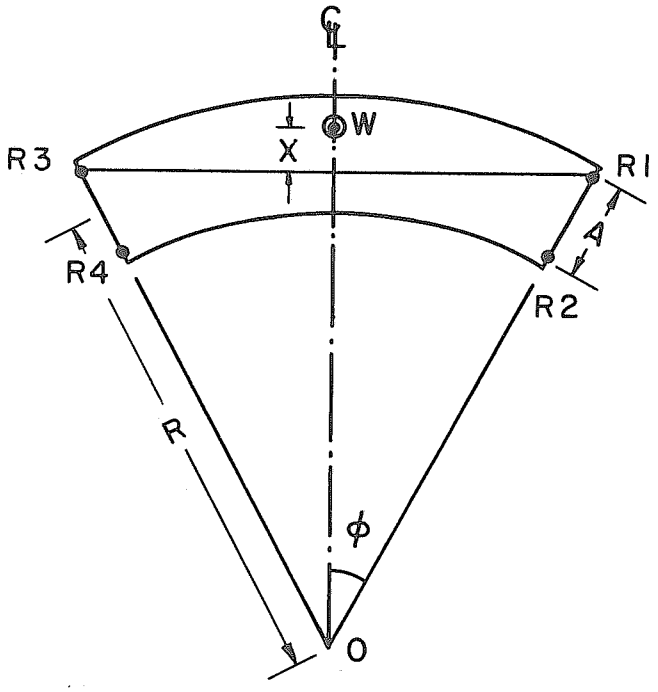

FIG. 7.2 PLAN VIEW OF A CURVED BRIDGE

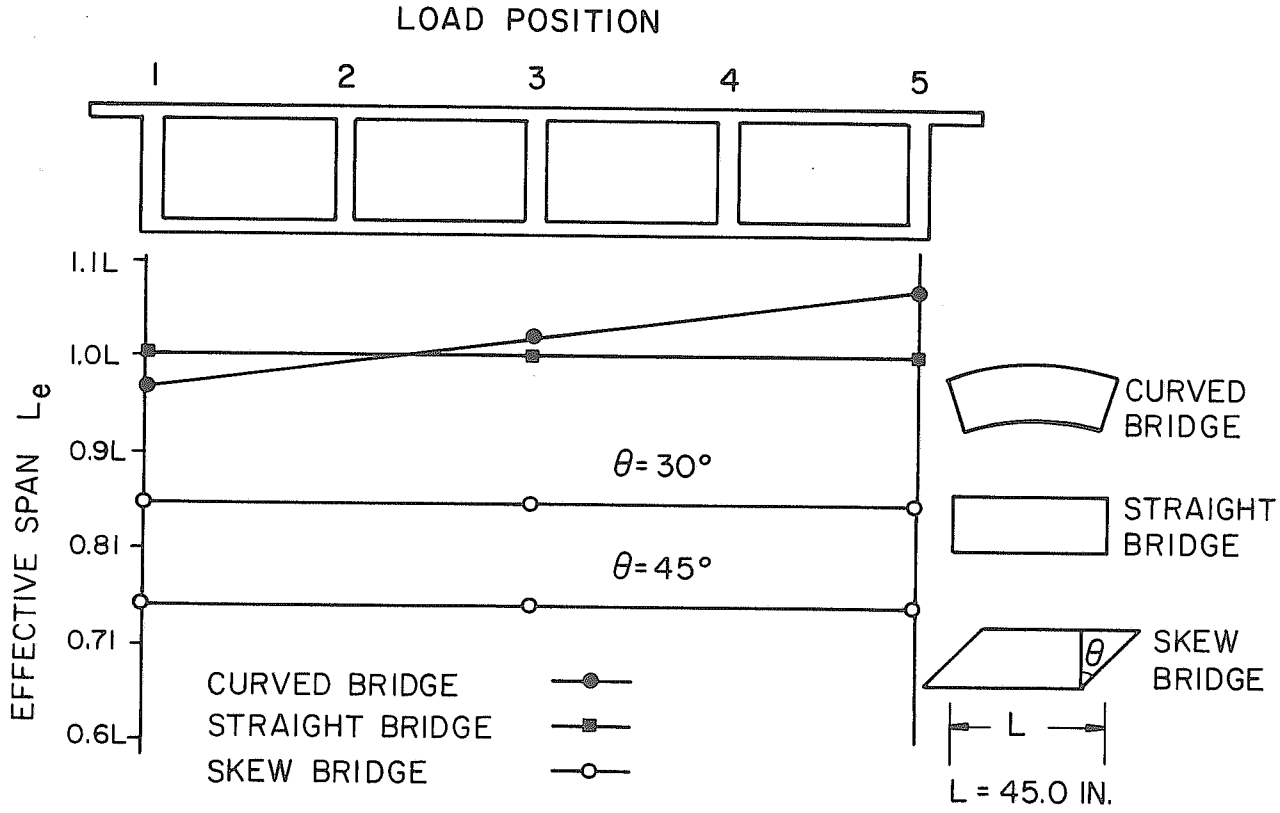

FIG. 7.3 VARIATION OF EFFECTIVE SPAN WITH LOAD POSITION AT MIDSPAN FOR CURVED, STRAIGHT AND SKEW BRIDGES

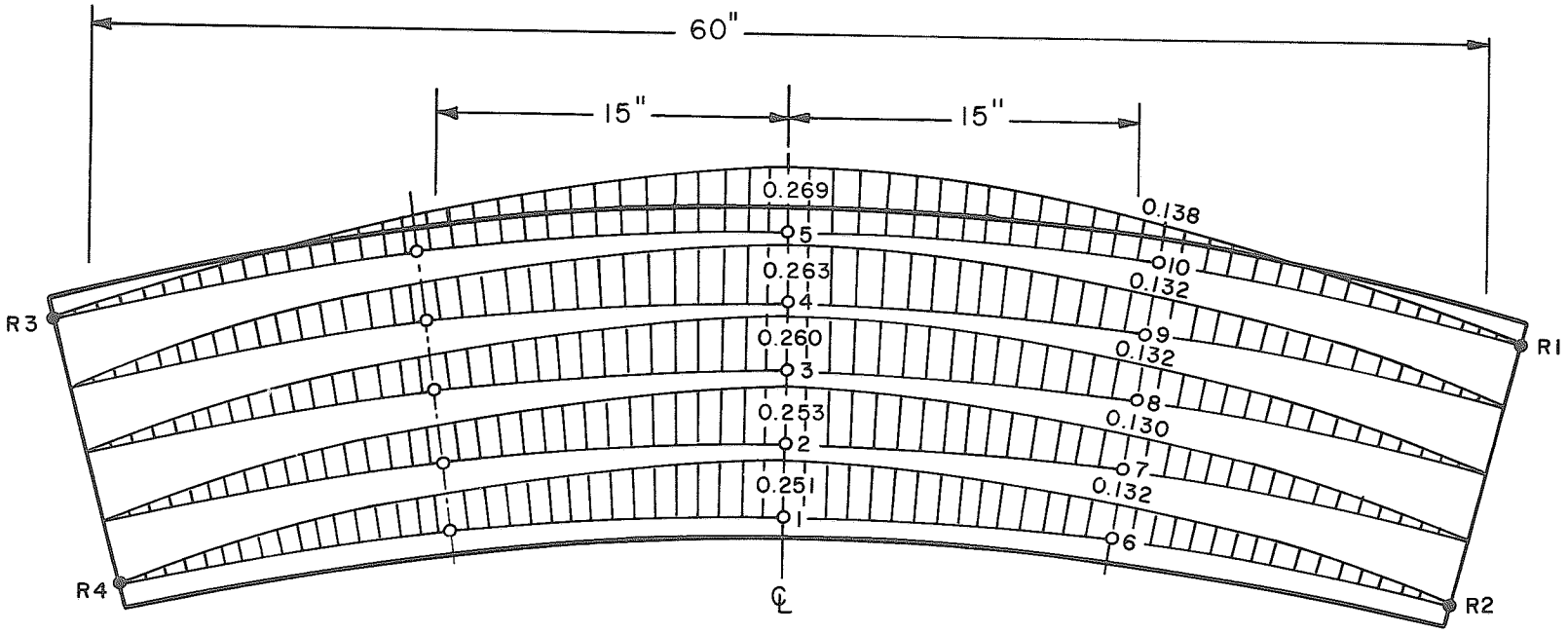

FIG. 7.4 INFLUENCE LINES FOR TOTAL LONGITUDINAL BENDING MOMENT AT MIDSPAN (COEFFICIENTS OF WL) MODEL 1A

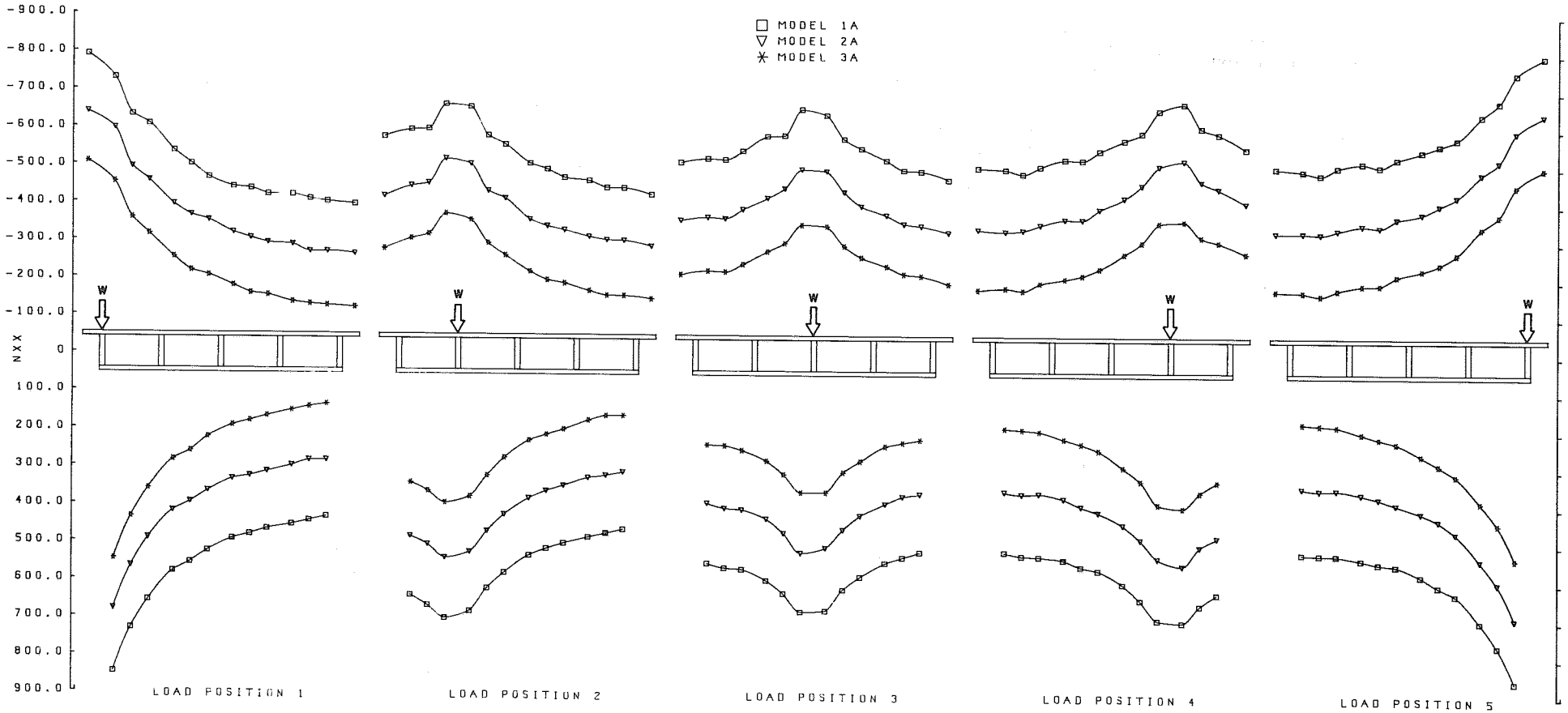

FIG.7.5 RADIAL DISTRIBUTION OF TANGENTIAL FORCES PER UNIT WIDTH IN TOP AND BOTTOM PLATES (NXX) AT SECTION 0-0 MODEL 1A MODEL 2A AND MODEL 3A

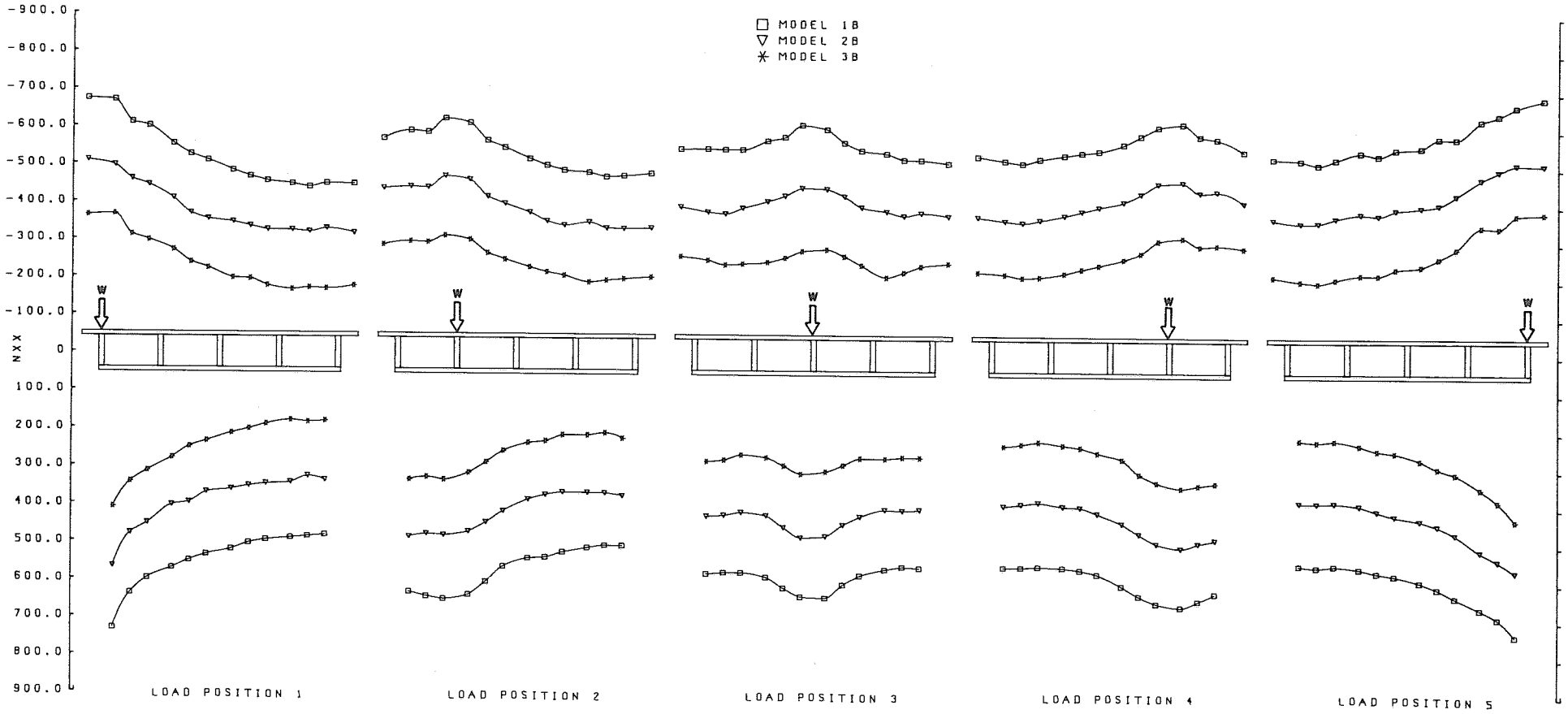

FIG.7.6 RADIAL DISTRIBUTION OF TANGENTIAL FORCES PER UNIT WIDTH IN TOP AND BOTTOM PLATES (NXX) AT SECTION 0-0 MODEL 1B MODEL 2B AND MODEL 3B

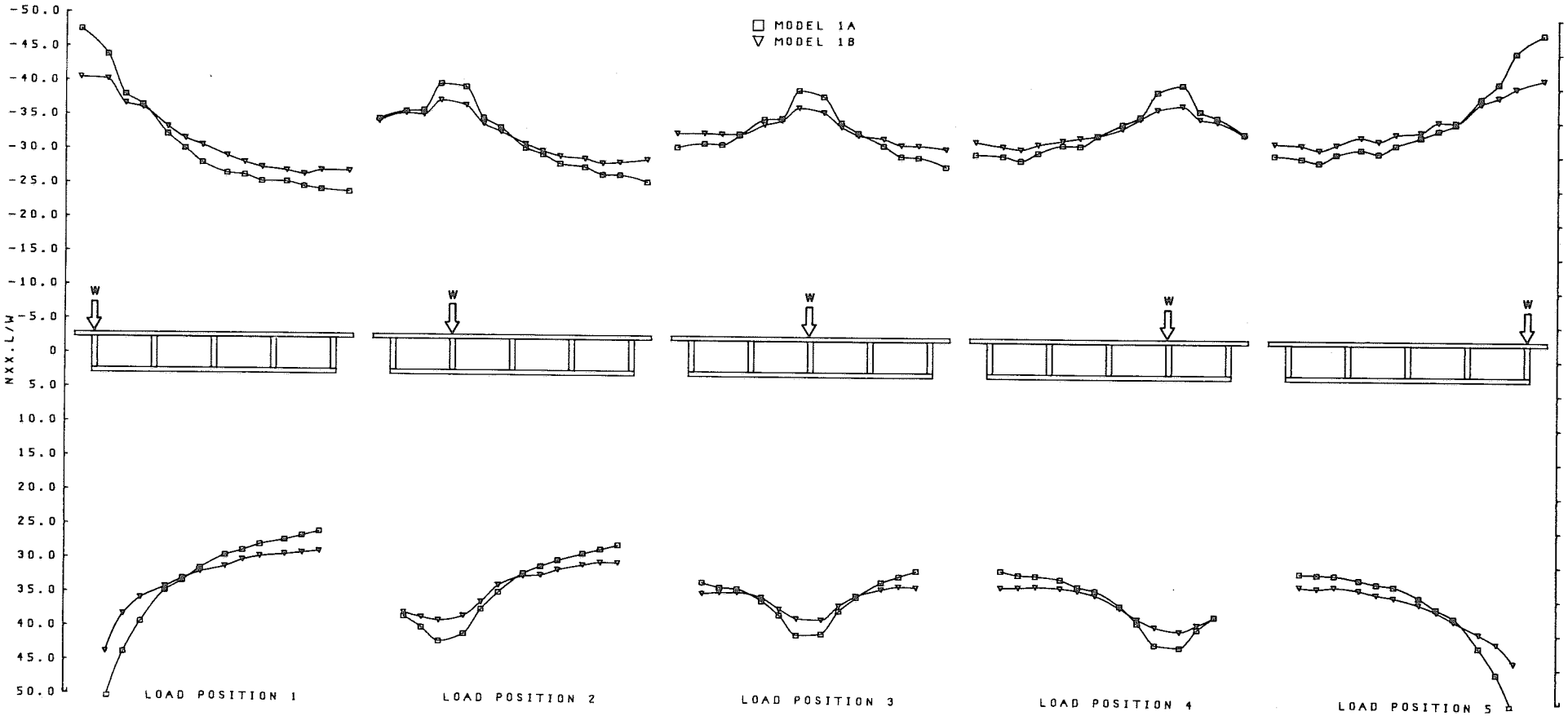

FIG.7.7 RADIAL DISTRIBUTION OF TANGENTIAL FORCES PER UNIT WIDTH IN TOP AND BOTTOM PLATES (NXX) AT SECTION 0-0 MODEL 1A AND MODEL 1B

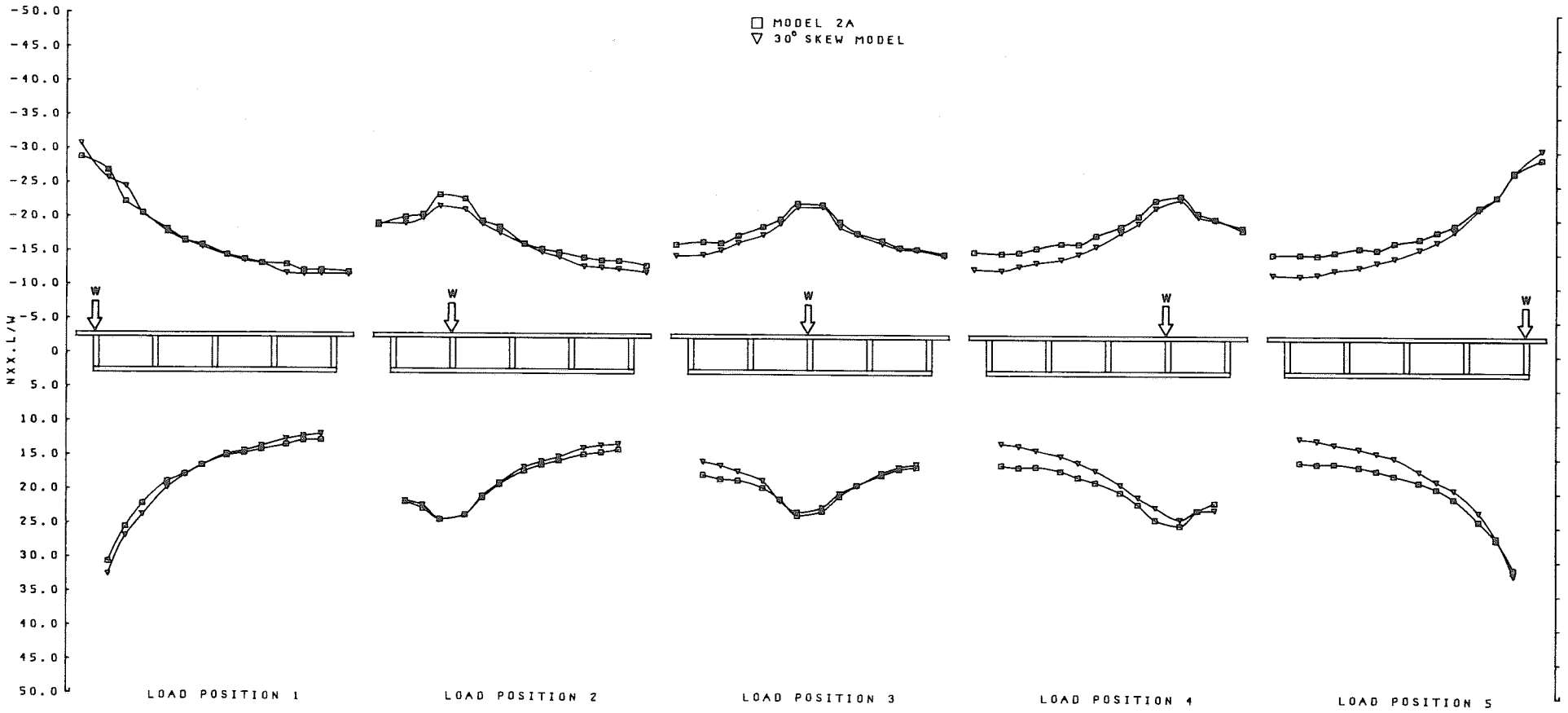

FIG.7.8 RADIAL DISTRIBUTION OF TANGENTIAL FORCES PER UNIT WIDTH IN TOP AND BOTTOM PLATES (NXX) AT SECTION 0-0
MODEL 2A AND 30° SKEW MODEL

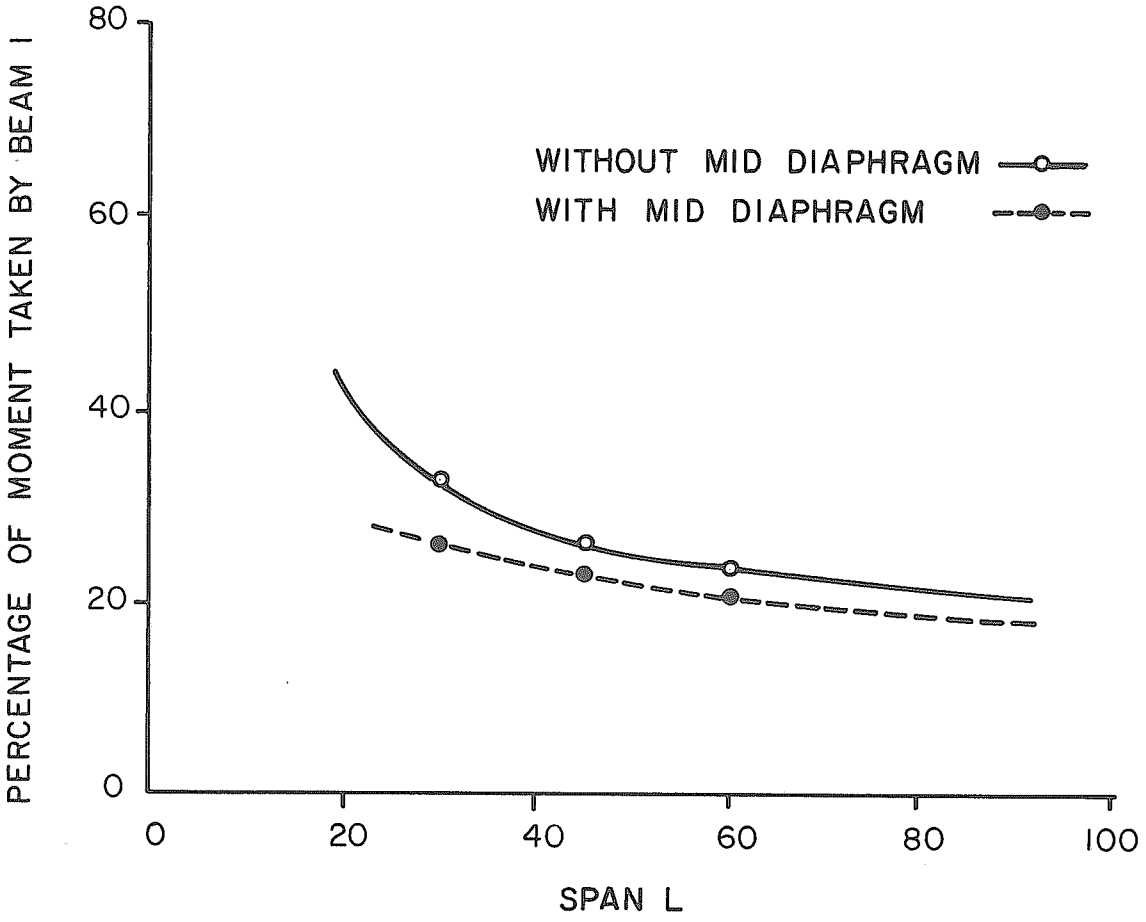

FIG. 7.9 VARIATION OF PERCENTAGE OF MOMENT WITH SPAN TAKEN BY BEAM NO.I FOR LOAD POSITION I

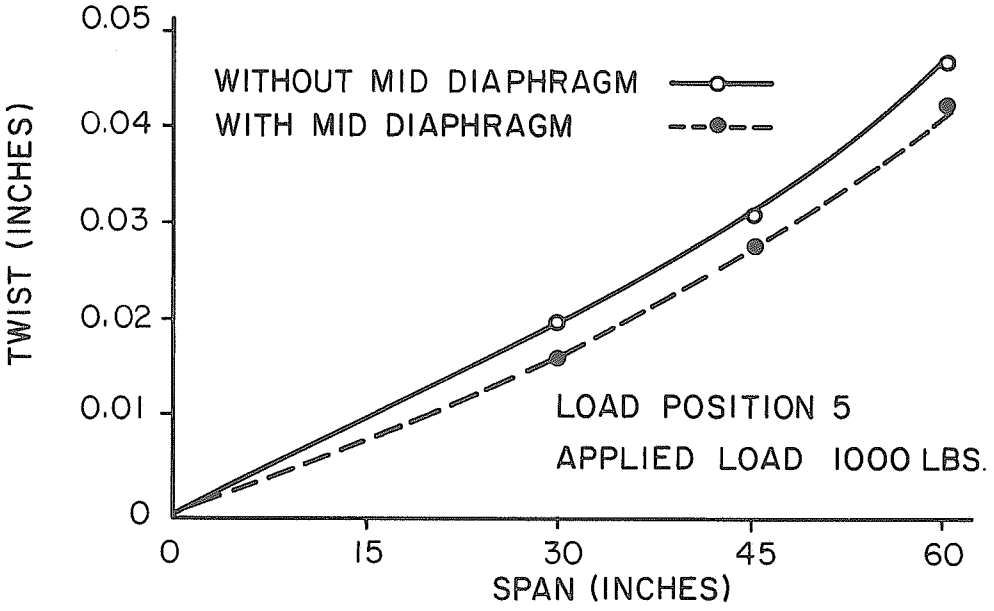

FIG. 7.10 VARIATION OF TWIST WITH SPAN LENGTH

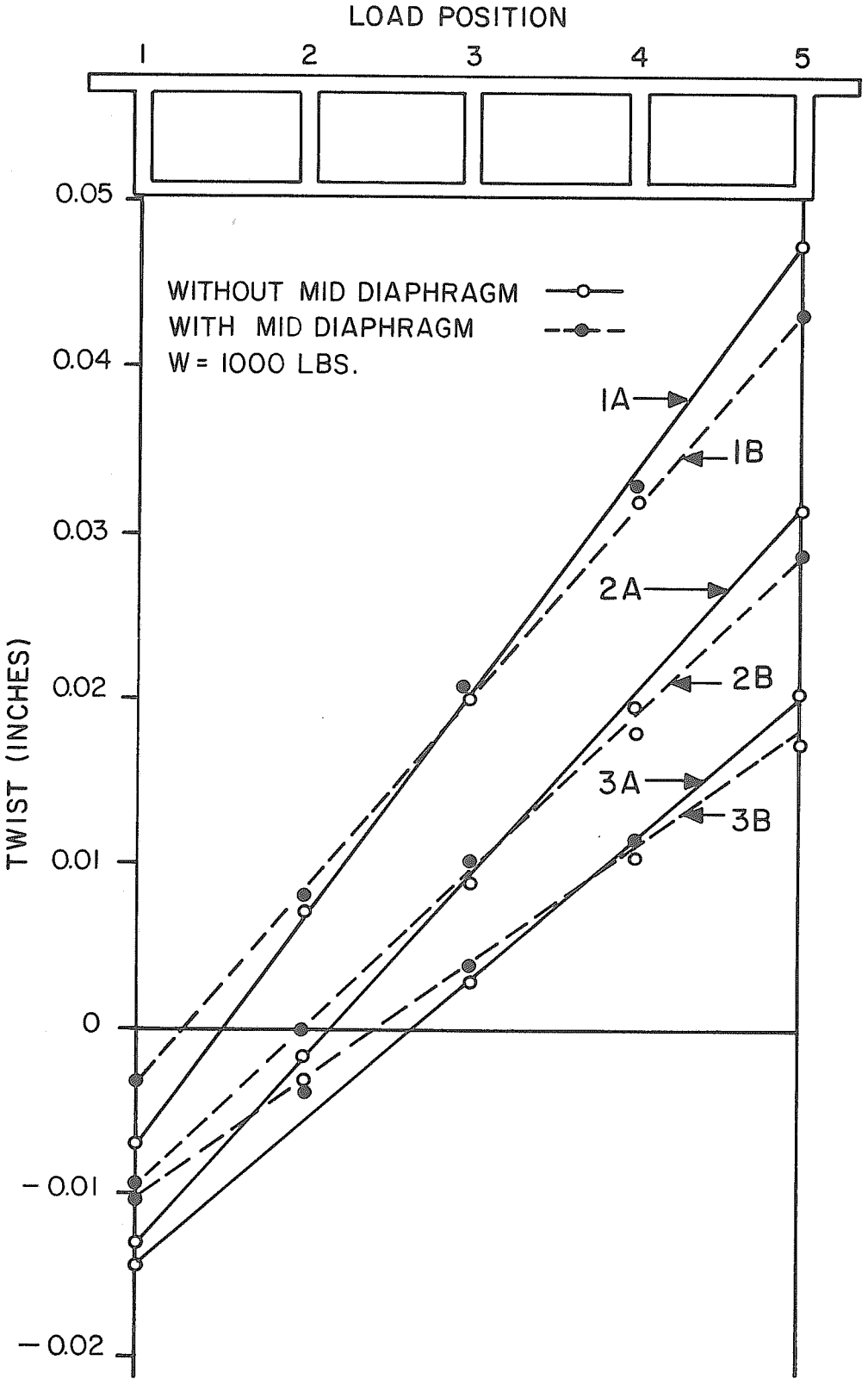

FIG. 7.11 VARIATION OF TWIST WITH LOAD POSITION AT MIDSPAN

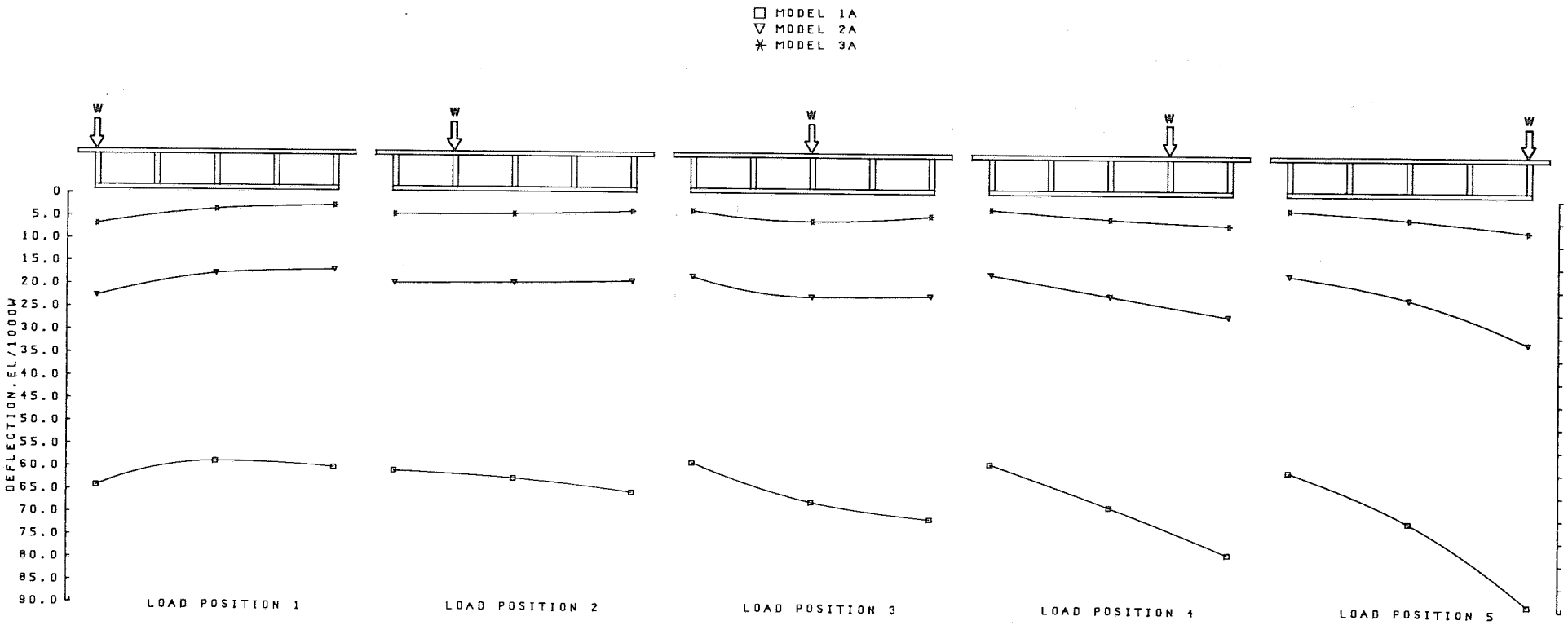

FIG.7.12 RADIAL DISTRIBUTION OF VERTICAL DEFLECTIONS AT MIDSPAN FOR MODEL 1A MODEL 2A AND MODEL 3A

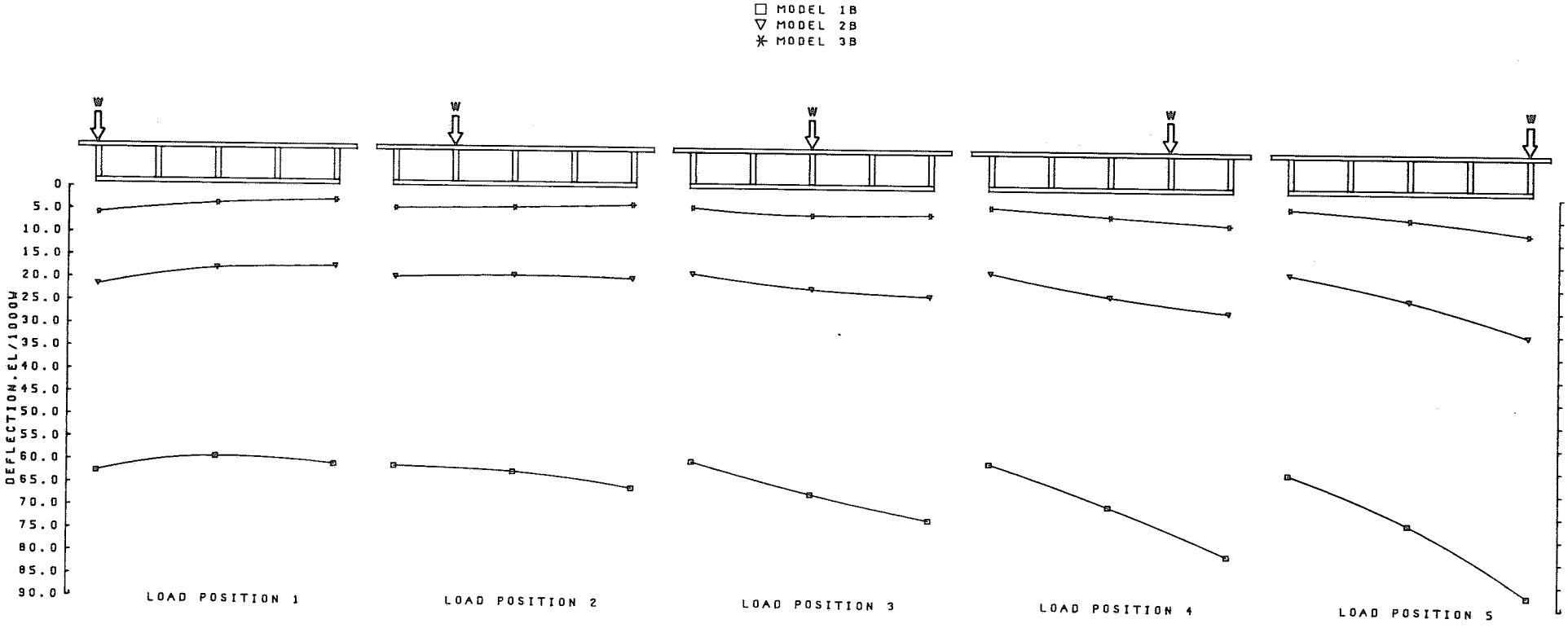

FIG. 7.13 RADIAL DISTRIBUTION OF VERTICAL DEFLECTIONS AT MIDSPAN FOR MODEL 1B MODEL 2B AND MODEL 3B

8. COMPARISON OF EXPERIMENTAL AND THEORETICAL RESULTS

8.1 General

A comparison between the model results presented in this report and results derived from theoretical studies on curved box-girder bridges is presented in this chapter. The response quantities compared include the total moment at midspan, total compressive and tensile forces at Section 0-0, distribution of moment between I-beams at Section 0-0, distribution of N_{xx} in plates, radial distribution of plate bending moments at Section 0-0 and deflections at midspan. The computer program used for the analysis of the bridge models assumes that the bridge is simply supported continuously along the two straight edges, which is equivalent to assuming infinitely stiff end diaphragms. Although the test model was not supported as assumed in the theoretical model, this difference in boundary conditions does not seem to make significant difference in the responses of the experimental and analytical models as the end diaphragms are sufficiently rigid in their own plane.

8.2 Theoretical Analysis

For the theoretical analysis of the curved box-girder bridges tested in this study, a computer program called 'CURSTR' [5] was used. This program which was developed at the University of California, Berkeley, is capable of analyzing curved folded plate structures simply supported at both ends and composed of elements that may in general be segments of conical frustra. The program is based on a harmonic analysis in the circumferential direction, with the loading expressed by Fourier Series, and on a finite element stiffness analysis in the transverse direction. The structure assembly and solution follows the direct

stiffness method. The structure may be subjected to surface or joint loads. The total number of harmonics to be used in the analysis can be specified depending upon the accuracy desired. Deflections usually converge very rapidly, and 5 to 10 nonzero harmonic terms are usually sufficient to describe most loading types. Stresses and moments do not converge as fast, especially for concentrated loads in which case at least 25 nonzero terms will be necessary for adequate accuracy. The program can be specified to calculate the I-beam moments together with the net compressive and tensile stress resultants for each I-beam at any section. A theoretical analysis of all the model bridges was made by this computer program, and a brief comparison of the computed data with the measured is given below.

8.3 N_{xx} Forces and Total Longitudinal Moments

Table 8.1 shows a comparison of computed and measured values of N_{xx} and total longitudinal moment at Section 0-0. The ratio of average N_{xx} of computed and test values was determined by computing the total compressive and tensile forces over the entire cross-section of the bridge at Section 0-0. The values in Table 8.1 represent average values of load positions 1, 3 and 5. Moments at Section 0-0 were calculated from reactions and applied loading. A comparison of moments at midspan is also given in Table 7.1 for midspan load positions for all models, which shows a close agreement. It can be seen in Table 8.1 that the computed and measured values of average N_{xx} and total longitudinal bending moment agree within 1%. However it was observed that the measured N_{xx} values were slightly higher in top and bottom plates than computed values, while the computed N_{xx} values were slightly higher in webs as compared with measured values and thus statics was satisfied in both cases.

Fig. 8.1 is a representative Calcomp plot which shows the radial distribution of experimental and theoretical N_{xx} values in plates at Section 0-0 for midspan load positions 1 through 5. It will be seen that the distribution trends in both cases are quite similar and the experimental and theoretical curves follow each other closely. The agreement in the top plate is better than the bottom plate except at the free edge of overhangs for load positions 1 and 5, where theoretical solution shows a stress drop.

8.4 Distribution of Longitudinal Moment between I-beams at Section 0-0

Distribution of longitudinal moment between the I-beams is a function of the distribution of N_{xx}. A comparison of the percentage of total moment taken by each beam at Section 0-0 is given in Table 8.3 for Models 1A, 2A and 3A, for the load positions 1, 3 and 5. It will be seen in Table 8.3 that the test and theoretical values generally agree within 2% which once again indicates that the distribution trends of N_{xx} values are similar for both theory and experiment and the N_{xx} values are close.

8.5 Radial Plate Bending Moments at Section 0-0

Fig. 8.2 shows a comparison of experimental and theoretical distribution of radial plate bending moments per unit length (M_{yy}) at Section 0-0 for Model 1A for load positions 1 through 5. Theoretical values are shown by dotted lines, and where they do not appear they are coincident with the experimental values. Fig. 8.2 shows that there is a close agreement between the measured and the computed plate bending moments, and the trends are similar in both cases. Since the radial bending moments do not change appreciably with span in both theory and experiment, the plot of Fig. 8.2 is a representative for all the models tested.

8.6 Deflections

Table 8.2 gives a comparison of computed and measured values of deflections at midspan under the Webs 1, 3 and 5 for Model 1A, 2A and 3A. The ratio of computed and test deflections given in Table 8.2 represent the average of load positions 1, 3 and 5. It will be seen in Table 8.2 that the test deflections are approximately 5%, 7% and 10% higher than computed deflections for Models 1A, 2A and 3A respectively indicating that the experimental model is slightly more flexible than the theoretical model. It may also be noted that the discrepancy between experimental and theoretical deflections increases from 5% to 10% as the span is reduced from 60 in. to 30 in. The main reason for the larger difference at smaller spans is probably the reduced accuracy in the measurement of deflections as a result of the rigid body motion of the bridge. This rigid body motion could result from the small axial flexibility of the load cells which will cause a greater percentage error when the deflections are small at smaller span. Another reason for the greater percentage difference in deflections at smaller spans could be the difference in boundary conditions of the experimental and theoretical models. However, the other response data are not affected by these differences.

A comparison of radial distribution of experimental and theoretical deflections at midspan is shown in Fig. 8.3 for Model 1A for the midspan load positions 1 through 5. It will be seen that the distribution curves are essentially parallel and show the same trends. The test values are approximately 5% higher than the theoretical values.

8.7 Conclusion

The agreement between the experimental and theoretical response data is very close, and it is concluded that the theory in its present form is sufficiently accurate for the elastic analysis of curved box-girder bridges.

Model No.	Computed Values/Test Values	
	Average N_{xx} at Section 0-0	Total longitudinal Moment at Section 0-0
1A, 1B	1.01	1.00
2A, 2B	1.01	1.00
3A, 3B	1.01	1.01

TABLE 8.1 COMPARISON OF COMPUTED AND MEASURED VALUES OF N_{xx} AND TOTAL LONGITUDINAL MOMENT AT SECTION 0-0

Model No.	Computed/Test Deflections at Midspan (Average of Load Positions 1, 3 and 5)		
	Under Web No. 1	Under Web No. 3	Under Web No. 5
1A	0.95	0.94	0.94
2A	0.94	0.93	0.93
3A	0.90	0.88	0.91

TABLE 8.2 COMPARISON OF COMPUTED AND MEASURED VALUES OF DEFLECTIONS AT MIDSPAN

Model	Beam No.	Percentage of Total Moment for Load Position					
		1		3		5	
		Test	Theory	Test	Theory	Test	Theory
1A	1	23.9	24.2	15.0	15.0	13.5	13.2
	2	24.8	24.9	22.7	22.7	19.5	19.4
	3	20.5	20.4	26.2	26.8	20.8	20.8
	4	18.4	18.4	21.9	21.8	26.1	26.6
	5	12.3	12.0	14.1	13.8	22.2	22.3
2A	1	26.7	26.6	14.5	14.1	12.4	12.1
	2	25.3	25.7	22.5	22.6	18.0	18.1
	3	19.7	19.7	27.5	28.2	20.0	20.2
	4	17.1	17.1	21.9	21.9	25.0	25.2
	5	11.2	10.9	13.6	13.1	24.6	24.4
3A	1	33.2	32.8	13.6	12.8	9.9	9.5
	2	27.3	27.5	22.2	22.4	15.1	15.0
	3	17.8	17.8	29.7	31.4	18.7	18.6
	4	13.6	13.7	21.6	21.6	26.6	27.1
	5	8.1	8.2	12.8	11.8	29.7	29.8

TABLE 8.3 COMPARISON OF PERCENTAGE OF TOTAL MOMENT TAKEN BY I-BEAMS AT SECTION O-O

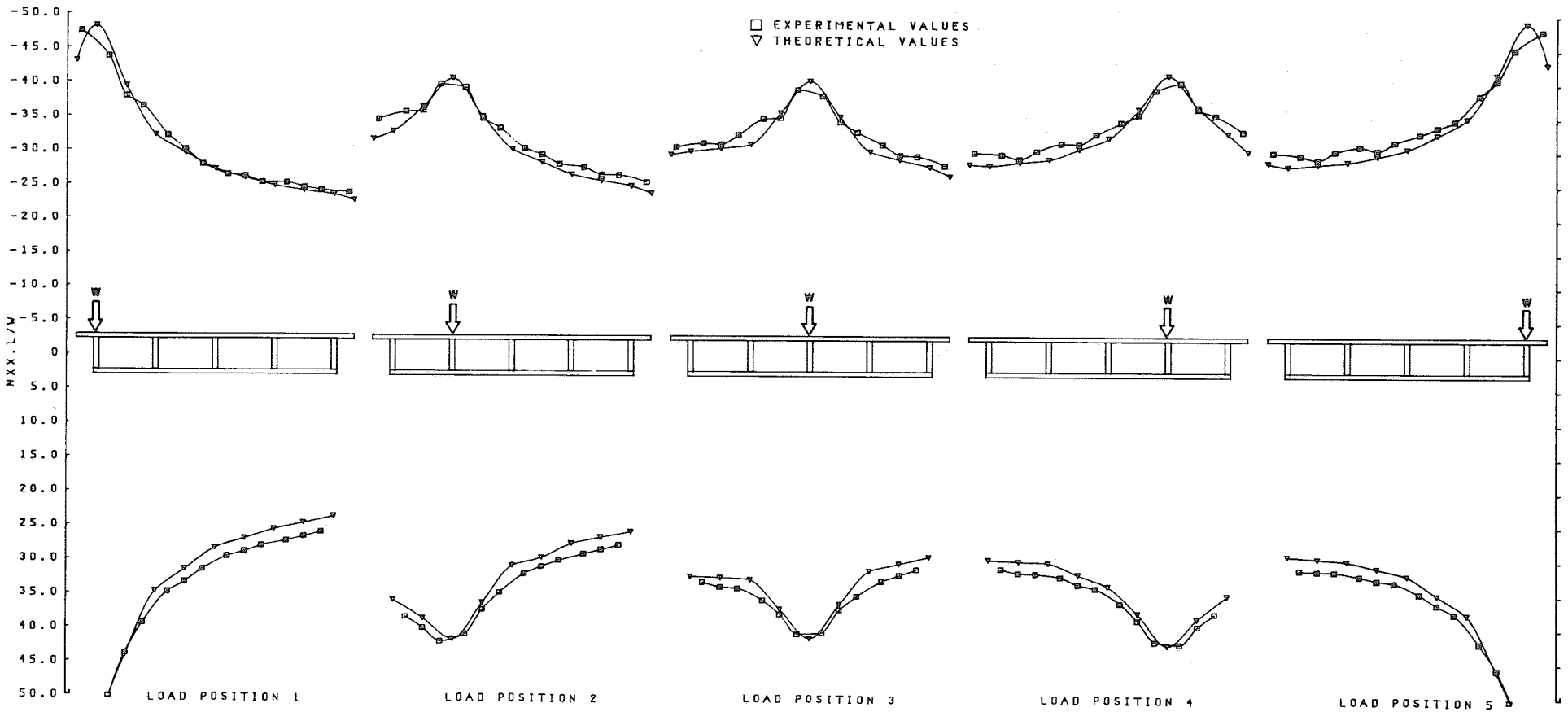

FIG.8.1 RADIAL DISTRIBUTION OF TANGENTIAL FORCES PER UNIT WIDTH IN TOP AND BOTTOM PLATES (NXX) AT SECTION 0-0
MODEL 1A

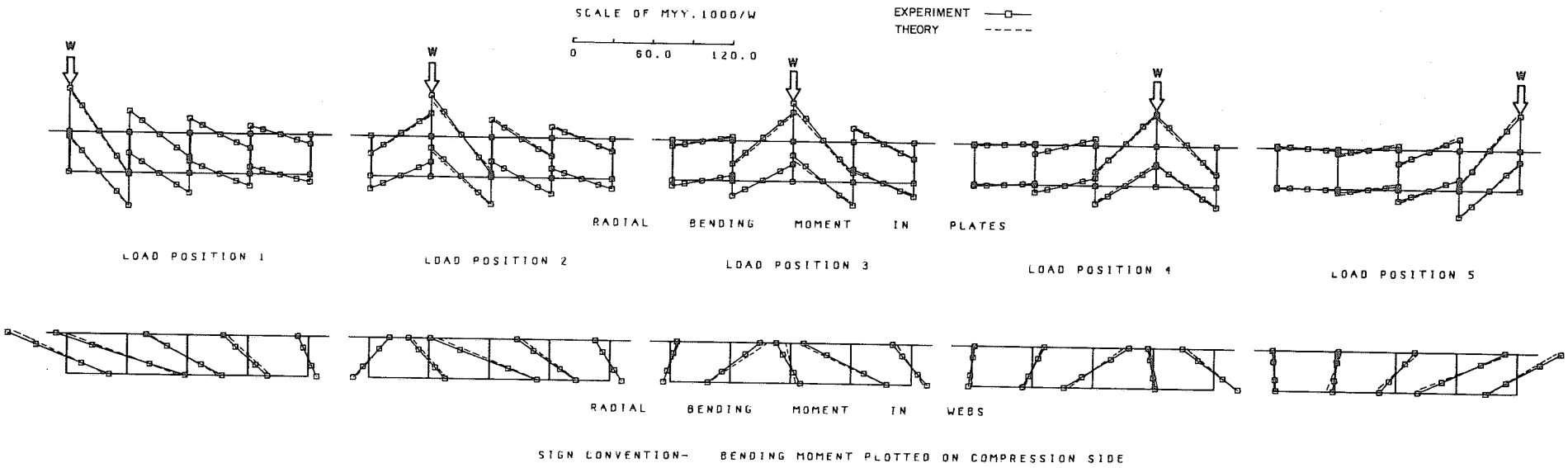

FIG.8.2 RADIAL DISTRIBUTION OF RADIAL BENDING MOMENT PER UNIT LENGTH (MYY) AT SECTION 0-0

MODEL 1A

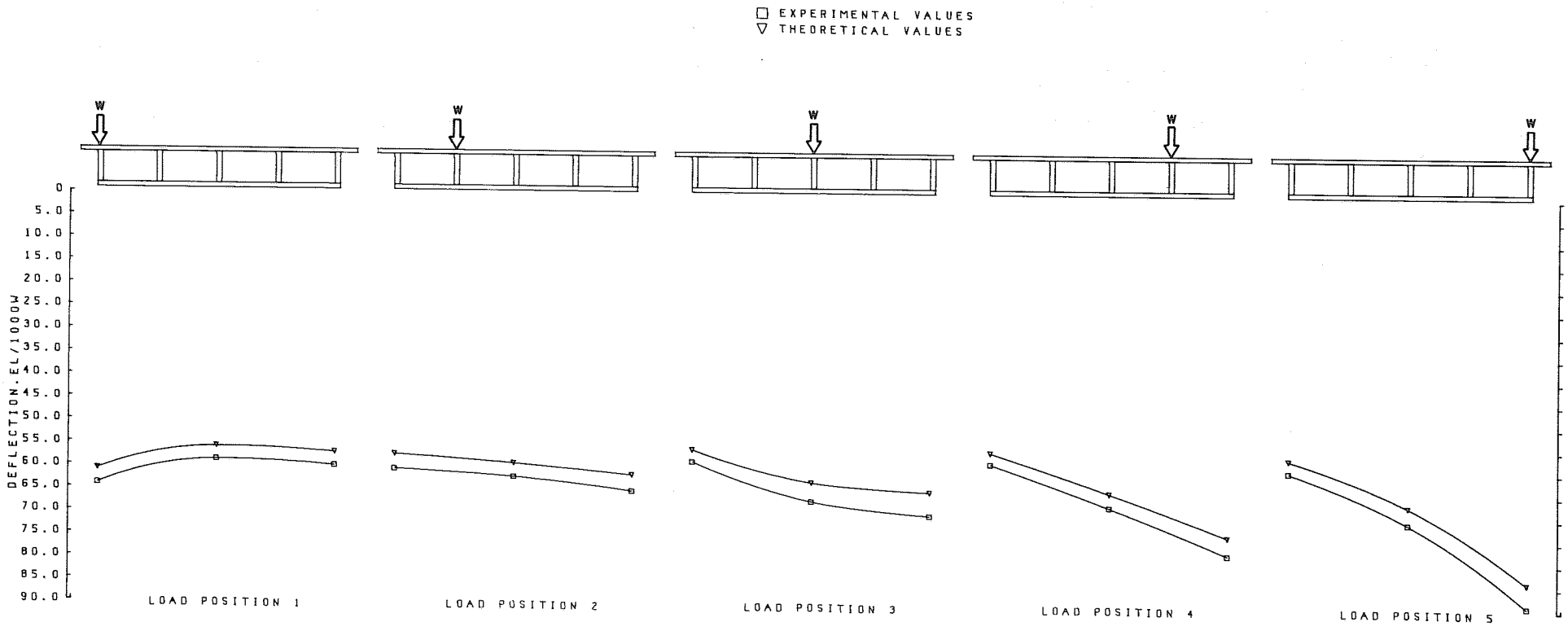

FIG. 8.3 RADIAL DISTRIBUTION OF VERTICAL DEFLECTIONS AT MIDSPAN FOR MODEL 1A

9. REFERENCES

1. Godden, W. G., and Aslam, M., "Model Studies of Skew Box-Girder Bridges," Report No. UC SESM 71-26, University of California, Berkeley, Calif., Dec., 1971.

2. Aneja, I., and Roll, F., "Model Analysis of Curved Box-Beam Highway Bridge," Journal of the Structural Division, ASCE, Vol. 97, No. ST12, Proc. Paper 8603, Dec., 1971, PP. 2861-2878.

3. Nicholls, J. I., and Fuchs, P., "A Comparison of Test Results and a Computer Analysis of a Single Cell Horizontally Curved Composite Box Bridge", University of Washington, Seattle, Washington, 1972.

4. "Standard Specifications for Highway Bridges", American Association of State Highway Officials, 9th ed., Washington, D.C., 1965.

5. Meyer, C., and Scordelis, A. C., "Analysis of Curved Folded Plate Structures," Report No. UC SESM 70-8, University of California, Berkeley, Calif., June 1970.

10. ACKNOWLEDGEMENTS

This investigation was conducted under the sponsorship of the State of California, Business and Transportation Agency, Department of Public Works, Division of Highways and U.S. Department of Transportation, Federal Highway Administration. The opinions, findings and conclusions expressed in this report are those of the authors and not necessarily those of the sponsors.

The authors would like to express their sincere appreciation to the following people who contributed to the success of the work:

Professor Scordelis, University of California, Berkeley, who initiated the study and supervised the theoretical studies referred to in Chapter 8. This project is part of a larger investigation he is conducting into the analysis and behavior of box-girder bridges.

Mr. Foster and Mr. M. Pitrola of the Structural Engineering Machine Shop who constructed the model and performed the necessary cut-back modifications.

Mr. D. L. Wasley who gave frequent help in running the Data Acquisition System, and Mr. L. Trescony who assisted with the instrumentation.